



HAL
open science

Contribution to the study of formation mechanisms of condensable by-products from torrefaction of various biomasses

Elvira Rodriguez Alonso

► **To cite this version:**

Elvira Rodriguez Alonso. Contribution to the study of formation mechanisms of condensable by-products from torrefaction of various biomasses. Chemical and Process Engineering. Institut National Polytechnique de Toulouse - INPT, 2015. English. NNT : 2015INPT0148 . tel-04240568

HAL Id: tel-04240568

<https://theses.hal.science/tel-04240568>

Submitted on 13 Oct 2023

HAL is a multi-disciplinary open access archive for the deposit and dissemination of scientific research documents, whether they are published or not. The documents may come from teaching and research institutions in France or abroad, or from public or private research centers.

L'archive ouverte pluridisciplinaire **HAL**, est destinée au dépôt et à la diffusion de documents scientifiques de niveau recherche, publiés ou non, émanant des établissements d'enseignement et de recherche français ou étrangers, des laboratoires publics ou privés.



Université
de Toulouse

THÈSE

En vue de l'obtention du

DOCTORAT DE L'UNIVERSITÉ DE TOULOUSE

Délivré par :

Institut National Polytechnique de Toulouse (INP Toulouse)

Discipline ou spécialité :

Génie des Procédés et de l'Environnement

Présentée et soutenue par :

Mme ELVIRA RODRIGUEZ ALONSO

le jeudi 3 décembre 2015

Titre :

CONTRIBUTION TO THE STUDY OF FORMATION MECHANISMS OF
CONDENSABLE BY-PRODUCTS FROM TORREFACTION OF VARIOUS
BIOMASSES

Ecole doctorale :

Mécanique, Energétique, Génie civil, Procédés (MEGeP)

Unité de recherche :

Laboratoire de Génie Chimique (L.G.C.)

Directeur(s) de Thèse :

M. CHRISTOPHE GOURDON

Rapporteurs :

M. FREDERIC MARIAS, UNIVERSITE DE PAU ET DES PAYS DE L ADOUR

M. YANN ROGAUME, UNIVERSITE DE LORRAINE

Membre(s) du jury :

M. FREDERIC MARIAS, UNIVERSITE DE PAU ET DES PAYS DE L ADOUR, Président

M. CHRISTOPHE GOURDON, INP TOULOUSE, Membre

M. JEAN-MICHEL COMMANDRE, CIRAD MONTPELLIER, Membre

Mme CAPUCINE DUPONT, CEA GRENOBLE, Membre

Contribution to the study of formation mechanisms of condensable by-products from torrefaction of various biomasses

Contribution à l'étude de mécanismes de formation des espèces condensables lors de la torréfaction de biomasses variées

“Those who are courageous, go headlong. They search all opportunities of danger. Their life philosophy is not that of insurance companies. Their life philosophy is that of a mountain climber, a glider, a surfer.

Not only in the outside seas they surf; they surf in their innermost seas. And not only on the outside they climb Alps and Himalayas; they seek inner peaks. Remember one thing: never forget the art of risking – never, never. Always remain capable of risking; wherever you can find an opportunity to risk, never miss it, and you will never be a loser. Risk is the only guarantee for being truly alive.

You need courage to risk; do not forget that courage is not the absence of fear, but rather the total presence of fear, with the courage to face it.”

Courage: The Joy of Living Dangerously (Osho)

REMERCIEMENTS

Je tiens à remercier beaucoup de monde pour ces trois années de thèse... :

D'abord, à Capucine Dupont, pour son encadrement, les soirées sushi, les restos, les longues discussions sur les méthodes de travail ;) J'ai découvert une femme très engagée avec son travail, mais aussi très humaine. Merci Capucine ! *¡¡Arriba el PSG!!*

A Christophe Gourdon, mon directeur de thèse, pour sa sympathie, son professionnalisme et sa bonne humeur !

A Laurent Heux, pour sa disponibilité, pour les longues discussions et la passion contagieuse pour ce qu'il fait.

Aux collègues du projet INVERTO, du LGC-ENSIACET Toulouse et du CIRAD Montpellier, pour ces bons moments passés ensemble au cours des réunions, avec une ambiance que je voudrais re-retrouver dans mon futur professionnel !

A Denilson Da Silva Perez, pour sa sympathie et son sourire permanent ! *Um beijinho !*

A ma famille, ma mère, mon père, ma sœur, pour m'avoir donné la vie, le contexte et le soutien qui m'ont amenée à finaliser cette thèse et à être la personne que je suis aujourd'hui.

A mes collègues du Labo Biomasse... : à Seb, pour sa bonne humeur et sa *comunicación*; à Marc, pour ces discussions dans nos bureaux en face; à Thierry C, pour les discussions spirituelles; à Guillaume B, pour son merveilleux bouquin; à Maguelone et Muriel, pour sa bonne humeur; à Lucia, pour les discussions n'importe où n'importe quand ; à Marion, pour les discussions autour du thé sur les chats et le chocolat; à Joseph, pour les discussions philosophiques qui ont réglé le monde ; à Céline, la *pitufina*, pour rendre le bureau plus vivant; à Maïté, Maxime et Clément pour ces discussions et conseils sur le théâtre; à Guillaume G, Emanuela, Chams... et beaucoup d'autres que j'ai rencontrés pendant ces trois années et demie au labo, merci pour cette expérience partagée avec vous !

A mes amis, ceux de ma ville d'origine Madrid : Teresa, Lara, Cristina, Lamis, Laura, Silvia, Iñi, Adri, Maria, Cris, Christian... Et à mes amis, ceux qui sont dispersés un peu partout : Raquel, Oscar, Marion, Martino... Merci pour ces bons, mais aussi mauvais moments passés ensemble, et pour que la distance ne soit jamais un obstacle à l'amitié J

A mes amis, ceux de ma ville d'adoption Grenoble :

-Au groupe d'italiens-espagnols : Xenia, Serena, Angel, Jaione, Leonardo, Raquel...
Merci pour les bons moments passés ensemble et que cela continue !! *En el mercado o donde haga falta...!!*

-A Juan (el traidor), pour son sens de l'humour et sa passion pour la musique, tous les deux très vrais.

-A Véro(nika), pour sa sympathie, sa créativité et son goût pour l'art qui m'ont marquée.

-A Pamela, parce que sa vision du monde et son courage m'ont toujours inspirée.
A Nina aussi.

-A Vero(nica), pour son amitié inconditionnelle, son optimisme vital et sa force intérieure. Bon courage pour ta fin de thèse *ñaña* !

-A Jose, pour son naturel, sa force, sa transparence, son humanité ... Mais aussi pour sa patience au téléphone ;)

A mon petit chat Abricot, parce que dans notre histoire je ne sais plus qui a aidé qui... 😊 Tu as été mon fidèle compagnon pendant les (longues) heures de rédaction du manuscrit !

A.M.A.G.

“There are essentially two things that will make you wise -- the books you read and the people you meet.” (Jack Canfield)

TABLE OF CONTENTS

Table des matières

TABLE OF CONTENTS.....	1
LIST OF TABLES	5
LIST OF FIGURES.....	7
NOMENCLATURE	13
INTRODUCTION.....	15
CHAPTER I: CONTEXT.....	21
1. THE FEEDSTOCK: LIGNOCELLULOSIC BIOMASS	23
1.1.. DEFINITION	23
1.2.. CONSTITUENTS AND STRUCTURE	23
1.3.. ELEMENTAL ANALYSIS	24
1.4.. CHEMICAL COMPOSITION.....	25
1.4.1. Cellulose	25
1.4.2. Hemicellulose	28
1.4.3. Lignin	30
1.4.4. Extractives	33
1.4.5. Ashes.....	34
2. THE PROCESS: TORREFACTION.....	35
2.1.. DEFINITION	35
2.2.. PRODUCTS	36
2.3.. MASS AND ENERGY BALANCES	37
2.1.. REACTIVITY OF BIOMASS	38
2.2.. PROPERTIES OF BIOMASS.....	39
2.3.. TECHNOLOGIES	39
3. THE FRAMEWORK: INVERTO PROJECT.....	41
4. OBJECTIVES.....	42
CHAPTER II: STATE-OF-THE-ART	43
1. INTRODUCTION.....	45
2. CHEMICAL EVOLUTION OF THE SOLID	45
2.1.. WHAT DOES CHEMICAL EVOLUTION OF THE SOLID STAND FOR?	45
2.2.. CHARACTERIZATION TECHNIQUES.....	45
2.2.1. Challenges of solid characterization during torrefaction.....	45

2.2.1.	<i>Comparison of characterization techniques</i>	46
2.2.1.	<i>Conclusion</i>	51
2.3.	¹³C SOLID-STATE NMR RESULTS DURING TORREFACTION	51
3.	PRODUCTION OF GASEOUS SPECIES	55
3.1.	ANALYSIS TECHNIQUES	55
3.1.1.	<i>Challenges in analysis of the gaseous phase obtained during biomass torrefaction at lab-scale</i>	55
3.1.2.	<i>Comparison of analysis techniques</i>	55
3.1.3.	<i>Conclusion</i>	59
3.2.	GC-MS RESULTS DURING TORREFACTION	59
4.	MODELLING OF TORREFACTION KINETICS	65
4.1.	TYPES OF MODELS	65
4.2.	MODELS OF SOLID DECOMPOSITION AND GASEOUS SPECIES FORMATION	66
4.2.1.	<i>Chemical species predicted</i>	66
4.2.2.	<i>Approach</i>	68
4.2.3.	<i>Experimental validation</i>	71
4.3.	CONCLUSION	72
	CHAPTER III: MATERIALS AND METHODS	75
1.	BIOMASSES	77
2.	COUPLING OF TGA-GC-MS	82
2.1.	THERMO-GRAVIMETRIC ANALYSIS (TGA)	83
2.1.1.	<i>Device description</i>	83
2.1.2.	<i>Experimental procedure</i>	83
2.1.3.	<i>Repeatability experiments</i>	85
2.2.	LOOPS STORAGE	86
2.2.1.	<i>Device description</i>	86
2.2.2.	<i>Experimental procedure</i>	87
2.3.	GAS CHROMATOGRAPH (GC)	89
2.3.1.	<i>Device description</i>	89
2.3.2.	<i>Experimental procedure</i>	89
2.4.	MASS SPECTROMETER (MS)	90
2.4.1.	<i>Device description</i>	90
2.4.2.	<i>Experimental procedure</i>	90
2.4.3.	<i>TGA-GC-MS data treatment</i>	91
3.	¹³C CP/MAS SOLID-STATE NMR	95
3.1.	DEVICE DESCRIPTION	95
3.2.	EXPERIMENTAL PROCEDURE	96

3.3.. SOLID-STATE NMR DATA TREATMENT	97
CHAPTER IV: EXPERIMENTAL RESULTS	99
1. INTRODUCTION	101
2. MASS LOSS OF SOLID	101
3. FORMATION OF CONDENSABLE SPECIES	108
3.1.. QUALITATIVE RESULTS	108
3.2.. QUANTITATIVE RESULTS	116
3.2.1. <i>Hydroxyacetone</i>	116
3.2.2. <i>Acetic acid</i>	119
3.2.3. <i>2-Furanmethanol</i>	122
3.2.4. <i>Eugenol</i>	124
3.2.5. <i>Isoeugenol</i>	126
3.3.. SEMI-QUANTITATIVE RESULTS	130
3.3.1. <i>Glycolaldehyde</i>	130
3.3.2. <i>Formic acid</i>	131
3.3.3. <i>Furfural</i>	133
3.3.4. <i>2-Methoxy-4-vinylphenol</i>	135
3.3.5. <i>Vanillin</i>	137
4. CHEMICAL EVOLUTION OF SOLID	141
4.1.. QUALITATIVE RESULTS	141
4.2.. QUANTITATIVE RESULTS	145
4.2.1. <i>Aromatics in lignin</i>	145
4.2.2. <i>C1 of cellulose</i>	147
4.2.3. <i>C4 and C6 of crystalline cellulose</i>	148
4.2.4. <i>C4 and C6 of amorphous cellulose</i>	150
4.2.5. <i>Methoxyl groups in lignin</i>	152
4.2.6. <i>Acetyl groups in hemicellulose</i>	154
5. SYNERGY OF RESULTS	157
5.1.. MASS LOSS AND CHEMICAL EVOLUTION OF THE SOLID	157
5.2.. PRODUCTION OF GASEOUS SPECIES AND CHEMICAL EVOLUTION OF THE SOLID	158
6. CONCLUSION	160
CHAPTER V: MODELLING	163
1. INTRODUCTION	165
2. APPROACH	165
3. PRODUCTS CONSIDERED	167
4. REACTION MECHANISMS	170
4.1.. CELLULOSE REACTIVITY	171

4.1.1.	<i>Decrystallization</i>	173
4.1.2.	<i>Dehydration</i>	173
4.1.3.	<i>Transglycosylation</i>	175
4.1.4.	<i>Depolymerization</i>	176
4.1.5.	<i>Fragmentation to form glycolaldehyde</i>	177
4.1.6.	<i>Fragmentation to form hydroxyacetone</i>	177
4.2..	HEMICELLULOSE REACTIVITY	178
4.2.1.	<i>Dehydration of C6 and C5 sugars</i>	180
4.2.2.	<i>Depolymerization of C6 and C5 sugars</i>	180
4.2.3.	<i>Fragmentation of acetyl groups</i>	181
4.2.4.	<i>Fragmentation of methoxyl groups</i>	181
4.2.5.	<i>Fragmentation of side chains to form formic acid</i>	182
4.2.6.	<i>Fragmentation of C6 and C5 sugars to form glycolaldehyde</i>	183
4.2.7.	<i>Fragmentation of carboxyl groups in C5 sugars</i>	183
4.2.8.	<i>Fragmentation of carbonyl groups in C6 sugars</i>	183
4.3..	LIGNIN REACTIVITY	184
4.3.1.	<i>Dehydration of alkyl chains</i>	186
4.3.2.	<i>Fragmentation of C_β-C_γ bonds</i>	186
4.3.3.	<i>Formation of eugenol</i>	186
4.3.4.	<i>Formation of 2-methoxy-4-vinylphenol</i>	187
4.3.5.	<i>Formation of vanillin</i>	188
5.	CONCLUSION	189
	CHAPTER VI: CONCLUSIONS AND PERSPECTIVES	191
	BIBLIOGRAPHY	197

LIST OF TABLES

Table 1. Proximate analysis of different biomasses (Castellano et al., 2015).	25
Table 2. Comparison of properties between raw and torrefied wood (Kiel, 2012).	39
Table 3. Main technologies of torrefaction (Casajus et al., 2012; Nocquet, 2012).	40
Table 4. Characterization techniques of biomass solid phase during torrefaction.	47
Table 5. Quantitative characterization through ¹³ C DP/MAS solid-state NMR of the raw and torrefied biomass (Park et al., 2013b).	54
Table 6. Analytical techniques used to detect condensable species during biomass torrefaction. .	56
Table 7. Identification of condensable species produced during biomass torrefaction by GC-MS..	61
Table 8. Mean yields (mg/g biomass) of the main condensable species produced in ash-wood torrefaction at different temperatures (Lê Thành et al., 2015).	62
Table 9. Comparison of chemical species predicted by models.	67
Table 10. Comparison of models which predict solid decomposition and formation of gaseous species during biomass torrefaction.	74
Table 11. Biomasses chemical properties and elemental analysis.	79
Table 12. Sugars composition in hemicellulose analysis.	80
Table 13. Helium properties in Chromatostock loops.	91
Table 14. Signal assignments for solid-state NMR spectra of biomasses.	96
Table 15. Condensable species produced during torrefaction of pine.	112
Table 16. Condensable species produced during torrefaction of ash-wood.	113
Table 17. Condensable species produced during torrefaction of miscanthus.	114
Table 18. Condensable species produced during torrefaction of wheat straw.	115
Table 19. Proportion of hydroxyacetone in the overall formation at each temperature.	118
Table 20. Comparative formation of hydroxyacetone (mg/g initial biomass).	119
Table 21. Proportion of acetic acid in the overall formation at each temperature.	121
Table 22. Comparative formation of acetic acid (mg/g initial biomass).	121
Table 23. Proportion of 2-furanmethanol in the overall formation at each temperature.	123
Table 24. Comparative formation of 2-furanmethanol (mg/g initial biomass).	123
Table 25. Proportion of eugenol in the overall formation at each temperature.	126
Table 26. Proportion of isoeugenol in the overall formation at each temperature.	128
Table 27. Comparative formation of isoeugenol (mg/g initial biomass).	128
Table 28. Synthesis of the quantitative analysis of condensable species formation.	129
Table 29. Proportion of glycolaldehyde in the overall formation at each temperature.	131
Table 30. Proportion of formic acid in the overall formation at each temperature.	133
Table 31. Proportion of furfural in the overall formation at each temperature.	135
Table 32. Proportion of 2-methoxy-4-vinylphenol in the overall formation at each temperature. ...	137
Table 33. Proportion of vanillin in the overall formation at each temperature.	139
Table 34. Synthesis of the semi-quantitative analysis of condensable species formation.	140

Table 35. Crystallinity index of the four biomasses.....	147
Table 36. Synthesis of quantitative characterization of the solid phase.	156
Table 37. Synthesis of original experimental results from TGA-GC-MS and solid-state NMR.	162
Table 38. Reactants in torrefaction mechanisms.	166
Table 39. Gaseous species considered as products in reaction mechanisms.	168
Table 40. Gaseous species considered as products in reaction mechanisms (continued).	169
Table 41. Reaction mechanisms of cellulose degradation.....	172
Table 42. Reaction mechanisms of hemicellulose degradation.....	179
Table 43. Reaction mechanisms of lignin degradation.	185

LIST OF FIGURES

Fig. 1. Global energy demand in 2011 (left) (IEA, 2013) and detail of biomass feedstock potentially available (right) (IEA, 2012).	17
Fig. 2. Principal processes, intermediate energy carriers and final products in thermochemical conversion of biomass (McKendry, 2002).	18
Fig. 3. Lignin-polysaccharide network in lignocellulosic biomass (Tsubaki and Azuma, 2011).	24
Fig. 4. Representation of the linear chain of cellulose (Vermerris and Abril, 2015).	26
Fig. 5. Cellulose content for several woody and non-woody biomasses (Da Silva Perez et al., 2015).	26
Fig. 6. Cellulose structure at different levels of aggregation (website of JRS, J. RETTENMAIER & SÖHNE group).	27
Fig. 7. Cellulose allomorphs (Kaplan, 1998).	28
Fig. 8. Structure of hemicellulose (Ochoa-Villarreal et al., 2012).	28
Fig. 9. Main sugar monomers in hemicellulose (Hansen and Plackett, 2008).	29
Fig. 10. Hemicellulose content for several woody and non-woody biomasses (Da Silva Perez et al., 2015).	29
Fig. 11. Model of lignin structure: in blue, syringyl (S unit); in green, guaiacyl (G unit); in red, <i>p</i> -hydroxyphenol (H unit) (Lupoi et al., 2015).	31
Fig. 12. Lignin monomers: in blue, sinapyl alcohol; in green, coniferyl alcohol; in red, <i>p</i> -coumaryl alcohol (Lupoi et al., 2015).	32
Fig. 13. Lignin content for several woody and non-woody biomasses (Da Silva Perez et al., 2015).	32
Fig. 14. Common monoterpenoids in biomass: (1) β -myrcene, (2) limonene, (3) β -phellandrene, (4) α -pinene, (5) β -pinene, (6) 3-carene, (7) borneol, (8) bornyl acetate, and (9) β -thujaplicin (Sjostrom, 1993).	33
Fig. 15. Extractives content for several woody and non-woody biomasses (Da Silva Perez et al., 2015).	34
Fig. 16. Ashes content for several woody and non-woody biomasses (Da Silva Perez et al., 2015).	35
Fig. 17. Evolution of an ash-wood sample during torrefaction. From left to right: raw biomass, and biomass torrefied at 250, 280 and 300°C under the same conditions (Lê Thành et al., 2015).	36
Fig. 18. Mass balance of products during torrefaction of several biomasses (Commandré and Leboeuf, 2015).	37
Fig. 19. Typical mass and energy balances of biomass torrefaction (Bergman et al., 2005).	38
Fig. 20. NIRS spectra of raw and torrefied beech at 220, 250 and 280°C for 1h (Rousset et al., 2011).	49
Fig. 21. FTIR spectra of torrefied pine at 240, 280 and 320°C (Zheng et al., 2012).	49

Fig. 22. ¹³ C CP/MAS solid-state NMR spectra of raw and torrefied samples of beech wood (Melkior et al., 2012).	50
Fig. 23. Mass loss, gaseous species produced and reaction mechanisms of beech torrefaction versus temperature (Melkior et al., 2012).	54
Fig. 24. GC-MS chromatogram of the gaseous phase produced during torrefaction of poplar sawdust at 230°C for 15 min (Candelier et al., 2011).	58
Fig. 25. Relative intensity obtained by GC-MS analysis of the major molecules produced during torrefaction of aspen for 90 min (Klinger et al., 2013).	58
Fig. 26. Mass balance of the main condensable species obtained after torrefaction of four biomasses at 250°C for 45 min (Commandré and Leboeuf, 2015).	64
Fig. 27. Torrefaction scheme adapted from Ranzi et al. (2008) (Anca-Couce et al., 2014).	69
Fig. 28. Kinetic scheme of biomass torrefaction proposed by Di Blasi and Lanzetta (1997).	70
Fig. 29. Principle of the kinetic model developed for biomass torrefaction by Nocquet et al. (2014b).	71
Fig. 30. The four biomasses: pine chips on the top left; ash-wood chips on the top right; miscanthus pellets on the bottom left; and wheat straw pellets on the bottom right.	78
Fig. 31. TGA-GC-MS device.	82
Fig. 32. TGA-GC-MS scheme.	82
Fig. 33. TGA scheme.	83
Fig. 34. Three-staged crucible for TGA torrefaction.	84
Fig. 35. Compared evolution of mass loss for ash-wood samples in a three-staged and a simple crucible.	86
Fig. 36. Chromatostock loops storage scheme.	87
Fig. 37. Sampling temperatures in TGA-GC-MS experiments.	88
Fig. 38. Temperature profile in the GC column.	90
Fig. 39. Production of isoeugenol during torrefaction of ash-wood.	93
Fig. 40. Production of 2-methoxy-4-vinylphenol during torrefaction of pine.	94
Fig. 41. Solid-state NMR device.	95
Fig. 42. Mass loss evolution of the four biomasses during dynamic torrefaction.	102
Fig. 43. Reaction rate evolution of the four biomasses during dynamic torrefaction.	103
Fig. 44. Mass loss evolution of the four biomasses during isothermal torrefaction.	105
Fig. 45. Reaction rate evolution of the four biomasses during isothermal torrefaction.	106
Fig. 46. Mass loss of several biomasses during torrefaction under isothermal conditions (T = 280°C, t = 2h, heating rate = 30°C/min) (Dupont et al., 2011).	108
Fig. 47. Production of hydroxyacetone during torrefaction.	117
Fig. 48. Production of acetic acid during torrefaction.	120
Fig. 49. Production of 2-furanmethanol during torrefaction.	122
Fig. 50. Production of eugenol during torrefaction.	125
Fig. 51. Production of isoeugenol during torrefaction.	127
Fig. 52. Production of glycolaldehyde during torrefaction.	130

Fig. 53. Production of formic acid during torrefaction.	132
Fig. 54. Production of furfural during torrefaction.	134
Fig. 55. Production of 2-methoxy-4-vinylphenol during torrefaction.	136
Fig. 56. Production of vanillin during torrefaction.	138
Fig. 57. Solid-state NMR spectra of pine samples: raw and torrefied at 200, 220, 240, 260, 280 and-300°C.	142
Fig. 58. Solid-state NMR spectra of ash-wood samples: raw and torrefied at 200, 220, 240, 260, 280 and-300°C.	143
Fig. 59. Solid-state NMR spectra of miscanthus samples: raw and torrefied at 200, 220, 240, 260, 280 and-300°C.	144
Fig. 60. Solid-state NMR spectra of wheat straw samples: raw and torrefied at 200, 220, 240, 260, 280 and-300°C.	145
Fig. 61. Evolution of the proportion of aromatics in lignin during torrefaction.	146
Fig. 62. Evolution of the proportion of C1 of cellulose during torrefaction.	148
Fig. 63. Evolution of the proportion of C4 of crystalline cellulose during torrefaction.	149
Fig. 64. Evolution of the proportion of C6 of crystalline cellulose during torrefaction.	149
Fig. 65. Evolution of the proportion of C4 of amorphous cellulose during torrefaction.	151
Fig. 66. Evolution of the proportion of C6 of amorphous cellulose during torrefaction.	152
Fig. 67. Evolution of the proportion of methoxyl groups in lignin during torrefaction.	153
Fig. 68. Evolution of the proportion of acetyl groups in hemicellulose during torrefaction.	155
Fig. 69. TGA-GC-MS and solid-state NMR synergy for pine.	159
Fig. 70. TGA-GC-MS and solid-state NMR synergy for ash-wood.	159
Fig. 71. TGA-GC-MS and solid-state NMR synergy for wheat straw.	160
Fig. 72. Van Krevelen diagram of chars.	171
Fig. 73. Intra-ring dehydration of cellulose: (a) enol form of anhydrocellulose, (b) keto form of anhydrocellulose, (c) transglycosylation to form a levoglucosan chain-end, (d) hydroxyl glucosidic chain-end, (e) unsaturation on the glucosidic chain-end, (f) elimination of water on C6, (g) formation of a vinylene group (Scheirs et al., 2001).	175

Abstract: The objective of the present work is to better understand chemical evolution of both solid and gaseous phases during torrefaction of various biomasses. Torrefaction experiments were carried out with a dynamic profile of temperatures between 200 and 300°C, under inert atmosphere, for pine, ash-wood, miscanthus and wheat straw. Mass loss and formation of condensable species were analyzed by TGA-GC-MS, and chemical evolution of solid phase was characterized by ¹³C CP/MAS solid-state NMR. Thirty condensable species could be detected; a half of these species were formed during the whole temperature range, and a third were formed by all biomass types. The main phenomena that occurred in solid phase were found to be decrystallization of cellulose, severe degradation of hemicellulose, devolatilization of acetyl groups, conservation of methoxyl groups and charring. It was also found that mass loss and chemical evolution of solid were not directly correlated for different biomasses. Based on the experimental results, a conceptual model was developed to describe biomass degradation during torrefaction. Thirty reactions were determined for the three major macromolecular constituents, namely cellulose, hemicellulose – represented by C5 and C6 sugars – and lignin – represented by H, G and S units. The main innovations of this model are in the detailed approach of hemicellulose and lignin compositions, as well as in the prediction of sixteen condensable and five permanent species, and six forms of solid char, through chemically meaningful and stoichiometrically valid reactions.

Keywords: biomass, torrefaction, reaction mechanisms, Thermogravimetric Analysis–Gas Chromatography–Mass Spectrometry, solid-state Nuclear Magnetic Resonance

Résumé : L'objectif des travaux est de mieux comprendre durant la torréfaction de différentes biomasses l'évolution chimique à la fois des phases solide et gaz. Des expériences de torréfaction ont été menées selon un profil de température dynamique entre 200 et 300°C, sous atmosphère inerte, sur du pin, du frêne, du miscanthus et de la paille de blé. La perte de masse et la formation des espèces condensables ont été analysées par ATG-GCMS, et l'évolution chimique de la phase solide par RMN du solide ¹³C CP/MAS. Trente espèces condensables ont été détectées ; la moitié a été formée dans l'ensemble de la gamme de température explorée et un tiers l'a été par toutes les biomasses. Les principaux phénomènes qui semblent associés à la dégradation du solide sont la décrystallisation de la cellulose, une sévère dégradation de l'hémicellulose, la dévolatilisation des groupes acétyles, la conservation des groupes méthoxys et la formation d'un résidu solide. Il a été par ailleurs montré que perte de masse et évolution chimique du solide n'étaient pas directement corrélées pour différentes biomasses. A partir de ces résultats expérimentaux, un modèle conceptuel a été développé pour décrire la dégradation de la biomasse. Trente réactions ont été associées aux trois constituants macromoléculaires principaux que sont la cellulose, l'hémicellulose et la lignine, respectivement représentées par deux sucres en C5 et C6 et par trois unités de type H, G et S. Ce modèle présente l'originalité de s'appuyer sur une description détaillée de ces deux derniers constituants et de prévoir la formation de seize espèces condensables, cinq gaz permanents et six formes de char solide, grâce à des réactions ayant un sens chimique et équilibrées d'un point de vue stœchiométrique.

Mots-clés : biomasse, torréfaction, mécanismes réactionnels, Analyse Thermogravimétrique-Chromatographie Phase Gaz–Spectrométrie de Masse, Résonance Magnétique Nucléaire solide

NOMENCLATURE

ASE	Accelerated Solvent Extractor	
Bi	Biot number	no unit
CP/MAS	Cross-Polarization/Magic Angle Spinning	
DGP	1,4:3,6-dianhydro- α -D-glucopyranose	
EI	Electron Ionization	
G	gram	
GC	Gas Chromatograph	
GJ	gigajoule	
H	hour	
HHV	High Heating Value	MJ/kg
INVERTO	INnovation in VEgetal chemistRy by TOrrrefaction	
Kg	kilogram	
L	liter	
LAC	3,6-dioxabicyclo[3.2.1]octan-2-one,1-hydroxy-,(1R)	
m ³	cubic meter	
mg	milligram	
min	minute	
mL	milliliter	
MJ	megajoule	
MS	Mass Spectrometer	
NMR	Nuclear Magnetic Resonance	
ppm	part per million	
Py'	extern Pyrolysis number	no unit
Re	Reynolds number	no unit
S	second	
T	tone	
T	temperature	°C
TGA	Thermo-Gravimetric Analysis	
W	weight of biomass	% (mass)
wmf	weight moisture-free of biomass	% (mass)
wmfh	weight moisture-free of hemicellulose	% (mass)
°C	degree Celsius	
μ g	microgram	
μ L	microliter	

INTRODUCTION

The global energy demand and the related greenhouse gas emissions due to the use of fossil energy sources, keep on increasing worldwide. This context encourages the development of renewable sources of energy, such as solar, wind, biomass, tidal and geothermal. These renewable sources constitute an alternative to the fossil sources, such as crude oil, natural gas and coal. Among the renewable options, biomass is the only source which is able to produce both energy and chemicals (van der Stelt et al., 2011). Today, renewable energy represents 13% of the global energy consumption, in which energy biomass sources – also called bioenergy – represent 10% (see Fig. 1) (Ho et al., 2014). In the future, various biomass feedstock are expected to contribute to this bioenergy (see Fig.1), with an increasing part constituted of residues from forestry and agriculture as well as of lignocellulosic crops.

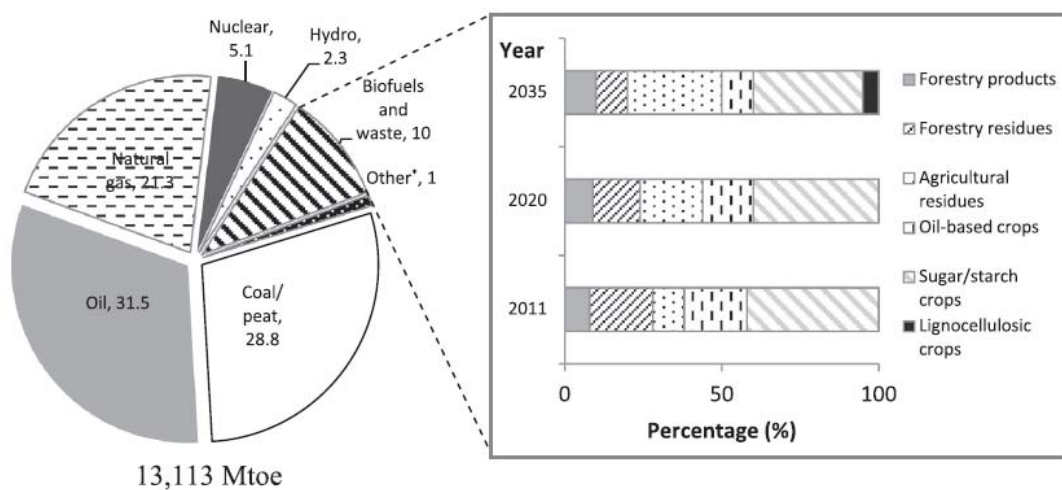


Fig. 1. Global energy demand in 2011 (left) (IEA, 2013) and detail of biomass feedstock potentially available (right) (IEA, 2012).

Bioenergy can be mainly obtained through two routes: thermochemical and biochemical conversion. Generally speaking, thermochemical route relies on the heating of biomass, while biochemical route involves the use of bacteria, microorganisms and enzymes. Thermochemical conversion seems to be a promising route complementary to biochemical route, as it can convert all biomass constituents, whereas biochemical route focuses on carbohydrates.

Thermochemical conversion of dry biomass mainly includes combustion, gasification and pyrolysis processes. They basically differentiate in the atmosphere applied, as combustion is carried out under excess of air, gasification under steam, CO₂ or default of air and pyrolysis in the absence of air. Furthermore, the three processes are associated to different final “products”: combustion only leads to heat and power, while gasification and pyrolysis also offer routes to obtain chemicals and fuels. Fig. 2 shows a scheme of the three thermochemical conversion processes, as well as the intermediate and final products.

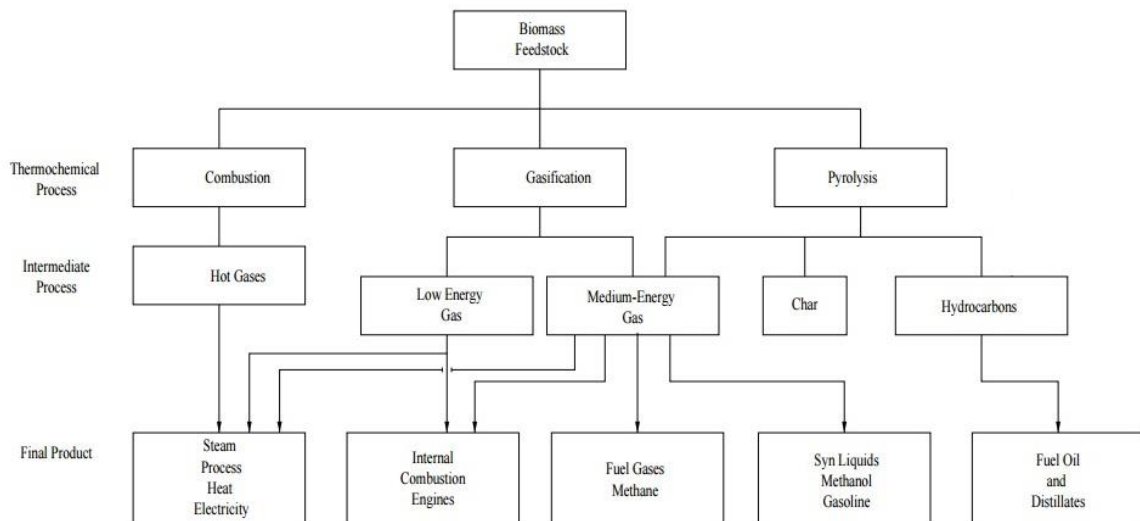


Fig. 2. Principal processes, intermediate energy carriers and final products in thermochemical conversion of biomass (McKendry, 2002).

In view of biomass thermochemical conversion industrial implementation, some of the physical and chemical properties of biomass can turn out to be problematic, in particular its high oxygen content, its high moisture content, its low density, its fibrous structure and its heterogeneous composition among tissues. Indeed, these properties decrease process efficiency and raise both technical and economic difficulties at the stages of collection, storage and transportation. Several pretreatment methods have been developed to counterbalance these disadvantages, and can be classified as thermal (e.g. torrefaction, drying) or mechanical (e.g. grinding, pelletizing). Under the

pretreatment operating conditions (temperature, pressure...), significant structural and chemical changes occur in biomass (Chen et al., 2015; Sierra et al., 2008; van der Stelt et al., 2011).

The present work focuses on the understanding of the pretreatment by torrefaction. Torrefaction is a mild thermal treatment whose severity is intermediate between drying and pyrolysis. It is carried out at temperatures within the interval of 200-300°C, under atmospheric pressure and in absence of oxygen. Torrefaction gives rise to a solid product, which is the torrefied biomass, and gaseous by-products, which are condensable species, such as water and acetic acid, and non-condensable species, mainly carbon dioxide and carbon monoxide. During torrefaction, the torrefied solid acquires mechanical and energy properties between coal and raw biomass, e.g. brown color, lower H/C and O/C ratios, hydrophobicity, increased energy density as well as improved grindability and flowability. These properties enhance biomass suitability for further combustion or gasification processes (Fisher et al., 2012). The torrefaction condensable by-products have been traditionally either burnt to obtain energy or removed as waste but may also be in a more innovative way chemically recovered as high added value green molecules, as tested in the frame of the collaborative French National Research Agency project associated to this PhD thesis, namely the INVERTO project.

Thereby, the objective of the present work is to contribute to better understand the chemical evolution of the solid product and the gaseous by-products formed during biomass torrefaction.

The manuscript is divided into six chapters, which are presented hereafter:

- Chapter I exposes the context of this work and describes the feedstock, the process, the framework and the objectives of the present work;
- Chapter II discusses the state-of-the-art on chemical evolution of the solid phase, production of gaseous species and modelling of biomass torrefaction;
- Chapter III refers to materials and methods employed in the present work, and describes biomasses investigated, as well as TGA-GC-MS and ^{13}C CP/MAS solid-state NMR devices;

- Chapter IV presents the experimental results from the present work, including mass loss of the solid, formation of condensable species, characterization of the solid, and the synergy potential between these results;
- Chapter V describes a conceptual model of biomass torrefaction founded on the experimental results obtained in the present work and on literature;
- Chapter VI draws out general conclusions from the study in relation with the objectives defined in Chapter I. To end, perspectives for future work both in short and long-terms are proposed.

CHAPTER I: CONTEXT

1. THE FEEDSTOCK: LIGNOCELLULOSIC BIOMASS

1.1. DEFINITION

The term “lignocellulosic biomass” refers to all vegetal matter existing on Earth. This includes wood, plants, agricultural products and vegetal wastes.

1.2. CONSTITUENTS AND STRUCTURE

Lignocellulosic biomass is mainly constituted by cellulose, hemicellulose and lignin. Crystalline cellulose fibers constitute the core of the complex lignocellulosic structure. Amorphous cellulose and hemicellulose are positioned among the fibrils of crystalline cellulose, and oriented in the same direction. Lignin plays a structural role by forming a matrix in which cellulose and hemicellulose are inserted (see Fig. 3) (Faulon et al., 1994; Sjostrom, 1993).

Lignocellulosic biomass also contains a minor proportion of water, extractives and ashes, which do not exercise a significant structural role (Raven et al., 1992).

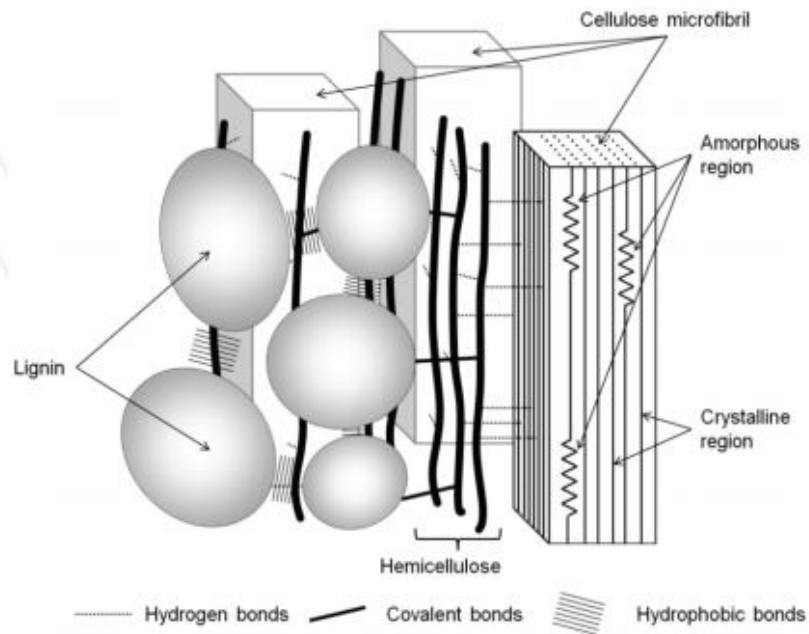


Fig. 3. Lignin-polysaccharide network in lignocellulosic biomass (Tsubaki and Azuma, 2011).

1.3. ELEMENTAL ANALYSIS

Elemental composition of biomass includes carbon, hydrogen and oxygen, which are major elements in biomass, as well as nitrogen, chlorine and sulfur, which are minor elements in biomass.

The work of Da Silva Perez et al. (2015) has investigated the elemental composition of several woody biomasses – beech, spruce, poplar and eucalyptus – and non-woody biomasses – wheat straw, triticale, fescue, miscanthus and switchgrass. Results have shown that the contents in carbon and hydrogen are very similar for all the biomasses. Regarding oxygen content, non-woody biomasses contain slightly less oxygen than woody biomasses. This is mainly due to differences in ash content. However, oxygen is calculated by difference, therefore this conclusion has to be taken with caution. The contents in nitrogen and chlorine are higher for non-woody biomasses than for woody biomasses. Chlorine content is higher for agricultural co-products (0.32%w), and wheat

straw, which is also an agricultural co-product, presents the highest sulfur content (0.16%w).

1.4. CHEMICAL COMPOSITION

The chemical composition of lignocellulosic biomass strongly depends on its source. Cellulose presents the same elemental composition in every biomass, whereas the compositions of hemicellulose and lignin vary among biomasses (Sjostrom, 1993). The proportions of the main biomass constituents vary significantly as a function of biomass species. These variations are significant for all constituents, except cellulose (see Table 1).

Table 1. Proximate analysis of different biomasses (Castellano et al., 2015).

Biomass	Unit	Cellulose	Hemicellulose	Lignin	Extractives	Ashes
Pine	%	23.56	44.16	28.46	6.00	0.96
Eucalyptus		19.15	34.33	30.31	6.85	2.83
Oak		21.94	36.44	24.44	5.32	3.10
Vine shoots		19.66	32.38	24.87	9.24	4.11
Poplar 1		20.33	42.65	25.19	4.62	2.79
Poplar 2		20.81	37.62	27.48	5.17	1.73
Oats		24.53	26.86	10.59	30.87	6.12
Triticale		20.86	34.75	11.07	29.39	6.88
Rice		24.08	37.09	13.82	13.98	12.35

1.4.1. Cellulose

Cellulose is a homopolysaccharide composed of D-glucopyranose monomers linked by $\beta(1\rightarrow4)$ -glycosidic bonds, with cellobiose as the repeating unit (see Fig. 4). The chemical formula of cellulose can be represented by $(C_6H_{10}O_5)_n$. The nature of the glycosidic bonds between glucose monomers leads to an arrangement in linear chains (Harmsen et al., 2010). In addition, since hydroxyl groups are distributed on both sides of the glucose chains, cellulose has a strong tendency to form intramolecular and intermolecular hydrogen bonds (Sjostrom, 1993).

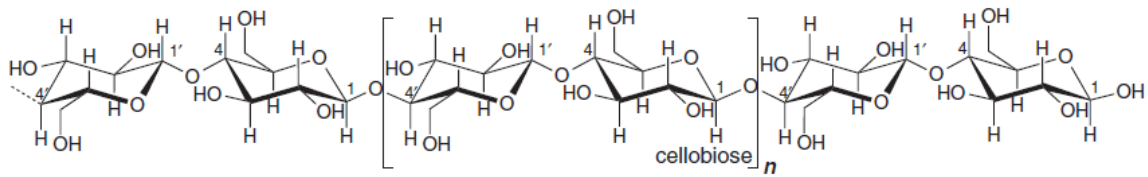


Fig. 4. Representation of the linear chain of cellulose (Vermerris and Abril, 2015).

Cellulose proportion in woody biomass is, in average, higher than in non-woody biomass. In the work of Da Silva Perez et al. (2015), cellulose content in woody biomasses tested ranges between 39 and 50%w, whereas for non-woody biomasses cellulose content is lower, between 27 and 30%w (see Fig. 5).

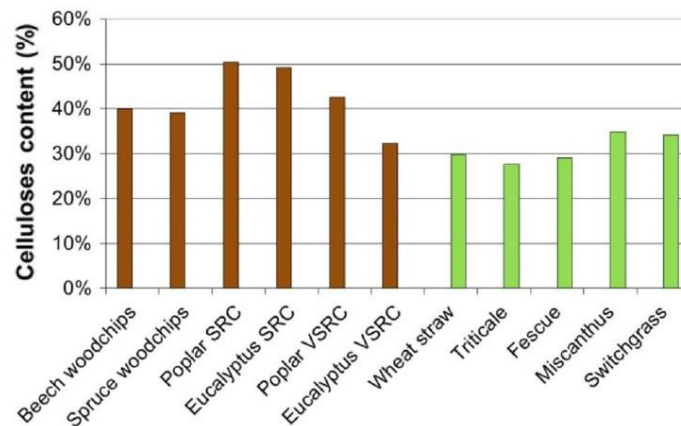


Fig. 5. Cellulose content for several woody and non-woody biomasses (Da Silva Perez et al., 2015).

Regarding cellulose structure, bundles of cellulose molecules aggregate to form micro-fibrils. Then, micro-fibrils build up macro-fibrils and, finally, they constitute fibers (see Fig. 6). As a consequence of this fibrous structure, cellulose has a high tensile strength and is insoluble in most solvents (Sjostrom, 1993). Besides, many properties of cellulose depend on its degree of polymerization, that is to say, the number of glucose

monomers which composes one cellulose polymer. The cellulose degree of polymerization depends on biomass species. It can extend to 17000, although it commonly ranges from 3000 to 10000 monomers (Kirk-Otmer, 2001).

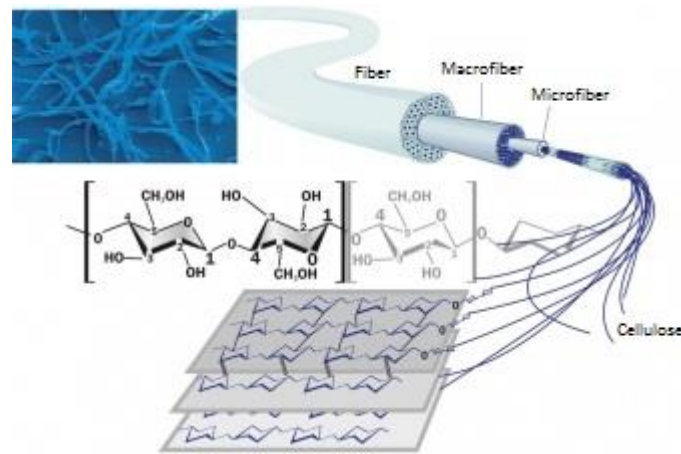


Fig. 6. Cellulose structure at different levels of aggregation (website of JRS, J. RETTENMAIER & SÖHNE group).

Inside the various fibrils of the cellulose macro-polymer, highly ordered regions – crystalline regions – alternate with less ordered ones – amorphous regions. Within crystalline regions, four different crystalline arrangements, the so-called allomorphs, have been identified (see Fig. 7):

- Cellulose I is the most abundant form found in nature, although its structure is not completely known due to its high complexity. The structure of cellulose I is a mixture of two crystalline forms: celluloses I_α and I_β. The proportions of these celluloses vary as a function of biomass species;
- Cellulose II can be obtained either by mercerization, which is an alkali treatment, or by regeneration, consisting of solubilization followed by recrystallization;
- Celluloses III_I and III_{II} can be formed from celluloses I and II, respectively, by treatment with liquid ammonia, and the reaction is reversible;
- Celluloses IV_I and IV_{II} can be obtained by heating celluloses III_I and III_{II}, respectively (Park et al., 2010).

biomass species (Sjostrom, 1993). In softwood hemicellulose, the main sugar structures are galactoglucomannan, arabinoglucuronoxylan and arabinogalactan. In hardwood hemicellulose, the main sugar structures are glucuronoxylan and glucomannan.

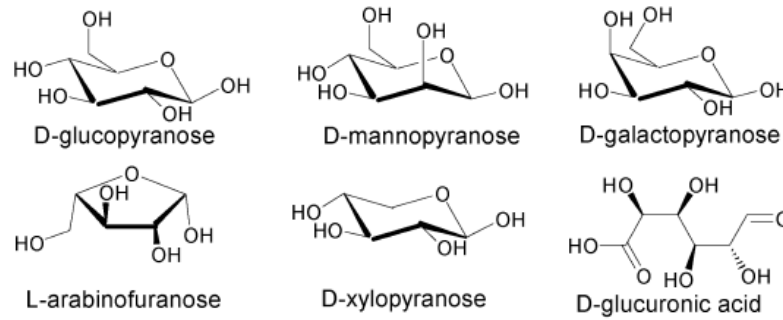


Fig. 9. Main sugar monomers in hemicellulose (Hansen and Plackett, 2008).

Hemicellulose proportion in non-woody biomasses is higher than in woody biomasses. In the work of Da Silva Perez et al. (2015), hemicellulose content in woody biomasses tested is of 22-33%w, whereas for non-woody biomasses hemicellulose content is of 31-38%w (see Fig. 10).

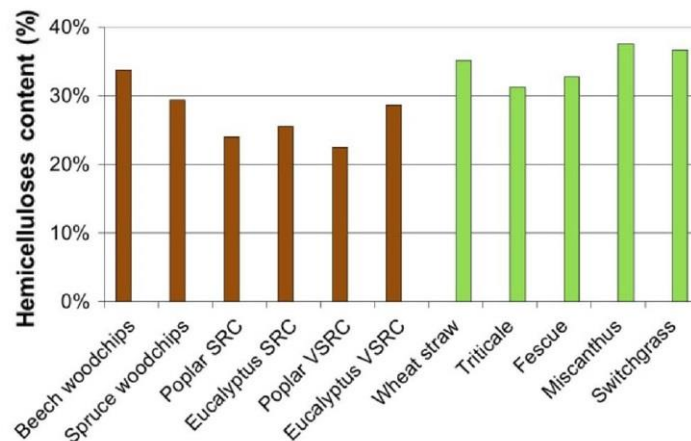


Fig. 10. Hemicellulose content for several woody and non-woody biomasses (Da Silva Perez et al., 2015).

The structure of hemicellulose is amorphous, mainly due to the highly branched structure and the presence of acetyl groups linked to the polymer. In contrast to cellulose, which is a long polymer, the degree of polymerization in hemicellulose reaches a maximum of 200 monomers. Hence hemicellulose is a relatively short polymer (Harmsen et al., 2010).

1.4.3. Lignin

Lignin is a heteropolymer with a very complex structure. Today, this structure is still not fully understood, yet some models have been proposed (see Fig. 11 for an example). The average chemical formula of lignin could be represented by $[C_9H_{10}O_3 \cdot (OCH_3)_{0.9-1.7}]_n$ (Chen and Kuo, 2011).

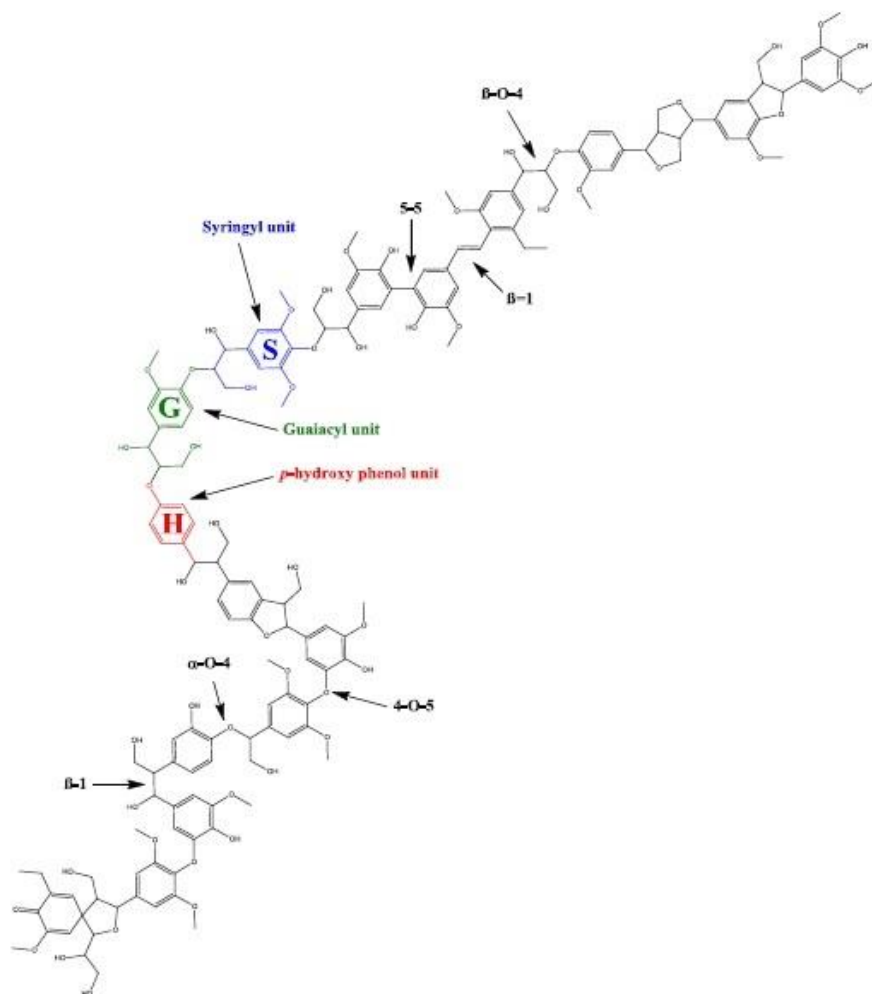


Fig. 11. Model of lignin structure: in blue, syringyl (S unit); in green, guaiacyl (G unit); in red, *p*-hydroxyphenol (H unit) (Lupoi et al., 2015).

Lignin is mainly composed of three phenylpropane monomers: sinapyl alcohol, coniferyl alcohol and *p*-coumaryl alcohol. Their respective phenylpropanoid units are: syringyl – usually represented as S unit –, guaiacyl – represented as G unit – and *p*-hydroxyphenol – represented as H unit. These three structures are constituted by the same phenylpropanoid skeleton, but they possess different degrees of oxygen-substitution on the phenyl ring. The H-unit consists of a 4-hydroxyphenyl ring, the G-unit has one hydroxyl group and one methoxyl group, and the S-unit has two methoxyl groups and one hydroxyl group (Banoub et al., 2015) (see Fig. 12). Three types of ether bonds link lignin units: β -aryl, diaryl and glyceraldehyde aryl (Tsubaki and Azuma, 2011).

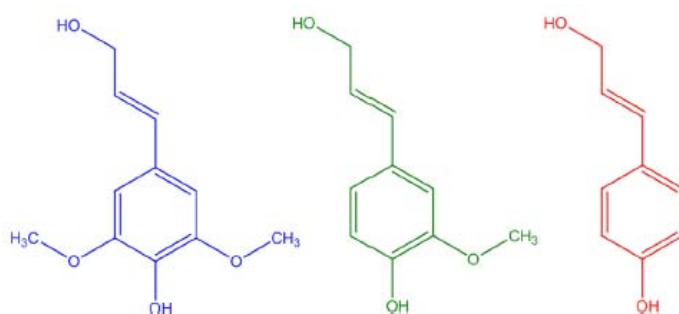


Fig. 12. Lignin monomers: in blue, sinapyl alcohol; in green, coniferyl alcohol; in red, *p*-coumaryl alcohol (Lupoi et al., 2015).

Lignin composition changes depending on biomass species, like hemicellulose. Softwood lignin mainly contains G units and to a less extent H units, while hardwood lignin is mainly composed of S units, and to a less extent of G units. In cereal crops, lignin is constituted by equivalent amounts of G and S units, whereas perennial crops are mostly constituted of H units (Banoub et al., 2015; Ragauskas, A.J., 2008).

Lignin proportion in woody biomass is, in average, higher than in non-woody biomass. In the work of Da Silva Perez et al. (2015), lignin content in woody biomasses tested is of 20-29%w, whereas for non-woody biomasses lignin content is of 17-23%w (see Fig. 13).

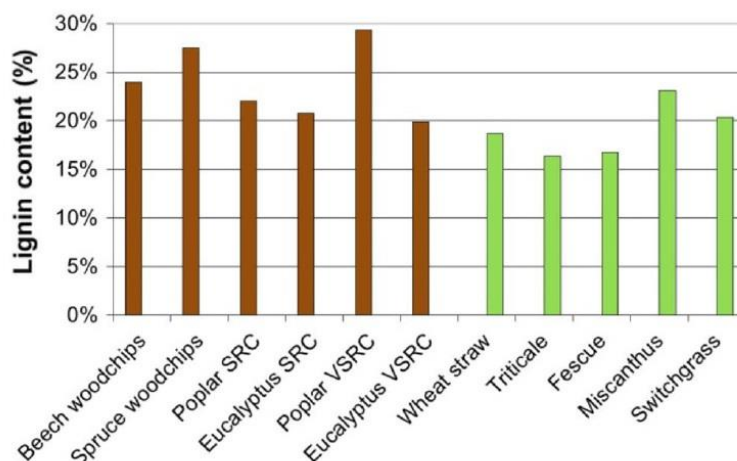


Fig. 13. Lignin content for several woody and non-woody biomasses (Da Silva Perez et al., 2015).

The measurement of lignin polymerization degree presents a high complexity, since lignin tends to fragment during its extraction from biomass structure. Bibliographic works have reported values of polymerization degree for lignin between 1000 and 20000 monomers (Banoub et al., 2015).

1.4.4. Extractives

Lignocellulosic biomass contains a small and variable amount of non-structural constituents which can be extracted by solvents, the so-called extractives (see Fig. 14 for some examples). The extractives fraction includes small molecules, like lipids, phenolic compounds, terpenoids, fatty acids, resin acids, steryl esters, sterol and waxes, but also heavier molecules, like soluble sugars and starch.

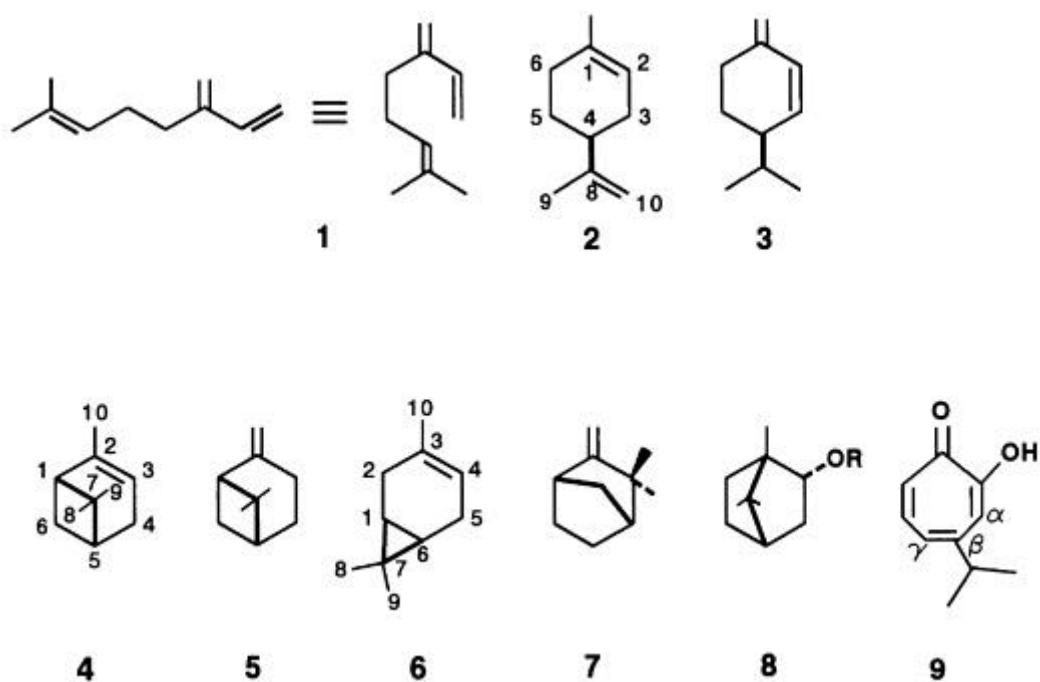


Fig. 14. Common monoterpenoids in biomass: (1) β -myrcene, (2) limonene, (3) β -phellandrene, (4) α -pinene, (5) β -pinene, (6) 3-carene, (7) borneol, (8) bornyl acetate, and (9) β -thujaplicin (Sjostrom, 1993).

In the work of Da Silva Perez et al. (2015), the extractives content in woody biomasses tested vary between 1 and 8%w, whereas values extend to 25%w for non-

woody biomasses (see Fig. 15). The reason for the high extractives content in non-woody biomasses may be due to the presence of soluble sugars and starch, whereas extractives content in woody biomasses is linked to “classic” extractives with low molecular mass (Da Silva Perez et al., 2015; Dorado et al., 2000).

Although extractives are in minor proportion in biomass, they can have an influence on biomass characteristics, such as wood strength or color. In some cases, extractives may even be toxic (Shebani et al., 2008).

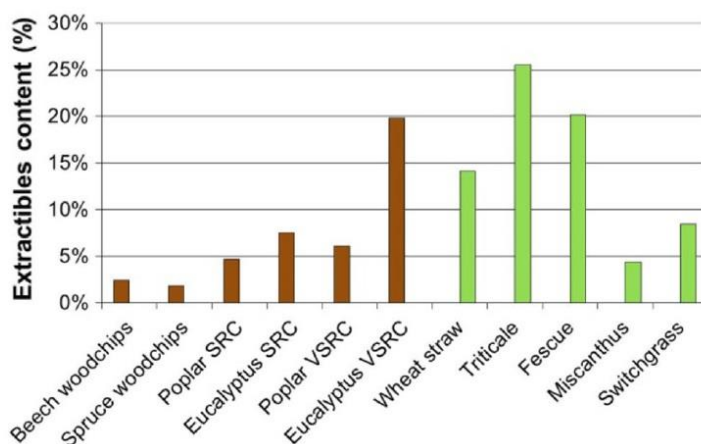


Fig. 15. Extractives content for several woody and non-woody biomasses (Da Silva Perez et al., 2015).

1.4.5. Ashes

Lignocellulosic biomass contains a low amount of inorganic matter, mostly found in ashes. They originate from salts deposited in cell walls, mainly under the form of metal salts. These salts can be carbonates, silicates, oxalates or phosphates. Different metal ions are contained in metal salts, and their presence and proportion depend on biomass type. In woody biomasses, the most abundant metal ions are calcium, potassium and magnesium. In non-woody biomasses, the most abundant metal ions are silicon, potassium and calcium. These metals can be either partially bound to the acetyl groups in xylan or held by biomass constituents through complexing forces (Sjostrom, 1993).

Ash content in woody biomasses is usually lower than in non-woody biomasses. In the work of Da Silva Perez et al. (2015), ashes content in woody biomasses tested represent between 1 and 4%w, while in non-woody biomasses ashes content represent between 3 and 9%w (see Fig. 16) (Da Silva Perez et al., 2015).

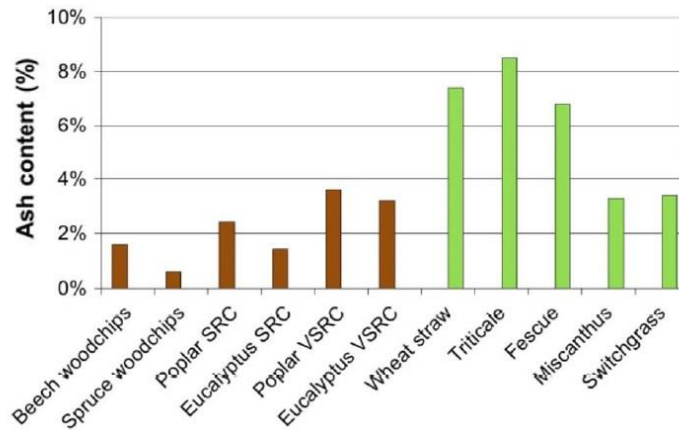


Fig. 16. Ashes content for several woody and non-woody biomasses (Da Silva Perez et al., 2015).

2. THE PROCESS: TORREFACTION

2.1. DEFINITION

Torrefaction is a thermal pretreatment of biomass carried out between 200 and 300°C, under atmospheric pressure and in absence of oxygen.

Biomass loses relatively more oxygen and hydrogen than carbon during torrefaction, which makes biomass acquire lower H/C and O/C ratios. This leads to densification of energy, as well as higher hydrophobicity, friability, grindability and flowability within torrefied biomass compared to raw biomass. It also simplifies the storage of biomass, since biomass becomes more resistant to fungi and bacteria (Hakkou

et al., 2006; van der Stelt et al., 2011). Macroscopically, it can be observed that biomass acquires brown or black color during torrefaction (see Fig. 17).



Fig. 17. Evolution of an ash-wood sample during torrefaction. From left to right: raw biomass, and biomass torrefied at 250, 280 and 300°C under the same conditions (Lê Thành et al., 2015).

2.2. PRODUCTS

The products of torrefaction are distributed into two phases:

- In the solid phase, torrefied biomass is formed;
- In the gaseous phase, condensable and non-condensable species are formed. Condensable species liquefy at room temperature, like water, acetic acid, furfural, methanol and phenol. Non-condensable or permanent species remain gaseous at room temperature, like carbon dioxide and carbon monoxide.

Fig. 18 shows the distribution of these three types of products in the overall mass balance obtained after torrefaction of several biomasses.

Permanent species typically represent one third of the overall torrefaction gas, whereas condensable species represent the other two thirds. Within condensable species, approximately one half is constituted by water, while the other half is constituted

by many different organic species, such as carboxylic acids, aldehydes and ketones (Nocquet et al., 2014a).

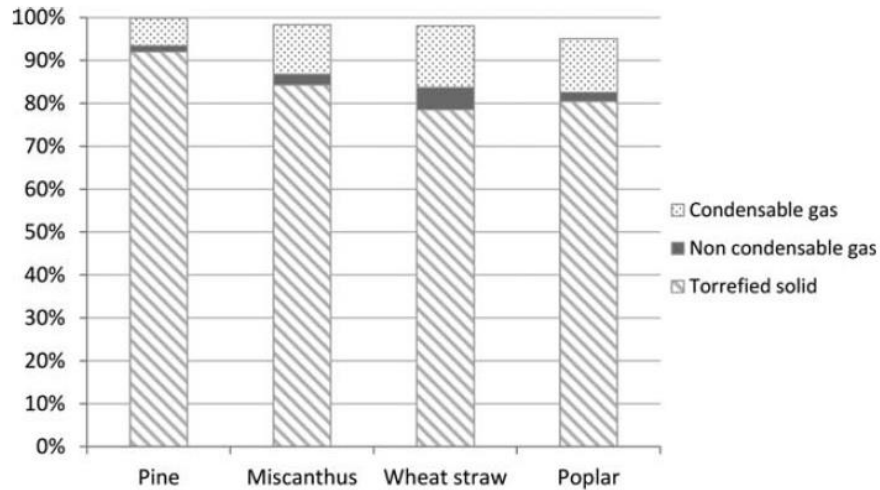


Fig. 18. Mass balance of products during torrefaction of several biomasses (Commandré and Leboeuf, 2015).

2.3. MASS AND ENERGY BALANCES

Fig. 19 shows typical overall mass and energy balances of torrefaction carried out within the temperature interval of 200-300°C. According to mass balance, 70% of the initial mass is retained in the torrefied solid, whereas 30% of the initial mass is contained in the gaseous phase, approximately. In contrast, energy balance indicates that the torrefied solid retains 90% of the initial energy, whereas the gaseous phase contains only 10% of the initial energy, approximately. Hence a gain of a 1.3 factor in the energy of the solid could be achieved thanks to torrefaction process (Bergman et al., 2005).

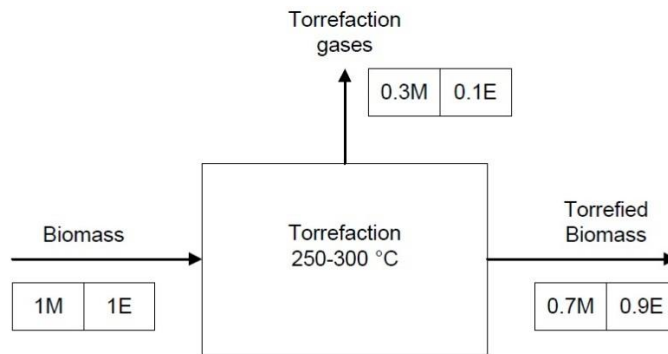


Fig. 19. Typical mass and energy balances of biomass torrefaction (Bergman et al., 2005).

2.1. REACTIVITY OF BIOMASS

Among the three macro-polymeric constituents of biomass, hemicellulose seems to be the most reactive constituent during torrefaction, followed by lignin and cellulose (Bergman et al., 2005).

Before 250°C, mass loss is mainly originated by the limited devolatilization and carbonization of hemicellulose. Lignin and cellulose are also degraded but in a minor extent, indeed they suffer significant chemical changes but low mass loss. After 250°C, the effects of torrefaction are more visible. Hemicellulose suffers extensive devolatilization and charring – which is a severe carbonization –, while lignin and cellulose already show limited devolatilization and carbonization (Bergman et al., 2005). This explains the fact that, in literature, torrefaction carried out at temperatures lower than 250°C has been called mild torrefaction, whereas torrefaction carried out at temperatures higher than 250°C has been called severe torrefaction (Chew and Doshi, 2011; Tumuluru et al., 2011; van der Stelt et al., 2011).

2.2. PROPERTIES OF BIOMASS

Torrefaction allows improving biomass properties from a logistic and end-use point of view (see Table 2). Torrefied biomass, in comparison with raw biomass, acquires (Kiel, 2012):

- Higher bulk density, volumetric energy density, low heating value (LHV) and fixed carbon;
- Lower moisture content, proportion of volatile matter, hygroscopicity and transport cost;
- Slower biodegradability.

Table 2. Comparison of properties between raw and torrefied wood (Kiel, 2012).

	Units	Wood pellets	Torrefied wood pellets
Moisture content	%w	7-10	1-5
Low heating value (LHV)	MJ/kg	15-17	18-24
Volatile matter	%wfm	75-84	55-65
Fixed carbon	%wfm	16-25	22-35
Bulk density	kg/L	0.55-0.65	0.65-0.80
Volumetric energy density	GJ/m ³	8-11	12-19
Hygroscopic properties	---	Hydrophilic	Moderately hydrophobic
Biological degradation	---	Moderate	Slow
Transport cost	---	Medium	Low

2.3. TECHNOLOGIES

Nowadays, the development of the torrefaction technologies is at a demonstration stage. However, in the short term, it should reach the industrialization stage.

Several competing technologies of torrefaction coexist. Some of these technologies have been specifically developed for torrefaction process, whereas others have been adapted from other thermal industrial uses. Table 3 presents the main reactors employed for torrefaction, their constructors and experimental conditions employed, as well as advantages/limitations of each technology.

Table 3. Main technologies of torrefaction (Casajus et al., 2012; Nocquet, 2012).

Reactor	Constructor	Experimental conditions	Advantages	Limitations
Multiple hearth furnace	Wyssmont TURBO-(DRYER®), USA	200-300°C 30-90 min	-Homogeneous torrefaction -Easy scale-up -Suitable for all types of biomass	-Expensive -Developed for low flowrates
	CMI, BE	200-300°C		
Moving bed	ECN (BO ₂ pellets™), NL	200-300°C	-Robust technology -Suitable for woody biomasses	-Carrier gas may present preferential pathways -Difficult scale-up -Not suitable for non-woody biomasses
	Thermya (Torspyd™), FR	240°C		
Cyclonic bed	Topell Energy (Torbed®), NL	280-320°C? Several min?	-Suitable for all types of biomass -Short residence times -Easy scale-up -Suitable for high flowrates	-Complex design -Difficult control of process
Torbed reactor	Torr-coal, NL	280-300°C? <100 min	-Robust technology -Well-known technology for drying -Suitable for the majority of biomasses	-Low efficiency on heat transfer -Heterogeneous torrefaction -High gas flow needed
	EBES AG, AUT	250-300°C		
	BioEnergy Development, SWE	?		
	4 Energy Invest, BE	?		
Vibrating belt	Atmosclear (Airless drying), CH	240-270°C	-Easy control of residence time and temperature -Easy scale-up -Suitable for the majority of biomasses	-Expensive maintenance
	Stramproy, NL	250-300°C		
Screw reactor	FoxCoal, NL	250-300°C	-Robust technology -Suitable for all types of biomass	-Difficult scale-up
	Biolake BV, NL	260-350°C		

In all these torrefaction technologies, condensable by-products are normally either removed as waste or burnt to obtain energy (Tumuluru et al., 2011). An innovative option would be to consider these species as high added-value chemicals. This is the central point of INVERTO project, discussed thereafter.

3. THE FRAMEWORK: INVERTO PROJECT

The INVERTO project stands for INnovation in VEgetal chemistRy by TORrefaction, and focuses on by-products of biomass torrefaction. The general objective of this project is to study the feasibility and interest of the chemical recovery of condensable species formed during torrefaction of lignocellulosic biomass. The approach must respond to a double question. Firstly, how to optimize the production of high added-value molecules from condensable species produced during biomass torrefaction. Secondly, whether this integrated energy/mass recovery allows improving the techno-economic and environmental performance of the process.

The specific objectives of the INVERTO project are related to:

- Mass balance of condensable species formed during torrefaction: an improvement on mass balances closure is aimed to more precisely know which condensable species could be potentially recovered;
- Prediction of yields on condensable species versus torrefaction parameters: the influence of experimental conditions and biomass species on the presence and quantity of condensable species formed during torrefaction is poorly known. A better knowledge about reaction mechanisms of torrefaction is necessary to understand and then optimize this transformation;
- Treatment of condensable species obtained during torrefaction: a critical point of the process is the treatment of condensable species in view of further extraction of the molecules of interest. The design and implementation of an adapted extraction/separation chain, as a function of downstream requirements, is essential and must be the focus of the development work;
- Viability of the process pathway: proving the feasibility of the process is necessary, but not sufficient. The viability of the process pathway must be proved from both economic and environmental points of view, by integrating the concepts of product price, toxicity and ecotoxicity, related to REACH regulation and durability within a framework of sustainability.

The objectives of the present work refer to the point of prediction of yields on condensable species versus torrefaction parameters, as explained thereafter.

4. OBJECTIVES

The general objective of this work is to contribute to better understand the chemical evolution of the solid and gaseous phases produced during biomass torrefaction. The first step is to study the different variables which could potentially have an influence on the evolution – experimental conditions and biomass type. The second step is to elucidate the reaction mechanisms which link degradation of the solid and formation of the gas during biomass torrefaction.

In order to attain this general objective, three specific objectives are considered:

- Identify and quantify chemical evolution of functional groups in the solid phase during biomass torrefaction, versus temperature and versus biomass species;
- Identify and quantify production of condensable species formed in the gaseous phase during biomass torrefaction, versus temperature and versus biomass species;
- Elucidate the reaction pathway which leads from reactants to products during biomass torrefaction.

These specific objectives are expected to be reached by the means of two devices. The ^{13}C CP/MAS solid-state NMR technique is employed to characterize the chemical evolution of the solid phase, while the TGA-GC-MS technique is employed to analyze the production of condensable species in the gaseous phase during biomass torrefaction. Then, the elucidation of torrefaction reaction mechanisms is based on the original ^{13}C CP/MAS solid-state NMR and TGA-GC-MS data obtained in the present work, as well as on the existing literature.

CHAPTER II: STATE-OF-THE-ART

1. INTRODUCTION

Three specific aspects are investigated in literature carried out on biomass torrefaction, in relation to the objectives presented in section 4 of chapter I:

- The chemical evolution of the solid phase during biomass torrefaction, versus temperature, residence time and biomass species;
- The production of condensable species in the gaseous phase during biomass torrefaction, versus temperature, residence time and biomass species;
- The modelling of solid degradation, gas formation and the associated reaction mechanisms during biomass torrefaction.

2. CHEMICAL EVOLUTION OF THE SOLID

2.1. WHAT DOES CHEMICAL EVOLUTION OF THE SOLID STAND FOR?

Biomass suffers a chemical evolution in composition and structure during torrefaction. More precisely, this evolution consists of changes in atoms layout within functional groups and changes in chemical bonds between atoms.

Methyl groups (-CH₃) and carbonyl groups (-CO-) are examples of functional groups, while simple bonds between carbons (C-C) and double bonds (C=C) are examples of chemical bonds.

2.2. CHARACTERIZATION TECHNIQUES

2.2.1. Challenges of solid characterization during torrefaction

The characterization of the solid phase during biomass torrefaction at lab-scale presents several challenges, related to the fact that:

- Biomass is a complex mixture of macro-polymers which contain many different functional groups and chemical bonds;
- Sample masses available are relatively small, typically from 10 mg up to 1g;
- Transformation occurs at high temperatures, up to 300°C.

2.2.1. Comparison of characterization techniques

Chemical evolution of the solid can be followed by the means of different characterization techniques. The principle of these techniques lies in the fact that, when biomass suffers chemical evolution, the signals emitted by the characterization device change. Then this change is detected and captured on a spectrum. Therefore, one crucial issue is to know which functional group or chemical bond corresponds to which signal.

The main techniques employed to characterize chemical evolution of biomass during torrefaction are NIRS (Near InfraRed Spectroscopy), FTIR (Fourier Transform Infrared Spectroscopy), XRD (X-Ray Diffraction) and ^{13}C solid-state NMR (Nuclear Magnetic Resonance). Table 4 lists these techniques, works which have employed the techniques, the objectives of works and the properties measured, as well as the advantages and limitations of each technique.

Table 4. Characterization techniques of biomass solid phase during torrefaction.

Technique	Work	Their objective	Measured properties	Advantages	Limitations
NIRS	Windeisen et al. (2009a)	Investigate the mechanical properties and chemical evolution in beech and ash-wood during torrefaction	Chemical evolution of main biomass constituents within biomass samples	-Fast -Non-destructive -Little or no sample preparation required -Possibility to measure energy and chemical properties (calorific value, ultimate and proximate analysis) -Quantitative	-Low sensitivity -Calibration needed on a large range of biomass samples
	Rousset et al. (2011)	Develop a numeric model to predict the combined effects of temperature and duration of beech torrefaction			
FTIR	Park et al. (2011)	Study the chemical changes of softwood during torrefaction in a pilot-scale reactor		-Fast -Quantitative	-Only relative values -Preparation of samples required
XRD	Wen et al. (2014)	Investigate the chemical evolution versus temperature during bamboo torrefaction, with a focus on lignin	Crystallinity of cellulose within biomass samples	-Non-destructive -Quantitative	-Specific (mostly used to measure crystallinity index) -Crystallinity index values only relative (higher values than in other methods)
¹³ C solid-state NMR	Ben and Ragauskas (2012)	Determine the effects of torrefaction temperature on the chemical structure of Loblolly pine	Chemical evolution of main biomass constituents within biomass samples	-Non-destructive -High selectivity -High resolution -Quantitative	-Time-consuming for satisfactory signal-to-noise ratios -Signals of one functional group can be overlapped by signals from other groups
	Melkior et al. (2012)	Investigate the chemical transformation of the main constituents in beech and elucidate the main reaction mechanisms			
	Park et al. (2013b)	Study the chemical and structural transformation of Loblolly pine during torrefaction and elucidate the main reaction mechanisms			
	Khazraie Shoulaifar et al. (2014)	Determine the chemical changes in the solid phase during torrefaction of birch			

NIRS and FTIR techniques are both based on infrared spectroscopy, which consists of the analysis of infrared light interacting with molecules. Infrared spectroscopy measures the vibrations of atoms; as a consequence, it is possible to determine functional groups contained in the solid, each of which corresponds to a defined stretching frequency or wavenumber. As an illustration, Fig. 20 shows an example of NIRS spectra and Fig. 21 of FTIR spectra. XRD technique is based on the measurement of the interference suffered by X-rays within the sample. When the sample is irradiated with a beam of monochromatic X-rays, the interaction with atoms in the sample results in diffracted X-rays. These rays generate spectra characteristic of chemical composition of the sample. Solid-state NMR is a nuclear magnetic resonance spectroscopy in which the sample is placed in a magnetic field. Certain nuclei of the solid sample, such as ^1H or ^{13}C , absorb the electromagnetic radiation and give in response a resonant frequency value. As an illustration, Fig. 22 shows an example of ^{13}C solid-state NMR spectra.

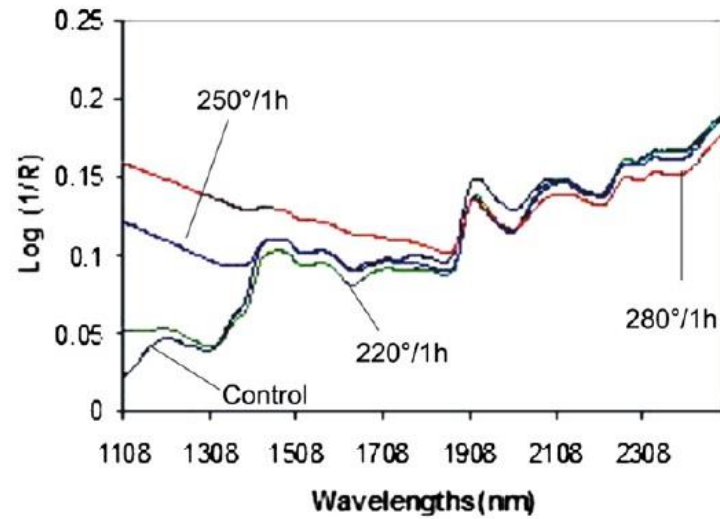


Fig. 20. NIRS spectra of raw and torrefied beech at 220, 250 and 280°C for 1h (Rousset et al., 2011).

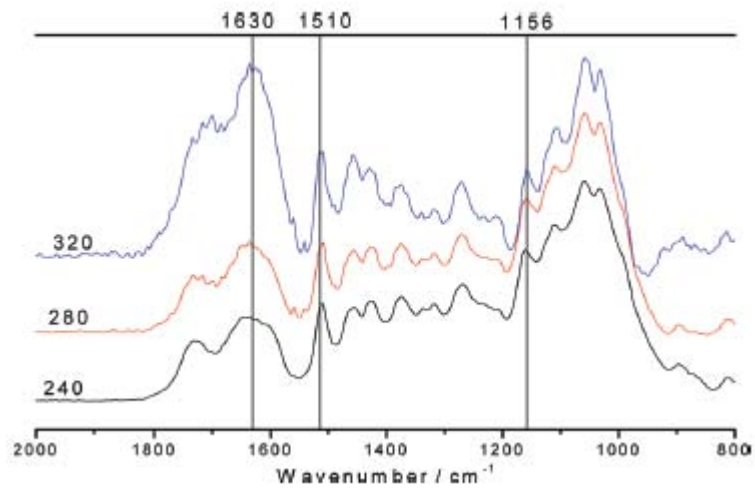


Fig. 21. FTIR spectra of torrefied pine at 240, 280 and 320°C (Zheng et al., 2012).

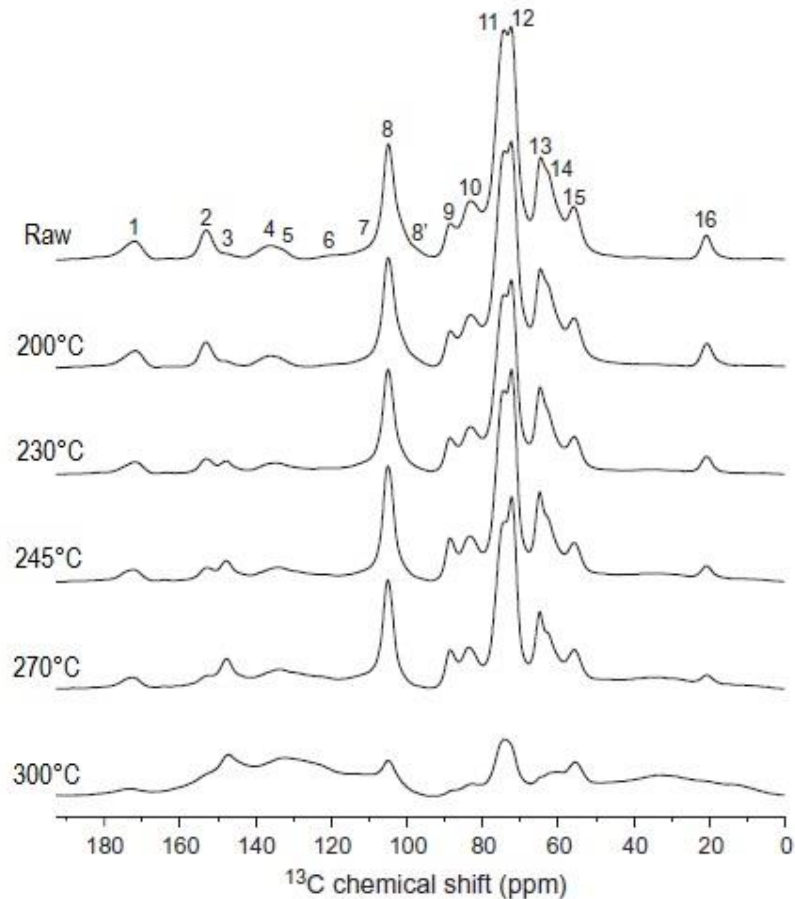


Fig. 22. ^{13}C CP/MAS solid-state NMR spectra of raw and torrefied samples of beech wood (Melkior et al., 2012).

As shown in Table 4, NIRS and FTIR present an important advantage, which involves the short duration of experiments. However, they also present major limitations when the objectives of the present work are considered. NIRS has a low sensitivity, which could hinder the detection of the least abundant functional groups within the solid. FTIR requires the preparation of a concentrated dilution of the sample in a suitable solvent and then transfer on a plate, which increases the analysis time. XRD is a technique employed for specific purposes, such as measure of crystallinity index or crystallite size. Although these measurements can be useful, they are not sufficient to describe the evolution of the three main biomass constituents. The last technique, ^{13}C solid-state NMR, presents the advantages of high selectivity and resolution, which could deal with the complexity of the torrefied solid phase. The only limitation of this technique lies in the

duration of experiments, which could extend to twelve of hours if the biomass sample is very condensed after torrefaction.

2.2.1. Conclusion

When putting together the different techniques available for characterization of the chemical evolution in the solid phase and the constraints associated to this characterization, ^{13}C solid-state NMR appears as a very good compromise. Thus the choice was made to employ it NMR in the present work, and to detail below the results obtained through this technique in literature.

2.3. ^{13}C SOLID-STATE NMR RESULTS DURING TORREFACTION

Qualitative chemical evolution of the solid during biomass torrefaction has been characterized with ^{13}C solid-state NMR by several authors, as shown in Table 4 of section 2.2. As explained above, with this technique, each peak on the spectrum corresponds to a signal value or interval of values, called chemical shift. Then each chemical shift is associated to an assignment, which represents a carbon located in a determined environment within the molecule. Carbon signals can be classified as carbonyls, aromatics and alkyls, which means that the carbon atom is located in a carbonyl group, an aromatic ring or an alkyl chain, respectively (Park et al., 2013b). Acetyl groups in hemicellulose are an example of assignment type carbonyl, carbon-carbon bonds in lignin are an example of assignment type aromatic, and carbons 4 of crystalline or amorphous cellulose are examples of assignment type alkyl (Ben and Ragauskas, 2012; David et al., 2009).

One of the reference works in characterization of torrefied biomass with solid-state NMR is the work of Ben and Ragauskas (2012). First of all, they studied torrefaction of pine wood at 250°C for 30 min, as reference. They found that the intensity of the signals corresponding to carbonyl and carboxyl groups slightly rose in comparison with raw biomass, which could indicate the formation of carbonyl and carboxyl groups during torrefaction. The intensity of the signal for aromatic C-O bonds increased, which would indicate the presence of more free hydroxyl groups on aromatic rings, due to the cleavage

of aryl ether bonds in lignin. The intensity of the signals for aromatic C-C bonds and aromatic C-H bonds in lignin increased. This could be attributed to both cleavage of aryl ether bonds in lignin, which would condense to form aromatic C-C bonds, and degradation of some carbohydrates, which would lead to the formation of aromatic C-C and C-H bonds. The intensity of the signal corresponding to C4 peaks of crystalline cellulose decreased, whereas the intensity of the signal corresponding to C4 peaks of amorphous cellulose increased. Despite the existence of overlapping from hemicellulose and lignin signals, this fact may be interpreted as a decrease in crystallinity index of cellulose. The intensity of the signal assigned to methoxyl groups in lignin significantly increased, which would mean that there is enrichment in methoxyls upon torrefaction. The intensity of the signal assigned to CH₂ groups in aliphatic chains remained almost unchanged after torrefaction, which could indicate that the degradation of aliphatic chains – mainly contained in extractives – is very limited during torrefaction.

Ben and Ragauskas (2012) studied the influence of temperature, using the above-mentioned reference. When comparing torrefaction carried out at different temperatures – 250°C and 300°C – for the same residence time – 30 min –, they found clear differences in solid chemical evolution. Pine torrefied at 300°C presented a higher intensity of signals assigned to carbonyl, carboxyl and aromatic carbons, as well as of signal for methoxyl groups. However, the intensity of the signal corresponding to acetyl groups contained in hemicellulose indicated that these groups were almost completely degraded.

The same authors studied the influence of residence time. When comparing torrefaction carried out for different residence times – 30 min and 4h – at the same temperature – 300°C –, Ben and Ragauskas (2012) observed that cellulose and hemicellulose were completely degraded after torrefaction for 4h, whereas lignin was very degraded but not completely. In this case, the torrefied solid contained a high proportion of carbonyl and aromatic carbons as well as methoxyl groups, which would mean that a condensed aromatic structure is formed as torrefaction progresses. They suggested that bonds between atoms into this complex structure might be C-O and C-C bonds.

To our knowledge, the influence of biomass species on chemical evolution of the solid during biomass torrefaction has not been studied by one author through solid-state

NMR yet. In literature, works have investigated only one woody biomass, although from different species among studies. Works have carried out torrefaction on softwood – pine in the case of Ben and Ragauskas (2012) and Park et al. (2013b) – or hardwood – birch in the case of Khazraie Shoulaifar et al. (2014) and beech in the case of Melkior et al. (2012). Besides, to the best of our knowledge, no work has characterized the chemical evolution of non-woody biomass through solid-state NMR.

To our knowledge, only one work has analyzed solid-state NMR results in terms of individual behavior of main biomass constituents during torrefaction (Melkior et al., 2012). Their work and conclusions are detailed below.

Few works have carried out a quantitative solid-state NMR characterization of torrefied biomass (Melkior et al., 2012; Park et al., 2013b). Quantification through solid-state NMR allowed Melkior et al. (2012) to observe that hemicellulose released acetyl groups from 200°C, and that cellulose degradation started at 245°C. Furthermore, they concluded that amorphous cellulose would be partly recrystallized from 200 to 245°C, and demethoxylation would be the dominant mechanism of lignin degradation from 200°C, mainly affecting syringyl units. These observations, together with the above-mentioned study of individual behavior of the main biomass constituents, enabled Melkior et al. (2012) to propose a scheme linking solid mass loss, gaseous species production and reaction mechanisms for beech samples during torrefaction, as shown in Fig. 23. The work of Park et al. (2013b) quantified the chemical evolution of solid during pine torrefaction at 270 and 300°C for 2.5 min, and obtained the results shown in Table 5. In view of these measurements, it seems that the condensed structure of the torrefied biomass would be mainly aromatic, probably due to the rearrangement and degradation of non-aromatic structures, as well as the decomposition of the few remaining carbohydrates.

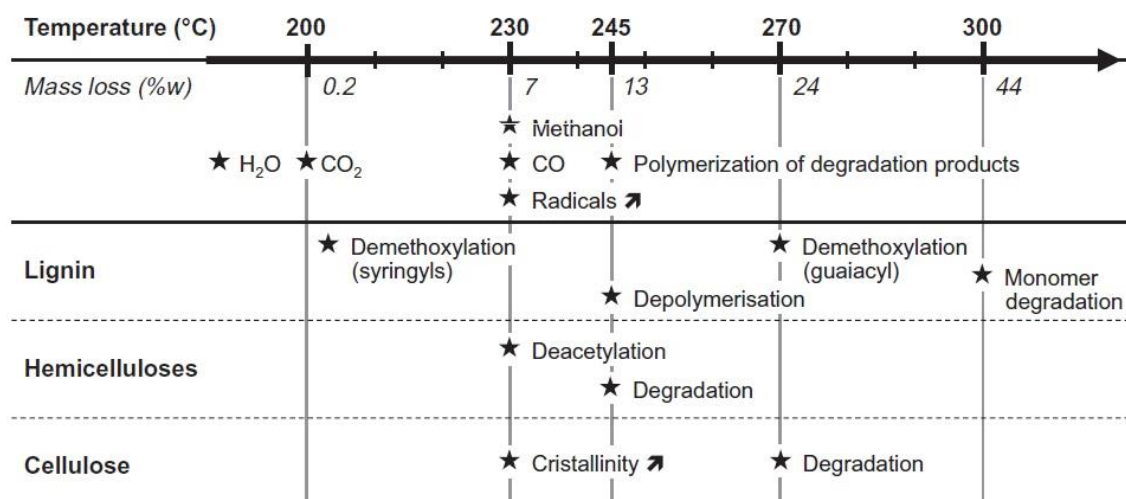


Fig. 23. Mass loss, gaseous species produced and reaction mechanisms of beech torrefaction versus temperature (Melkior et al., 2012).

Table 5. Quantitative characterization through ^{13}C DP/MAS solid-state NMR of the raw and torrefied biomass (Park et al., 2013b).

	Carbonyls (%)	Aromatics (%)			Alkyls (%)
		C-O	Protonated	Non-protonated	
Raw	3.6	4.7	31.1		60.6
270°C	2.8	6.1	18.7	19.9	52.5
300°C	4.5	5.1	19.2	29.5	41.7

Up to now, the ^{13}C solid-state NMR results obtained during biomass torrefaction in literature have shown that:

- When torrefaction severity increases in terms of temperature and time, a condensed aromatic structure seems to appear within the biomass solid phase, at the same time that the three main constituents of biomass degrade;
- Polysaccharides would be completely degraded at high temperature of torrefaction – around 300°C –, contrary to lignin, which would not be totally degraded under the same conditions.

However, to our knowledge, the influence of biomass species on chemical evolution of the solid during torrefaction has not been investigated yet, and quantification of solid chemical evolution has been barely carried out, although it seems to provide more accurate data on the individual behavior of the main biomass constituents, as well as on the reaction mechanisms present during biomass torrefaction.

3. PRODUCTION OF GASEOUS SPECIES

3.1. ANALYSIS TECHNIQUES

3.1.1. Challenges in analysis of the gaseous phase obtained during biomass torrefaction at lab-scale

The analysis of the gaseous phase obtained during biomass torrefaction at lab-scale presents several challenges, related to the fact that:

- High amount of chemical species conform the gaseous mixture;
- Chemical species released have different weights and polarities;
- Some species are present in low concentrations.

3.1.2. Comparison of analysis techniques

Several analysis techniques have been employed to analyze condensable species produced during biomass torrefaction. The main single techniques employed in literature are MS (Mass Spectrometry), HPLC (High-Performance Liquid Chromatography), FTIR (Fourier Transform Infrared Spectroscopy), whereas the main coupled techniques are GC-MS (Gas Chromatography-Mass Spectrometry) and GC-FID (Gas Chromatography-Flame Ionization Detector). Table 6 presents these techniques, works which have employed the techniques and the objectives of these works, as well as the advantages and limitations of each technique.

Table 6. Analytical techniques used to detect condensable species during biomass torrefaction.

Technique	Work	Their objective	Advantages	Limitations
MS	Aziz et al. (2012)	Study the influence of temperature on torrefaction of oil palm biomass	<ul style="list-style-type: none"> -High sensitivity -On-line measurement -Quantitative 	<ul style="list-style-type: none"> -No separation of different compounds in a mixture -No differentiation of compounds with the same molecular weight -Low intensities may be masked by higher intensities of signal -Only mass spectra provided, not peaks -Destructive
	Shang et al. (2013)	Develop a kinetic model to predict the mass loss and gas evolution during torrefaction of wheat straw		
HPLC	Prins et al. (2006a)	Study the influence of temperature and residence time on the yield and composition of solid and gas produced during torrefaction of deciduous and coniferous wood	<ul style="list-style-type: none"> -Fast (short elution times of several min) -Quantitative 	<ul style="list-style-type: none"> -Need of condensation for liquid injection -Need of specific columns for different families of compounds
FTIR	Chen et al. (2014)	Study the influence of temperature and residence time on fuel properties, energy and mass yields, carbon and oxygen yields, during torrefaction of rice husk	<ul style="list-style-type: none"> -High sensitivity (depending on cell length and resolution) -Fast -On-line measurement -Quantitative 	<ul style="list-style-type: none"> -Variable sensitivity depending on cell length and compounds -Low resolution for complex mixtures -Low intensities may be masked by higher intensities of signal -Simultaneous evolution of several compounds (co-elution) may hinder identification -Need of standard of all compounds -Need of heating the cell to avoid condensation
	Nocquet et al. (2012)	Study the solid mass loss and gaseous species yields during torrefaction of beech and its constituents		
GC-MS	Klinger et al. (2013)	Elucidate the scheme of reaction mechanisms and develop a semi-empirical model for torrefaction of aspen wood	<ul style="list-style-type: none"> -High separation capability for complex mixtures -High sensitivity for low concentrations, even traces (yields of 0.01%) -Quantitative 	<ul style="list-style-type: none"> -Time-consuming (several h) -Destructive -Need of specific columns for compounds families
	Khazraie Shoulaifar et al. (2014)	Study chemical evolution during torrefaction of birch wood		
	Pelaez-Samaniego et al. (2014)	Study the influence of temperature on yield, chemical composition and deposition pattern of lignin liquid intermediates on wood cells during torrefaction of ponderosa pine		
	Lê Thành et al. (2015)	Perform a qualitative and quantitative analysis of condensable species produced during torrefaction of pine, ash wood, miscanthus and wheat straw		
GC-FID	Theng and Doshi (2014)	Study the evolution of gas and liquid by-products versus temperature during torrefaction of palm mesocarp fiber	<ul style="list-style-type: none"> -High separation capability for complex mixtures -Quantitative 	<ul style="list-style-type: none"> -Only detects combustible carbon atoms -Destructive

MS is an analytical technique based on the measurement of the mass-to-charge ratio of ions in the gas phase, which have been previously obtained by, for instance, bombarding with electrons. This provokes molecules to break into charged fragments or ions, which are then separated according to their mass-to-charge ratio, usually by applying an electric or magnetic field. HPLC technique consists of making a liquid mixture pass through a column filled with a solid adsorbent. As molecules in the complex mixture have different polarities, they interact differently with the adsorbent solid material. Thus molecules of the mixture are retained on the adsorbent and released at different flow rates. FTIR fundamentals applied to solid have been explained in section 2.2 of the present chapter, and can also be applied to the analysis of condensable species in a liquid or gaseous phase. The coupling of GC and MS allows combining the detection of molecules by MS with their separation by GC. The principle of separation in GC is the same as in the HPLC column, since the column separates the molecules of the mixture. This allows the separation of molecules clusters inside the GC before entering the MS detector, which improves the accuracy of results. Fig. 24 shows an example of chromatogram obtained by GC-MS, whereas Fig. 25 shows an example of GC-MS data treated to compare the evolution of several gaseous species during biomass torrefaction. The coupling of GC-FID is based on the passing of the gaseous mixture under an air flame into which organic molecules are oxidized, and then charged to become ions. These ions produce an electrical signal which is detected and measured.

Water analysis deserves a special mention due to its complexity, since water is an abundant, small and polar molecule obtained during biomass torrefaction. Works in Table 6 have handled the issue measuring water by MS (Shang et al., 2013), HPLC (Prins et al., 2006a), FTIR (Chen et al., 2014; Nocquet, 2012), GC-MS (Klinger et al., 2013) or Karl Fischer volumetric titration (Lê Thành et al., 2015). However, other works have chosen not to carry out measurement of water (Khazraie Shoulaifar et al., 2014; Pelaez-Samaniego et al., 2014; Theng and Doshi, 2014).

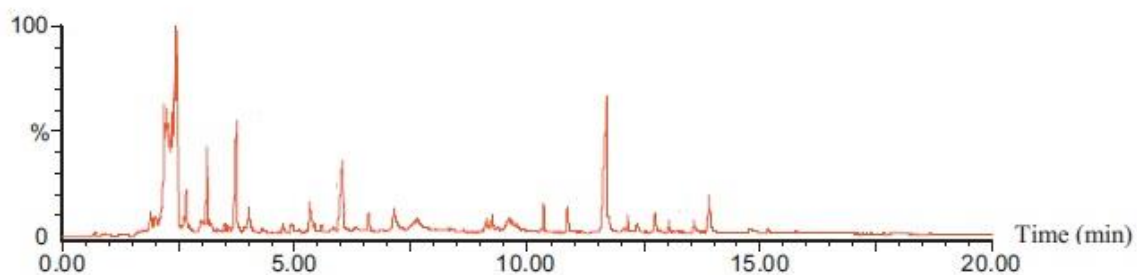


Fig. 24. GC-MS chromatogram of the gaseous phase produced during torrefaction of poplar sawdust at 230°C for 15 min (Candelier et al., 2011).

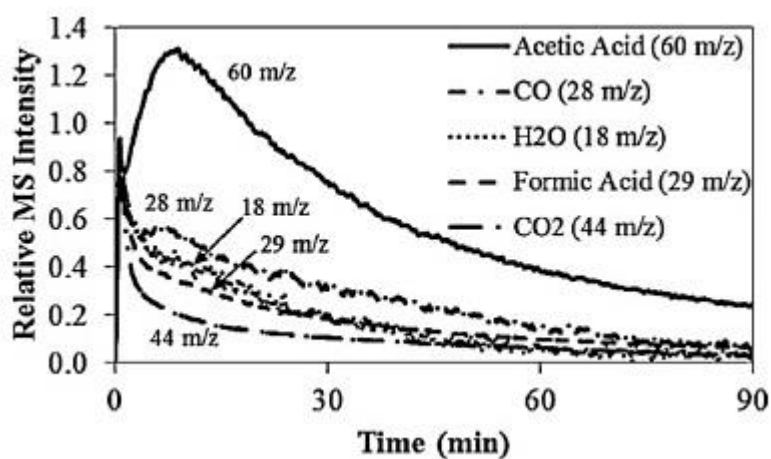


Fig. 25. Relative intensity obtained by GC-MS analysis of the major molecules produced during torrefaction of aspen for 90 min (Klinger et al., 2013).

As shown in Table 6, MS and GC-MS techniques present a high sensitivity, which is essential to analyze the low concentration of gaseous species in the mixture. However, MS cannot separate compounds in complex mixtures, like the mixture obtained during biomass torrefaction. HPLC involves short elution times of analysis, which is a significant advantage. However, samples for HPLC analysis require condensation, during which some light compounds –such as formaldehyde – might escape. FTIR allows to avoid the escape of species thanks to on-line analysis of gases. However, the main drawbacks of FTIR are the risk of species co-elution and the fact that the most intense signals may mask the least concentrated ones, which could hinder detection of diluted species. GC-MS

technique joins the high separation capability of the GC and the high sensitivity of the MS. Nevertheless, it can lead to long analyses and require specific columns depending on compounds families present in the mixture, although this can be easily solved by employing columns adapted to a large spectra of molecules polarities. Finally, GC-FID presents a high separation capability, like GC-MS, but has the major drawback of detecting only combustible carbon atoms, like $-CH_2-$ or $-CH_3$. This means that molecules which contain only carbon and hydrogen are well detected, but molecules which also contain other atoms, like oxygen, emit a weaker response. Thus GC-FID seems not to be recommendable for the present work.

3.1.3. Conclusion

When putting together the different techniques available for analysis of the gaseous phase obtained during biomass torrefaction at lab-scale and the challenges associated to this measurement, GC-MS appears as a very good compromise. Thus the choice was made to employ it in the present work. Moreover, as the major limitation of this technique is the long time required for analysis, it was decided to develop a heated samples storage, which would enable to collect several samples of the gaseous phase, at different times of torrefaction within the same experiment.

As a basis for our experimental study, the results obtained through this technique during literature torrefaction experiments are detailed below.

3.2. GC-MS RESULTS DURING TORREFACTION

Condensable species production during biomass torrefaction has been analyzed with the GC-MS technique in literature by many authors, as indicated in Table 6.

Works which have identified condensable species formed during biomass torrefaction thanks to GC-MS are shown in Table 7. The condensable species most commonly identified in literature are the most abundant ones, such as water, acetic acid, furfural, methanol, formic acid and hydroxyacetone (or 2-propanone, 1-hydroxy-). Table 7 presents the works which have identified condensable species by GC-MS, their objective,

the feedstock and experimental conditions employed, and the condensable species detected. It can be observed that works did not detect the same number of species. Bergman et al. (2005) identified thirty-four species, whereas other works like Chen et al. (2011a) identified five or less species. No species was common to all works. However, some species were common to most of works, like acetic acid, furfural and formic acid. Other species were common only to few works, like vanillin, phenol and 2,6-dimethoxyphenol. Less species were detected only in one work, like hydroxyacetone, methylfurfural and hydroxymethylfurfural. This lack of agreement in identified species among works may be due to differences in experimental conditions applied and feedstock employed for the study of torrefaction.

Table 7. Identification of condensable species produced during biomass torrefaction by GC-MS.

Work	Their objective	Feedstock	Experimental conditions	Condensable species
Bergman et al. (2005)	Better understand biomass torrefaction process by investigating the effect of several parameters, as well as process simulations and designs	Willow, woodcuttings, demolition wood	250-300°C 7.5-30 min	Furfural, 5-methyl-2-furaldehyde, acetaldehyde, 2(5H)-furanone, ethylene, glycol diacetate, ethanol, pyrrole, 1-hydroxy-2-butanone, eugenol, isoeugenol, propionic acid, 3,4,5-trimethoxytoluene, furan-2-methanol, furan-3-methanol, methanol, methylacetate, methylformiate, hydroxyacetone, cyclohexanone, butanone, propanal, pyrrole-2-carboxaldehyde, 2-butenal, phenol, 2-methoxyphenol, 3-methoxyphenol, 4-methoxyphenol, 2,6-dimethoxyphenol, acetone, 3-methoxypyridine, 4-methoxypyridine, 2-methoxypyridine, acetic acid, formic acid
Candelier et al. (2011)	Study the influence of temperature and biomass type on formation of gaseous by-products during biomass torrefaction	Pine, Silver fir	180, 200, 210, 220, 230°C 15 min	Acetic acid, furfural, methylfurfural, hydroxymethylfurfural, phenol, 2-methoxy-, phenol, 2,6-dimethoxy-, vanillin, syringaldehyde, acetovanillin, acetosyringone
Chen et al. (2011b)	Investigate the behavior of Lauan wood blocks during torrefaction and influence of experimental conditions on biomass properties	Lauan wood	220, 250, 280°C 0.5, 1, 1.5, 2h 30°C/min	Phenol, phenol, 2-methoxy-, phenol, 4-methyl-, eugenol, vanillin
Commandré and Leboeuf (2015)	Quantify gaseous by-products and evaluate solid grindability after torrefaction of various biomass types	Pine, miscanthus, poplar, wheat straw	250°C 45 min 10°C/min	Acetaldehyde, acetic acid, formaldehyde, formic acid, 2-furanmethanol, furfural, glycolaldehyde dimer, 2-propanone-1-hydroxy-, propanoic acid
Anca-Couce et al. (2014)	Develop a kinetic scheme to predict product composition of beech woodchips torrefaction	Beech	250, 285°C	Formaldehyde, acetaldehyde, acetone, methanol, ethanol, glycolaldehyde, acetic acid, water, glyoxal, lactic acid, formic acid

Many works have investigated the influence of temperature on formation of condensable species during torrefaction. Candelier et al. (2011) carried out torrefaction of ash sawdust from 180°C until 230°C for 15 min. As temperature increased, they observed higher quantities of acetic acid, furfural, methylfurfural and hydroxymethylfurfural. Vanillin was present in small quantities from 180°C, syringaldehyde from 210°C,

acetovanillin from 200°C, and their quantities also increased with temperature. Lê Thành et al. (2015) quantified almost twenty condensable species produced at 250, 280 and 300°C of dwell time. They found that all these species increased in quantity as temperature increased (see Table 8). In the case of anhydrosugars – LAC, DGP and levoglucosan –, quantities were low during torrefaction at 250°C, but strongly increased for higher temperatures. In these works, there was no specific reference to whether the overall composition of the gaseous phase varies with temperature or not.

Table 8. Mean yields (mg/g biomass) of the main condensable species produced in ash-wood torrefaction at different temperatures (Lê Thành et al., 2015).

Condensable species	250°C	280°C	300°C
Water	77.4	104.1	153.5
Acetic acid	27.1	40.8	48.2
2-Propanone,1-hydroxy-	1.9	5.9	12.1
Methanol	6.6	9.7	12.1
Glycolaldehyde dimer	1.8	4.6	9.2
2-Furanmethanol	2.1	3.4	5.7
Formic acid	3.7	5.6	6.7
Formaldehyde	2.9	3.6	2.9
2-Methoxy-4-vinylphenol	0.8	1.8	2.1
2-Butanone,1-hydroxy-	1.2	2.6	3.1
Furfural	1.7	2.5	2.9
LAC	0.3	0.7	1.1
DGP	0.4	1.1	2.2
1-Acetyloxy-2-propanone	0.4	1.0	1.3
Propanoic acid	0.4	0.9	1.4
Levoglucosan	0.2	0.6	1.7
3-Methyl-1,2-cyclopentanedione	0.3	0.6	1.6
Isoeugenol	0.6	0.9	1.1
2,6-Dimethoxyphenol	0.4	1.1	1.8
Phenol-2-methoxy-	0.1	0.4	0.8

To the best of our knowledge, no work has investigated the influence of residence time on formation of condensable species during torrefaction. In the present work, a study of the evolution of condensable species formation versus time during biomass torrefaction is carried out.

Lê Thành et al. (2015) investigated the influence of biomass species on the formation of condensable species during torrefaction. They investigated four biomasses

representative of different families of behavior – pine, ash-wood, miscanthus and wheat straw –, which are the biomasses investigated in the INVERTO project (see section 3 of chapter I). They observed that ash-wood produced about three times more methanol than pine, whereas pine released much more LAC than wheat straw, for which LAC was below the quantification limit. Pine produced the lowest amount of acetic, formic and propanoic acids among the four biomasses – with the exception of formic acid produced from wheat straw. They claimed that these three acids could be produced by degradation of hemicelluloses, hence this difference in quantity formed during torrefaction would be due to a different composition of pine hemicellulose in comparison with the other three biomasses. Commandré and Leboeuf (2015) also studied the influence of biomass species on the formation of condensable species during torrefaction. They torrefied pine, miscanthus, poplar and wheat straw. Fig. 26 gives mass balances of the main condensable species produced during torrefaction of the four biomasses. They observed that acetic acid was the main species produced by all biomasses, except pine. Formaldehyde and glycolaldehyde dimer were produced by all biomasses, except wheat straw. Propanoic acid was produced by pine and wheat straw, and furfural was the only condensable species to be produced by all biomasses. They suggested that the reason for these differences in product distribution may lie in differences in hemicellulose composition among biomasses. Nevertheless, they did not carry out experimental measurement of sugars content in hemicellulose.

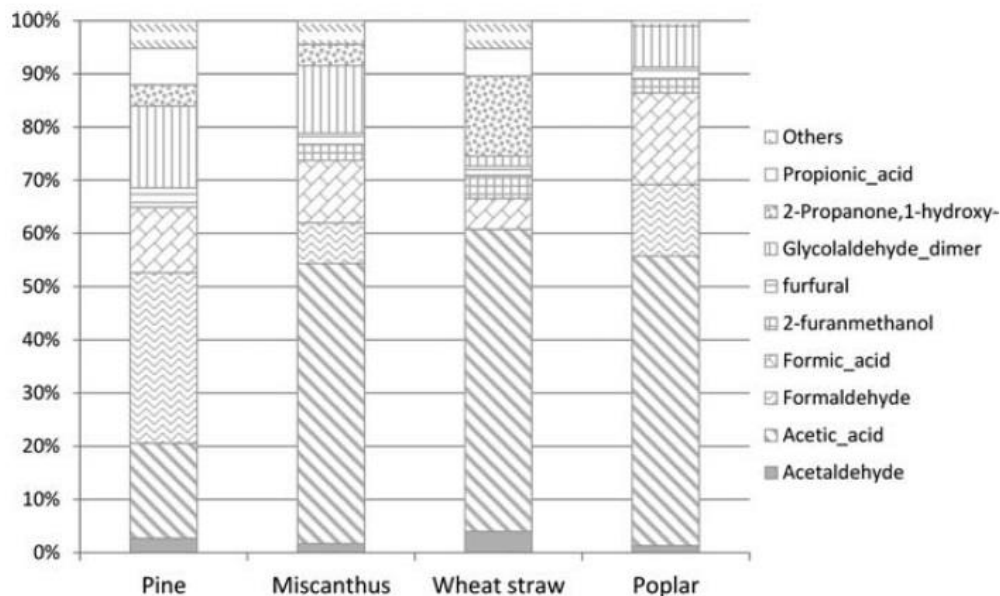


Fig. 26. Mass balance of the main condensable species obtained after torrefaction of four biomasses at 250°C for 45 min (Commandré and Leboeuf, 2015).

Nocquet et al. (2014a) investigated the production of condensable species during torrefaction of each main constituent of beechwood. Cellulose and xylan – which represented hemicellulose – were commercial constituents extracted from beech, whereas milled wood lignin had been extracted from the beech sample employed in the work. They observed that formic acid was produced only by xylan, formaldehyde was mainly produced by lignin and cellulose – probably due to the presence of hydroxymethyl groups in these constituents –, and methanol was produced only by lignin and xylan – probably due to the presence of methoxyl groups in these constituents. An interesting result was observed regarding the production of acetic acid, as it was one of the major products of beech torrefaction, but was neither produced by lignin, cellulose nor xylan. This would confirm the hypothesis which proposes that acetic acid may come from the hydrolysis of the acetyl groups in hemicellulose, which had previously been removed during the extraction of xylan from beechwood.

To our knowledge, up to now, no work has carried out torrefaction of biomass and quantification of the condensable species formed by TGA-GC-MS. This type of study will be carried out in the present work.

Up to now, the GC-MS results obtained during biomass torrefaction in literature have shown that:

- There is lack of agreement regarding identification of condensable species among works, which may be due to the differences in experimental conditions applied and types of biomass investigated;
- The variation of condensable species yields versus temperature has been widely reported, however, no reference has been found to mention whether the overall composition of the gaseous phase varies with temperature or not;
- The variation of condensable species yields versus biomass type has also been reported. It has been suggested that it is due to the differences in hemicellulose composition among biomasses. However, no experimental measurement of sugars content in hemicellulose has been carried out;
- The extraction method of biomass constituents can affect the reactivity during torrefaction. In particular, the removing of acetyl groups (present in xylan) during extraction would delete the production of acetic acid.

To our knowledge, up to now, no work has investigated the influence of residence time on formation of condensable species during torrefaction, and no work has carried out torrefaction of biomass and quantification of the condensable species formed by TGA-GC-MS.

4. MODELLING OF TORREFACTION KINETICS

4.1. TYPES OF MODELS

There are quite a few recent works which have proposed kinetic models of biomass torrefaction (Anca-Couce et al., 2014; Bach et al., 2014; Bates and Ghoniem, 2012; Cavagnol et al., 2013; Nocquet et al., 2014b; Patuzzi et al., 2013a; Prins et al., 2006b; Ren et al., 2013; Sarvaramini et al., 2013; Shang et al., 2013).

Kinetic models of biomass torrefaction can be classified into two groups. The first group is composed of the majority of models, which only predict solid decomposition (Bach et al., 2014; Cavagnol et al., 2013; Patuzzi et al., 2013b; Prins et al., 2006b; Ren et al., 2013; Sarvaramini et al., 2013; Shang et al., 2013). The second groups is composed of the minority of models, which link the prediction of solid decomposition and gaseous species formation (Anca-Couce et al., 2014; Bates and Ghoniem, 2012; Nocquet et al., 2014b). It has to be highlighted that models which predict solid decomposition and gaseous species formation are more recent than works which only predict solid decomposition.

Among models which predict the formation of specific gaseous species, Anca-Couce et al. (2014) have proposed a kinetic scheme based on the scheme proposed by Ranzi et al. (2008), whereas Bates and Ghoniem (2012) and Nocquet et al. (2014b) have proposed a kinetic scheme based on the scheme proposed by Di Blasi and Lanzetta (1997). The approach of these three models is particularly interesting for our study, thus they are thereafter detailed.

4.2. MODELS OF SOLID DECOMPOSITION AND GASEOUS SPECIES FORMATION

4.2.1. Chemical species predicted

Different chemical species have been the target of models which predict the formation of specific gaseous species linked to solid decomposition.

Anca-Couce et al. (2014) targeted the formation of 14 condensable and 5 permanent gases, as well as 4 forms of char. Condensable species considered in the model were water, acetic acid (represented as AA in the model), hydroxyacetaldehyde (HAA) –also known as glycolaldehyde –, glyoxal (GLYOX), acetaldehyde (CH_3CHO), hydroxymethylfurfural (HMFU), propanal ($\text{C}_3\text{H}_6\text{O}$) –also known as acetone –, formaldehyde (CH_2O), methanol (CH_3OH), ethanol (ETOH), *p*-coumaryl alcohol (*p*-COUMARYL), phenol (PHENOL), propanedial ($\text{C}_3\text{H}_4\text{O}_2$) – also known as malondialdehyde –

and sinapaldehyde (FE2MACR). Permanent gases considered in the model were carbon monoxide (CO), carbon dioxide (CO₂), methane (CH₄), hydrogen (H₂) and ethylene (C₂H₄).

Nocquet et al. (2014b) proposed a model to predict the formation of 6 condensable and 2 permanent gases. Condensable gases considered in the model were water, formaldehyde, acetic acid, furfural, methanol and formic acid, whereas permanent gases were carbon dioxide and carbon monoxide.

Bates and Ghoniem (2012) proposed a model to predict the production of 7 condensable and 2 permanent gases. Condensable species considered in the model were water, acetic acid, formic acid, methanol, lactic acid, furfural and hydroxyacetone. Permanent gases considered were carbon dioxide and carbon monoxide.

Table 9 shows the comparison of chemical species formation predicted by the three models.

Table 9. Comparison of chemical species predicted by models.

	Anca-Couce et al. (2014)	Nocquet et al. (2014b)	Bates and Ghoniem (2012)
Condensable gas	water acetic acid methanol		
	formaldehyde		---
	---	furfural formic acid	
	glycolaldehyde glyoxal acetaldehyde hydroxymethylfurfural acetone ethanol p-coumaryl alcohol phenol propanedial sinapaldehyde	---	lactic acid hydroxyacetone
Permanent gas	carbon monoxide carbon dioxide		
	methane hydrogen ethylene	---	
Char	4 forms of char	no char	

Thus, regarding condensable species predicted by these models, Table 9 shows that some of the species modelled by Bates and Ghoniem (2012) were also modelled by Anca-Couce et al. (2014), but not formic acid, methanol, lactic acid, furfural and hydroxyacetone. The majority of condensable species modelled by Nocquet et al. (2014b) were included in the model of Anca-Couce et al. (2014), except furfural and formic acid. The permanent gases modelled by Bates and Ghoniem (2012) and Nocquet et al. (2014b) were included in the model of Anca-Couce et al. (2014). Only the model of Anca-Couce et al. (2014) included char species.

4.2.2. Approach

The scheme proposed by Anca-Couce et al. (2014), shown in Fig. 27, was based on the scheme proposed by Ranzi et al. (2008), originally purposed for pyrolysis of small ash-free biomass particles. Anca-Couce et al. (2014) adapted this scheme to torrefaction conditions, since direct application of the scheme correctly predicted solid and total volatile yields, but did not correctly predict the yield of some condensable species, such as water and acetic acid. The adapted scheme eliminated some of the reactions proposed by Ranzi et al. (2008) for pyrolysis, such as the formation of levoglucosan from cellulose and the depolymerization of hemicellulose to xylose. The majority of the reactions conserved were assumed to be common to pyrolysis and torrefaction, which may be disputable since ranges of temperatures are different for these two processes. The scheme of Anca-Couce et al. (2014) considered biomass to be composed of cellulose, hemicellulose and three types of lignin, without interactions among them. Cellulose torrefaction was described through one reaction which produces two types of volatiles and chars. Hemicellulose torrefaction was based on two series reactions. The first reaction produces acetic acid, two types of volatiles and chars, and a solid activated hemicellulose. The solid activated hemicellulose reacts to produce two types of volatiles and chars. Lignin torrefaction was based on the reaction of three pseudo constituents of lignin defined as LIG-C, LIG-H and LIG-O units, which are lignin units of reaction richer in carbon, hydrogen and oxygen, respectively. Each of these units was mathematically defined, however this definition had no chemical meaning. LIG-C torrefaction was based

on two series reactions, as for hemicellulose. The first reaction produces volatiles, char and LIG-CC, a lignin unit even richer in carbon. LIG-CC decomposes to form two types of volatiles and chars. LIG-H and LIG-O produce volatiles and LIG-OH, a lignin unit richer in hydroxyl groups. The LIG-OH decomposes to form three types of volatiles and char, and sinapaldehyde. Thus the decompositions of LIG-H and LIG-O follow a similar pathway, different from that of LIG-C. The model of Anca-Couce et al. (2014) included six parameters in reaction mechanisms of cellulose, hemicellulose and lignin degradation, which represented the fraction of reactants which form products in a determined reaction.

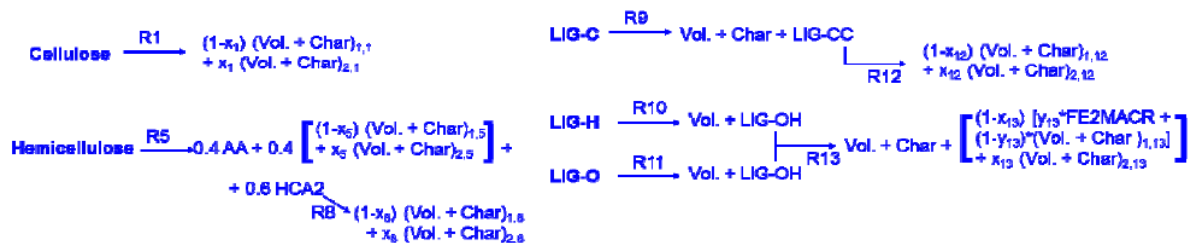


Fig. 27. Torrefaction scheme adapted from Ranzi et al. (2008) (Anca-Couce et al., 2014).

The model of Nocquet et al. (2014b) was based on the kinetic scheme previously proposed by Di Blasi and Lanzetta (1997), initially proposed to model the degradation of xylan under torrefaction between 200 and 340°C (see Fig. 28). In this model, biomass is considered to be composed of cellulose, hemicellulose – represented by xylan and acetyl groups – and lignin. Thereby, four kinetic sub-models were added to describe the degradation of each of the components (see Fig. 29). Acetyl groups were introduced as a sub-model in order to represent the formation of acetic acid through hydrolysis of acetyls. To obtain the model, the additive law was applied so that the contributions of the four sub-models were added. Each of the four reactions in Fig. 28 were assumed to follow kinetics of order one, and kinetic parameters to obey Arrhenius law. Volatile fractions V1 and V2 were assumed to be made up of the eight condensable species mentioned in Table 9. To describe the composition of the volatile fractions, one parameter was associated to each species for each reaction. Then the global yield of the species *i* was the sum of the yield obtained in reaction 1 and in reaction 2. Since the composition of

volatiles was approximately the same within the range of temperatures investigated, it was assumed to be constant with temperature. Moreover, the composition of the volatile fractions was assumed to be constant with time. Some of the parameters associated to species were taken equal to zero, since in (Nocquet et al., 2014a) it was observed that each constituent did not produce every species:

- Cellulose formed carbon dioxide, carbon monoxide, water, formaldehyde and furfural;
- Lignin formed carbon dioxide, carbon monoxide, water, formaldehyde, furfural and methanol;
- Xylan formed carbon dioxide, carbon monoxide, water, formaldehyde, methanol and formic acid;
- Acetyl groups only formed acetic acid.

The main novelty of this work is that Nocquet et al. (2014b) considered the existence of interactions between biomass constituents – which were proved to exist from 280°C and higher temperatures, in the experiments performed by the authors (Nocquet et al., 2014a). The interactions between cellulose and the other two biomass constituents – hemicellulose and lignin – were considered in the model by the means of a corrective factor. Acetyl groups, however, were considered not to have any interaction with the three main constituents.

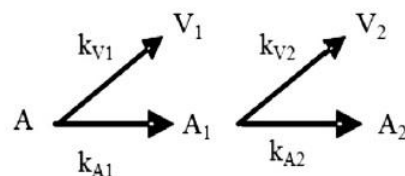


Fig. 28. Kinetic scheme of biomass torrefaction proposed by Di Blasi and Lanzetta (1997).

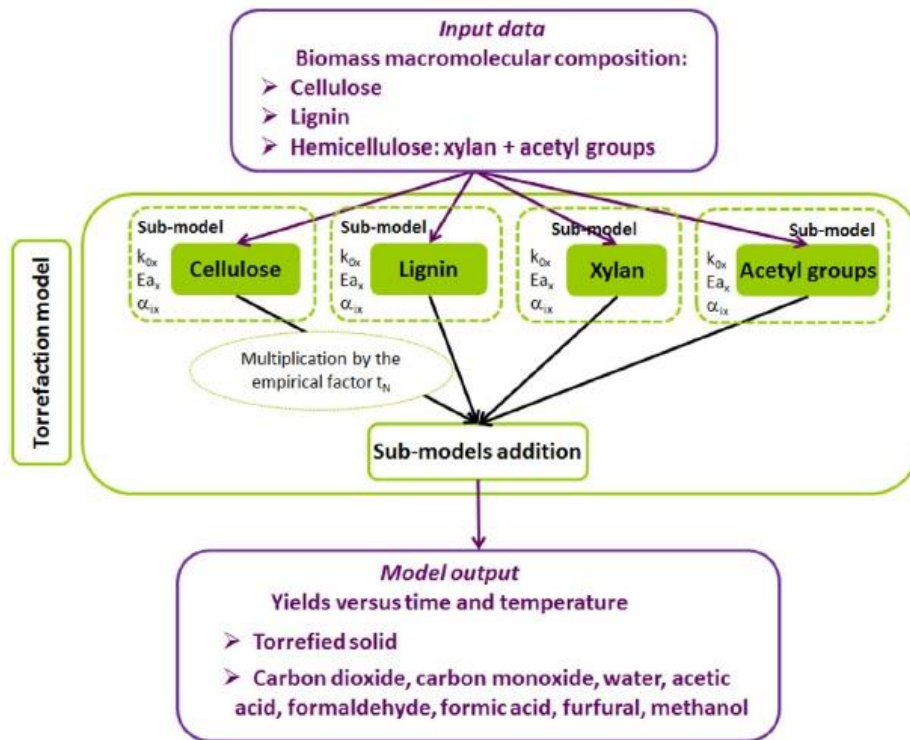


Fig. 29. Principle of the kinetic model developed for biomass torrefaction by Nocquet et al. (2014b).

The model of Bates and Ghoniem (2012) was also based on the kinetic scheme of Di Blasi and Lanzetta (1997), and its approach is close to the model of Nocquet et al. (2014b). Nevertheless, they differed in the fact that Bates and Ghoniem (2012) considered that both total mass and composition of the volatiles could vary as a function of time. Given the narrow temperature range of their experiments, between 230 and 300°C, composition in individual species of V1 and V2 were assumed to be constant with temperature, which is in agreement with Nocquet et al. (2014b).

4.2.3. Experimental validation

The three models were compared to experimental data for validation. Nevertheless, Nocquet et al. (2014b) and Anca-Couce et al. (2014) carried out their own experiments, whereas Bates and Ghoniem (2012) used experimental data from a previous work (Zanzi et al., 2002).

The model of Bates and Ghoniem (2012) predicts that condensable species represent 70-80% of the total gaseous yield, whereas the experimental data observed 80-90%. The CO₂/CO ratio predicted by the model was in agreement with the experimental measurements. Thus the model satisfactorily predicts the global yields of condensable and non-condensable gaseous species. They also evaluated the prediction of the carbon, hydrogen and oxygen fractions retained by the solid product, with good agreement. However, no information was given on condensable species yields.

In the work of Nocquet et al. (2014b), most modelling results were satisfactorily validated with experimental results, in particular regarding the yields of the eight volatile species predicted. The relative difference was of 35% or less for the major condensable species, and slightly higher (50%) for carbon monoxide. The results were less satisfactory for two minor species, namely formic acid (200%) and furfural (300%). This high difference could be explained by the very low quantities of these species formed in the experiments but even though, the order of magnitude was found to be correct and sufficient for a first rough estimation in process design.

In the model of Anca-Couce et al. (2014), the final solid yield was satisfactorily predicted, although evolution versus time was not precisely described. They validated the yields of water and condensable species, the latter classified into four groups: carbonyls+alcohols, furans, sugars and phenolics. The prediction was satisfactory for the yields of the four groups of condensable species; however, the water yield was under-predicted.

4.3. CONCLUSION

The comparison of the few existing models predicting condensable species during biomass torrefaction can be summarized through Table 10. This table shows that to develop a torrefaction model which predicts condensable species during biomass torrefaction, one should:

- Consider the individual reactivity of the three main biomass constituents – cellulose, hemicellulose and lignin;

- Detail the chemical composition of these biomass constituents to predict the differences in results observed among different types of biomass;
- Consider the potential interactions among biomass constituents;
- Elucidate the reactions associated to the interval of temperatures of torrefaction;
- Consider not only the formation of condensable and permanent gaseous species, but also the formation of solid char;
- Detail the pathway from reactants to products through reactions with stoichiometric coefficients.

Table 10. Comparison of models which predict solid decomposition and formation of gaseous species during biomass torrefaction.

	Anca-Couce et al. (2014)	Nocquet et al. (2014b)	Bates and Ghoniem (2012)
Reference kinetic scheme	Ranzi et al. (2008)	Di Blasi and Lanzetta (1997)	
Chemical species predicted	14 condensable gases 5 permanent gases 4 forms of char	6 condensable gases 2 permanent gases	7 condensable gases 2 permanent gases
Own experimentation	Yes		No
Composition of the volatiles fraction vs. time	?	Constant	Variable
Composition of the volatiles fraction vs. temperature	?	Constant	Constant
Limitations	No detailed approach of cellulose (crystalline/amorphous)		
	No detailed approach of hemicellulose (composition in sugars)		
	Lignin units defined mathematically, but lacking of chemical meaning	No detailed approach of lignin (composition in units)	
	Reactions with stoichiometric coefficients, but lacking of chemical meaning	No reaction with stoichiometric coefficients proposed	
	Char without any chemical meaning	No char predicted	
	No interaction among constituents considered	Interaction among constituents considered with one corrective factor	No interaction among constituents considered
	---	No detailed approach on which reactant produces which gaseous species	

CHAPTER III: MATERIALS AND METHODS

1. BIOMASSES

Biomass potentially useable in thermochemical processes presents a large diversity. As a consequence, in the present work, four biomasses were chosen to represent each biomass family:

- Pine represents the softwood family. It has been harvested in Aveyron (South West of France);
- Ash-wood represents the hardwood family. It has been harvested in Aveyron (South West of France);
- Miscanthus represents the perennial energy crops family. It has been harvested in Montans (South West of France);
- Wheat straw represents the agricultural residues family. It has been harvested in Montans (South West of France).

As shown in Fig. 30, pine and ash-wood samples were received in the form of wood chips, whereas miscanthus and wheat straw samples were in the form of pellets. The reason is that woodchips are a suitable feedstock for industrial torrefaction process; however, crops and agricultural residues occupy high volume and do not present suitable properties for industrial process. Sampling has been carried out, following the standard XP CENT/TS 14780, from a sample of several t to a sample of several kg.



Fig. 30. The four biomasses: pine chips on the top left; ash-wood chips on the top right; miscanthus pellets on the bottom left; and wheat straw pellets on the bottom right.

Both pine and ash-wood were dried, whereas miscanthus and wheat straw had not been treated in any way. The reason for drying is that wood presented around 50%w of moisture content, which means that biomass could rapidly degrade during the storage period. Crops and agricultural residues, however, only presented around 20%w of moisture content. For pine and ash-wood, drying was carried out at 60°C during 24h. The temperature was fixed at 60°C so as to mainly remove water, but retain the maximum of extractives. This way, extractives can be analyzed together with torrefaction products. As shown in Table 11, moisture content after drying is similar for the four biomasses, between 8 and 10%w. Therefore, the influence of this parameter is considered to be similar for the four biomasses during torrefaction.

Feedstock was prepared following the XP CEN/TS 14780 standard for sample preparation of solid biofuels. Biomass samples were ground below 300 μm in order to ensure sample homogeneity and representativeness.

Chemical properties and elemental analysis of biomasses are shown in Table 11, and analysis of sugars composition in hemicellulose is shown in Table 12. Proximate and ultimate analyses were carried out following standards on solid biofuels, except for

extractives content, which was measured by internal methods because no standard exists.

Table 11. Biomasses chemical properties and elemental analysis.

Magnitude	Standard	Unit	Pine	Ash-wood	Miscanthus	Wheat straw
Moisture	EN 14774-1	%w	10.0	13.3	8.0	9.6
Ash	XP CEN/TS 14775	%wmf	1.3	2.8	2.8	8.3
Extractives	Internal method		8.4	10.0	8.6	15.7
Cellulose	TAPPI standard T249 cm-85		36.7	39.0	45.7	33.8
Hemicellulose	TAPPI standard T249 cm-85		26.1	21.9	22.8	21.7
Lignin	TAPPI T222 om-83		27.5	26.3	20.2	20.5
C	XP CEN/TS 15104		51.3	49.2	48.3	45.2
H	XP CEN/TS 15104		6.2	5.9	6.0	5.7
N	XP CEN/TS 15104		<0.3	0.3	<0.3	0.8
O	By difference		42.5	44.5	45.7	48.4
Al	EN 15290		ppm wmf	350	204	65
As	EN 15297	0.2		<0.1	<0.1	<0.1
Ca	EN 15290	2128		8792	2539	4081
Cd	EN 15297	<0.4		<0.4	<0.4	<0.4
Cr	EN 15297	1.2		1.0	1.2	4.0
Fe	EN 15290	288		146	91	296
Mg	EN 15290	597		606	329	735
P	EN 15290	75		257	291	1247
Hg	EN 15297	0.1		0.1	<0.1	<0.1
K	EN 15290	590		2663	3364	8823
Mn	EN 15297	42		16	70	59
Ni	EN 15297	<1.5		<1.5	<1.5	<1.5
Na	EN 15290	57		56	56	325
Pb	EN 15297	2.3		0.6	<0.5	6.0
Ti	EN 15290	50.0		15.0	6.8	33.0
Zn	EN 15297	15.0		6.6	6.3	31.0
B	NF EN ISO 11885	4.7		14.1	<1.5	<1.5
Si		2074		985	7009	25226

Table 12. Sugars composition in hemicellulose analysis.

Functional group/sugar	Standard	Unit	Pine	Ash-wood	Miscanthus	Wheat straw
Acetyl	Internal method	%wmf	1.7	3.6	2.6	1.7
Mannan	TAPPI T249 cm-85/ TAPPI T249 cm-85/ASTM E1758 - 01(2007)	%wmfh	10.3	1.2	0.3	0.4
Xylan	TAPPI T249 cm-85/ TAPPI T249 cm-85/ASTM E1758 - 01(2007)		5.0	14.3	17.2	16.0
Galactan	TAPPI T249 cm-85/ TAPPI T249 cm-85/ASTM E1758 - 01(2007)		1.7	0.6	0.4	0.9
Arabinan	TAPPI T249 cm-85/ TAPPI T249 cm-85/ASTM E1758 - 01(2007)		1.0	1.6	1.9	2.3
Other sugars	TAPPI T249 cm-85/ TAPPI T249 cm-85/ASTM E1758 - 01(2007)		6.4	0.6	0.4	0.6

Analysis of biomass main constituents in Table 11 shows that lignin content was determined by weighting the solid residue after sulfuric acid dissolution of samples, according to the Klason method. For cellulose and hemicellulose, samples were totally hydrolyzed in sulfuric acid, and the sugar monomers were quantified by chromatography. Cellulose and hemicellulose contents were estimated by modelling from sugar quantification (Jacob et al., 2013). Composition in major biomass constituents varies between 34-45%wmf for cellulose, 22-26%wmf for hemicellulose and 20-28%wmf for lignin, which are typical values found in literature (Da Silva Perez et al., 2015).

Extractives content was measured using an ASE (Accelerated Solvent Extractor) to carry out extraction with 2 cycles at 1500 psi. Firstly, it was done with water at 110°C then with acetone at 95°C. Once solvents were evaporated, the residues were weighted as the extractives content (Jacob et al., 2013). The extractives content ranges from 8 to 16%wmf. These values are higher than expected, since they are usually lower than 10%wmf (Sjostrom, 1993). High values of extractives content can be due to the extraction

method, which may extract some inorganic matter (e.g. silica) and/or organic matter (e.g. starch), in addition to “classic” extractive species, especially in extraction from wheat straw.

Regarding ash content, pine shows the lowest value, ash-wood and miscanthus present higher ash contents – and similar between them –, and wheat straw shows the highest ash content close to 10wmf%. These ash contents are in agreement with bibliographic data (Da Silva Perez et al., 2015; Vassilev et al., 2010).

In elemental analysis, oxygen was calculated by difference, considering that $C+H+N+O=100$. Carbon content varies between 45-51%wmf, hydrogen content is around 6%wmf and oxygen content varies between 42-48%wmf. The content in these three elements varies in a narrow range of values from one biomass to another, which has been reported before in literature (Da Silva Perez et al., 2015). However, nitrogen content varies among biomasses from a non-detectable quantity up to 1%wmf, thus the content in this element varies in a wider range. In addition, nitrogen content is higher for wheat straw than for the other three biomasses, which has also been reported before (Da Silva Perez et al., 2015).

Composition in ashes is variable, in terms of type and proportion of inorganic species, among biomasses. Wheat straw contains significantly higher amounts of Si, Na, K and P than the other three biomasses, ash-wood contains more Ca and B, and pine contains more Pb. These observations are consistent with literature (Da Silva Perez et al., 2015).

In Table 12, analysis of sugars composition in hemicellulose shows that the four biomasses contain a similar proportion of acetyl groups in hemicellulose. Acetyl groups are mainly contained in xylan, but are also present in other sugars. Ash-wood, miscanthus and wheat straw contain similar proportions of sugars, with comparable proportions of mannan and galactan, which are sugars with 6 carbons or C6 sugars. Ash-wood, miscanthus and wheat straw also contain similar proportions of xylan and arabinan, which are sugars with 5 carbons or C5 sugars. On the contrary, pine contains a high proportion of mannan, almost absent in the other three biomasses, and less xylan. This difference in sugars composition of softwood hemicellulose has been previously reported

in literature (Sjostrom, 1993). The unidentified fraction of sugars is higher for pine than for the other three biomasses, and could be mainly composed of glucose monomers.

2. COUPLING OF TGA-GC-MS

Torrefaction of biomass samples and analysis of condensable species formed were carried out with the TGA-GC-MS device (see Fig. 31 for device and Fig. 32 for scheme). As a matter of fact, the entire facility is a coupling of four devices: TGA (Thermogravimetric Analyzer), loops storage of gaseous samples, GC (Gas Chromatograph) and MS (Mass Spectrometer). They are described in detail thereafter.



Fig. 31. TGA-GC-MS device.

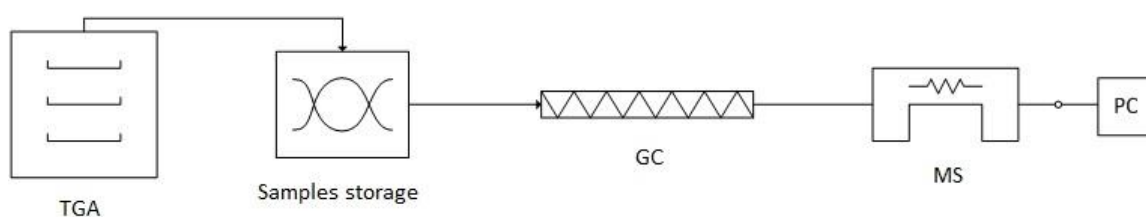


Fig. 32. TGA-GC-MS scheme.

2.1. THERMO-GRAVIMETRIC ANALYSIS (TGA)

2.1.1. Device description

Torrefaction was carried out in a Thermogravimetric Analyzer SETARAM ATG92 (see Fig. 33 for scheme). Inside, there was a cylindrical furnace in which torrefaction of the biomass sample was carried out. The biomass sample was contained in a crucible, which was placed inside the furnace.

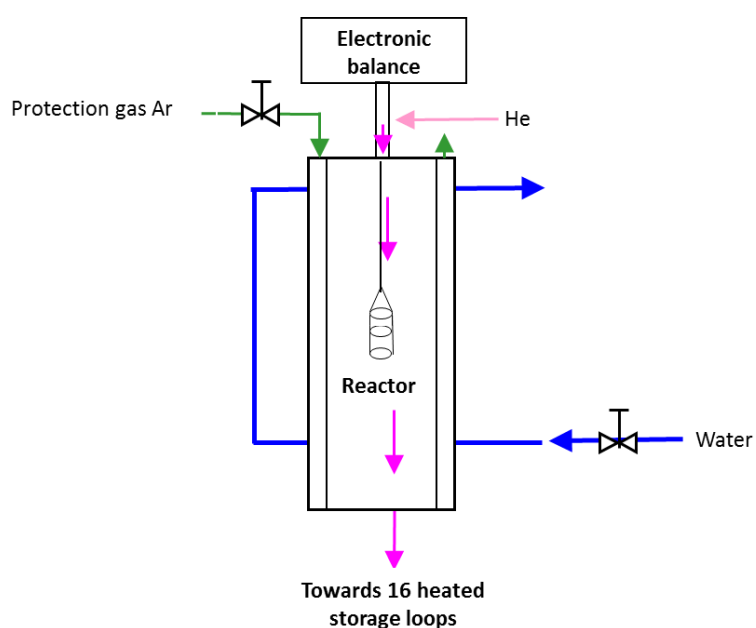


Fig. 33. TGA scheme.

2.1.2. Experimental procedure

Biomass samples were placed into a three-stage crucible, whose dimensions were 1.2 cm in width and 2.3 cm in height (see Fig. 34). These dimensions allowed to keep the crucible inside the isothermal zone of the TGA furnace.



Fig. 34. Three-staged crucible for TGA torrefaction.

Torrefaction experiments were carried out under a dynamic profile of temperatures. Temperature rose from room temperature with a heating rate of 5°C/min, until the final temperature of torrefaction between 200 and 300°C. Then the sample was removed so as to stop further reactivity.

In order to make sure that identical temperature was applied on the whole biomass, the crucible was placed in the isothermal zone of the furnace. Moreover, to ensure that torrefaction experiments were carried out under chemical regime and that a homogeneous torrefaction took place, particle size and mass of samples were reduced. The values were established as: maximal particle size of 300 µm and maximal sample mass of 150 mg.

Torrefaction was carried out under inert atmosphere. In the present work, this atmosphere was made up of helium. The reason for this choice is that helium was the carrier gas in the GC-MS, so using helium all along the facility avoided gaseous samples from being diluted in different gases. The flow rate of the helium was 40 mL/min.

A sample mass of around 100 mg was necessary to dispose of a reliable enough MS signal, since forming a higher quantity of gas led to a more intense signal. By calculating reaction characteristic times for samples of 100 mg and less, it was checked out that there were not heat limitations related to external control (González-Martínez, 2015). This is why a three-stage crucible, instead of a simple crucible, was chosen as

support for the biomass sample. The three-staged crucible can contain a higher mass sample (around 100 mg) than a simple crucible (around 35 mg).

Mass loss of torrefied samples was normalized to 100% at 200°C, in order to compare mass variations after drying. This mass loss until 200°C corresponds mainly to remaining water, although some extractive species can also be released (Nocquet, 2012). Mass loss until 200°C represents a maximum of 6%w of the raw biomass in the present work.

2.1.3. Repeatability experiments

Two types of tests were carried out during torrefaction with the three-stage crucible:

- Firstly, repeatability of experiments with the three-stage crucible was tested, by carrying out two experiments under the same experimental conditions. The temperature profile was dynamic from room temperature until 300°C with a heating rate of 5°C/min. Then the sample was removed to stop further reactivity. Two samples of 100 mg of ash-wood, ground to 300 µm, were torrefied. Experiments showed a relative difference lower than 2% in terms of mass loss between experiments with the three-stage crucible (see Fig. 35). Hence experiments carried out in the three-stage crucible were considered to be repeatable.
- Secondly, a comparison between experiments with the three-stage crucible and with a simple crucible was carried out. Four experiments, two for each crucible, were compared (see Fig. 35). Four samples of 100 mg of ash-wood, ground to 300 µm, were torrefied. The temperature profile was dynamic from room temperature until 300°C with a heating rate of 5°C/min. Experiments showed a relative difference lower than 3% in terms of mass loss when comparing the simple crucible and the three-stage crucible. Therefore the evolution of mass loss for samples in the simple crucible and the three-stage crucible were identical.

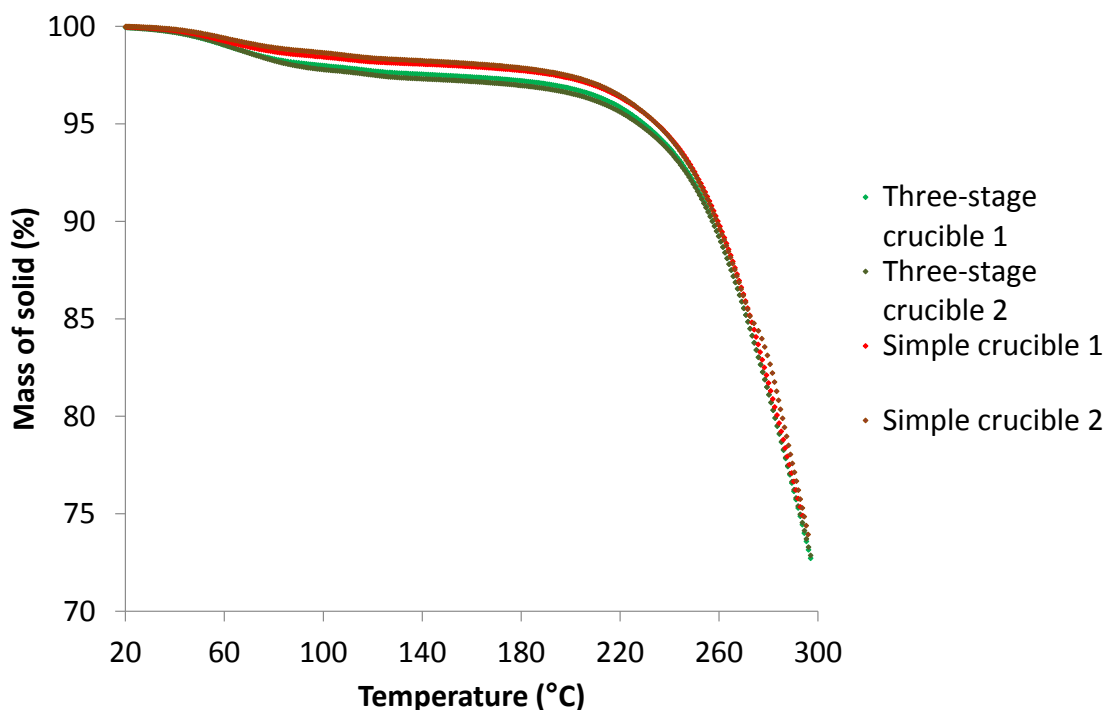


Fig. 35. Compared evolution of mass loss for ash-wood samples in a three-staged and a simple crucible.

2.2. LOOPS STORAGE

2.2.1. Device description

The gaseous species formed during torrefaction of biomass in the TGA furnace were led to the Chromatostock loops storage (see Fig. 36 for scheme). The role of this device was to keep samples heated at 200°C inside the loops, in order to maintain their gaseous state. After being stored, these gaseous samples were sent to analysis in the GC-MS. The storage device was made up of 16 loops, and each loop contained a volume of 500 μL .

The 16 loops of the Chromatostock could adopt two positions:

- In position V1, the loop received the gaseous sample originated in the TGA furnace;

- In position V2, the loop released the gaseous sample and sent it to the GC-MS, where the sample was analyzed.

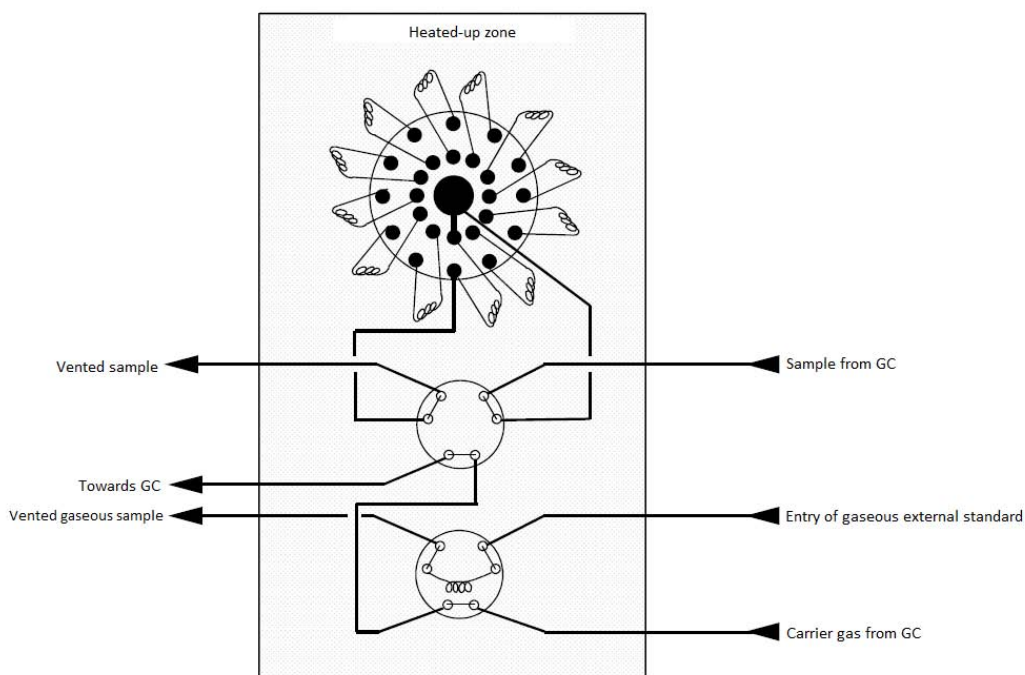


Fig. 36. Chromatostock loops storage scheme.

2.2.2. Experimental procedure

Gaseous samples were stocked one by one in each of the loops on the V1 position. The sampling was done at torrefaction temperatures of 200, 210, 220, 230, 240, 250, 260, 270, 280, 290 and 300°C, attained by the biomass sample in the TGA (see Fig. 37). Then the V2 position was activated and samples were sent one by one for analysis to the GC-MS.

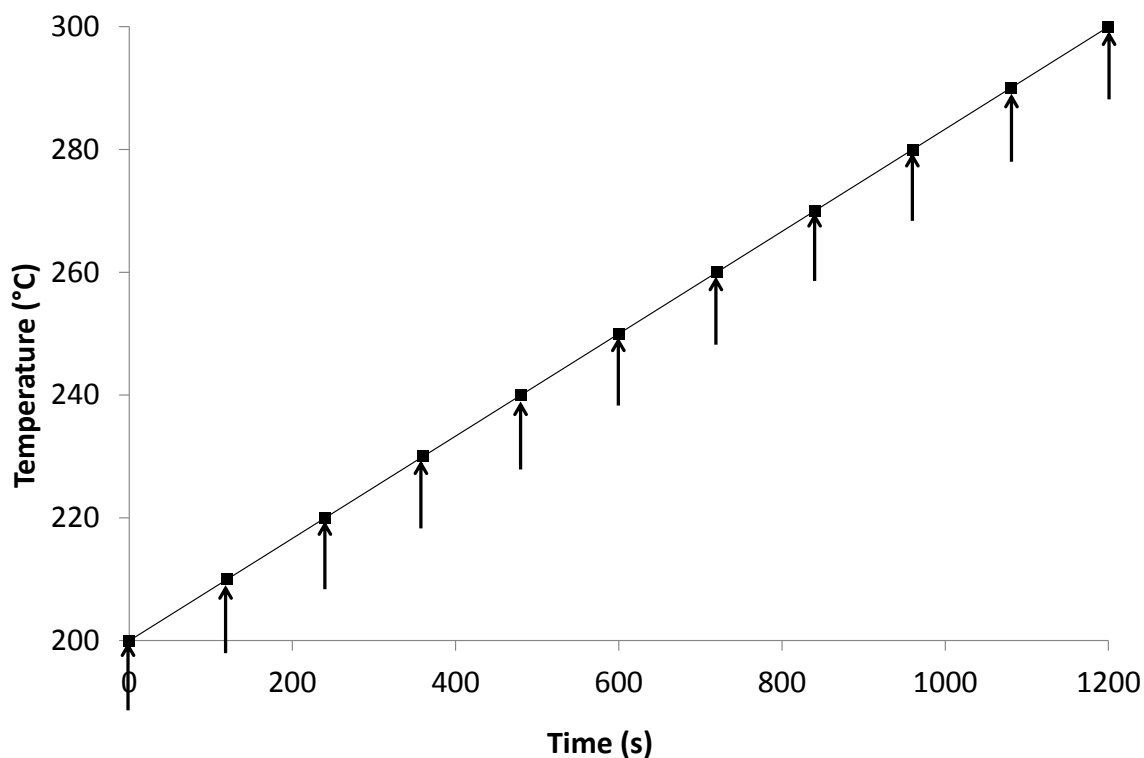


Fig. 37. Sampling temperatures in TGA-GC-MS experiments.

A set of experiments was carried out to verify the existence or not of secondary reactions within gaseous samples stocked in the Chromatostock loops. A sample of 100 mg of ash-wood was torrefied. Two samples of gaseous phase produced at 300°C were stocked (at 200°C) into two different loops. One of them was right away analyzed, whereas the other one was stocked for 18h. These conditions of temperature and storage time were chosen as the most extreme values of the TGA-GC-MS experiments. Chromatograms showed similar profiles, i.e. the same species were present after torrefaction of the sample which had not been stocked and the sample which had been stocked for 18h. This indicates that kinetics of gas-to-gas reactions were negligible during the sample storage of 18h, hence it can be claimed that no significant secondary reactions took place during storage of gaseous samples in the loops.

2.3. GAS CHROMATOGRAPH (GC)

2.3.1. Device description

The gaseous samples stocked in the Chromatostock loops were led to the Gas Chromatograph device, which was a GC Perkin-Elmer Clarus 580. The capillary column was a Perkin-Elmer Elite-1701 with a composition of 14% cyanopropylphenil-85% dimethyl polysiloxane, a non-polar stationary phase. The dimensions of this capillary column were 60 m in length, 0.25 mm in internal diameter and 0.25 μm in film thickness. On the internal surface of this capillary column, chemical species were adsorbed (attracted) and desorbed (released). Depending on their polarity, molecules were adsorbed on different adsorption sites and desorbed at different elution times. Due to the non-polar nature of this column, the lower the polarity of molecules was, the earlier they were adsorbed onto the capillary column. As temperature rose in the column, molecules started to desorb.

2.3.2. Experimental procedure

Fig. 38 showed the temperature program in the GC column, which allowed a good separation of peaks, especially of the light carboxylic acids.

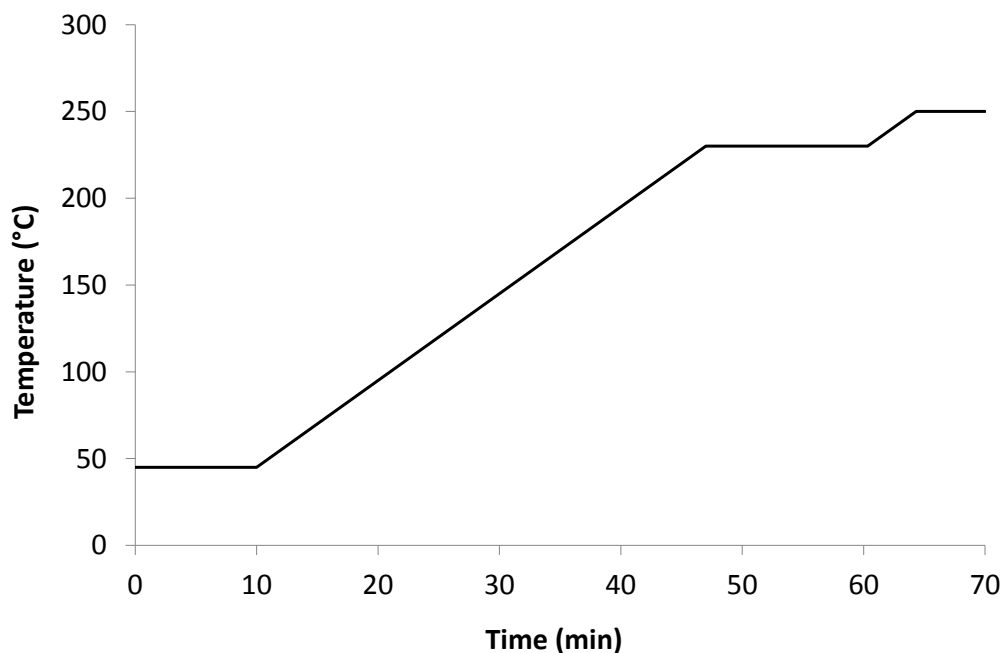


Fig. 38. Temperature profile in the GC column.

2.4. MASS SPECTROMETER (MS)

2.4.1. Device description

After the GC separation, gaseous species were sent to the Mass Spectrometer device. The MS Perkin-Elmer Clarus SQ8S allowed qualitative and quantitative analysis of the volatile species. It contained an Electron Ionization (EI) ion source, a mass analyzer and a detector. Molecules were fragmented in the ion source, then fragments were analyzed and finally identified in the detector.

2.4.2. Experimental procedure

One chromatogram of 70 min duration was obtained for each sample, which had been previously sampled at torrefaction temperatures between 200 and 300°C.

In the present work, the identified m/z values of molecules fragments ranged from 28 to 300. Once the species was identified, it could be quantified by measuring the integrated area under the corresponding peak. Thanks to an external standard calibration, a straight line correlated integrated area under the peak to an absolute quantity of gaseous species (Fougeroux, 2014).

The carrier gas in the GC-MS was helium, with a flow rate of 1 mL/min, which was established with the objective of creating a laminar regime inside the GC column. Calculations were made to check out whether the flow regime was laminar or not. Considering that the inner diameter of Chromatostock loops was of 0.5 mm, the Reynolds number (Re) was calculated for the two extremes of the temperatures interval applied. As it can be observed in Table 13, Re varied as a function of temperature.

Table 13. Helium properties in Chromatostock loops.

Property	Unit	20°C	300°C
Density	kg·m ⁻³	0.164	0.084
Viscosity	Pa·s	1.96·10 ⁻⁵	3.12·10 ⁻⁵
Re	---	0.36	0.11

These values much lower than the transition Re which is 2300 (Frank M. White, n.d.). As the transition Re indicates the change from laminar regime to turbulent regime, this means that the helium flow inside the GC column was under a laminar regime. Hence, inside the GC capillary column, gaseous species carried by helium were adsorbed onto the column and released one by one in series, without mixing. This ensured that species followed always in the same order the pathway from the GC forwards the MS.

2.4.3. TGA-GC-MS data treatment

To carry out quantification, standards were made from 1 μ L of condensable species which was diluted to make different concentrations. When the standard solution was injected in the GC column, a split of 1/10 was applied. Then a conversion factor of 10⁻⁴ correlates peak area (A_p) and concentration of species.

To carry out semi-quantification, the normalized peak area (NA_p) of condensable species is calculated taking into account the peak area (A_p), the initial sample mass (m_i) and the mass loss suffered by the sample during torrefaction, as indicated in equation (1).

$$(1) NA_p = \frac{A_p}{m_i} \cdot ML$$

The repeatability of experiments in TGA-GC-MS has been analyzed. Results have shown that the quantitative difference in formation of condensable species, obtained during two identical torrefaction experiments, is not negligible. This difference in values can vary in a factor between 3 to 7 times. Thus, quantitative and semi-quantitative experiments on condensable species formation are not repeatable for now. However, the trends of formation of condensable species obtained during two identical torrefaction experiments, appear to be very similar, as shown in Fig. 39 and Fig. 40. Thus, trends of condensable species formation in quantitative and semi-quantitative experiments are repeatable. These similarities between identical experiments, in terms of trends of condensable species formation, appear to be present for all species from all biomasses. The example in Fig. 39 shows the formation of isoeugenol during torrefaction of two identical ash-wood samples, under the same experimental conditions. In this example, it can be observed that the values of isoeugenol yield are of the same order of magnitude for both experiments at each temperature. However, the absolute values are significantly different, since the experiments of set 1 produce 3-4 times more eugenol than the experiments of set 2, from 240°C. The trends in evolution of eugenol yield are similar in both sets of experiments: the formation is negligible until 240°C, then it starts to increase; this increase accelerates between 240 and 280°C, then it decelerates from 280 to 300°C. The example in Fig. 40 shows the formation of 2-methoxy-4-vinylphenol during torrefaction of two identical pine samples, under the same experimental conditions. The values of normalized peak area of 2-methoxy-4-vinylphenol are of the same order of magnitude for both experiments at each temperature. However, the absolute values are significantly different, since the experiments of set 1 produce around 3 times more 2-methoxy-4-vinylphenol than the experiments of set 2, from 240°C. The trends in evolution of 2-methoxy-4-vinylphenol normalized peak area are similar in both sets of experiments: the formation is negligible until 240°C, then it starts to increase; this increase accelerates

between 240 and 300°C, except for pine 1 between 280 and 300°C, where there is no increase.

The reason for the relative lack of repeatability of TGA-GC-MS experiments could lie in either the pollution which tends to accumulate into the storage loops, or the differences in configuration of the TGA-GC-MS from one set of experiments to another, sometimes carried out at distant periods of time.

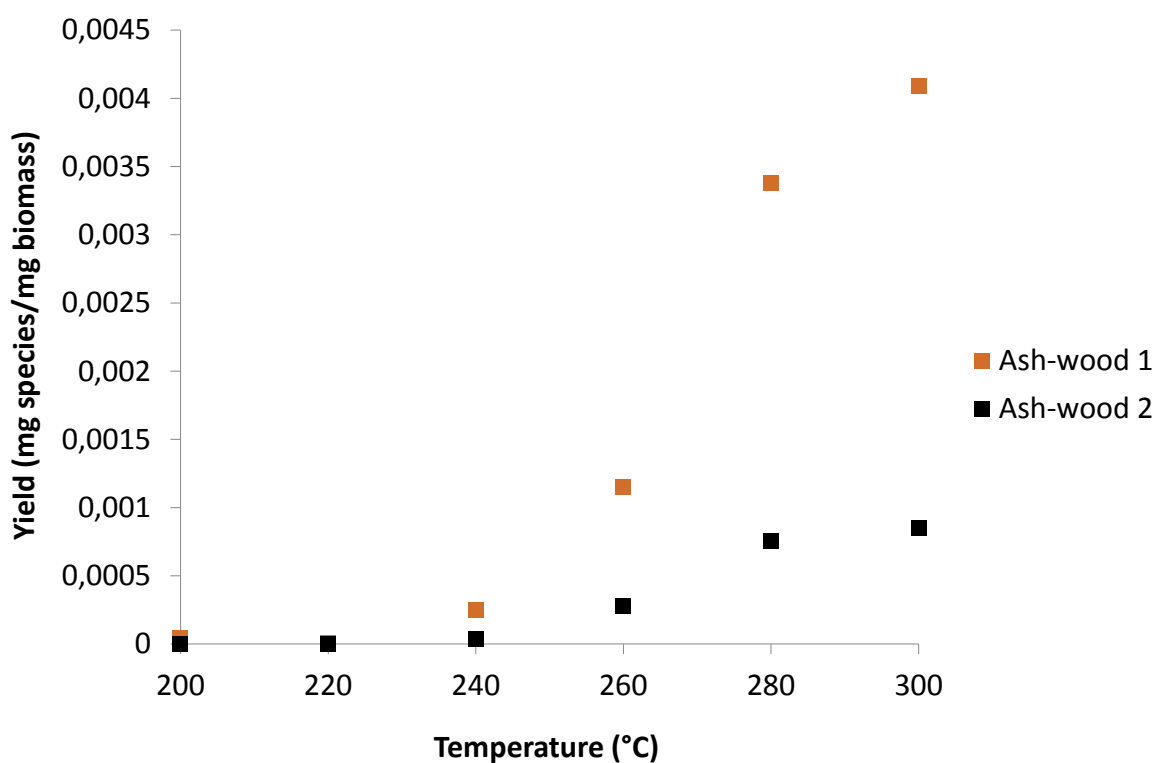


Fig. 39. Production of isoeugenol during torrefaction of ash-wood.

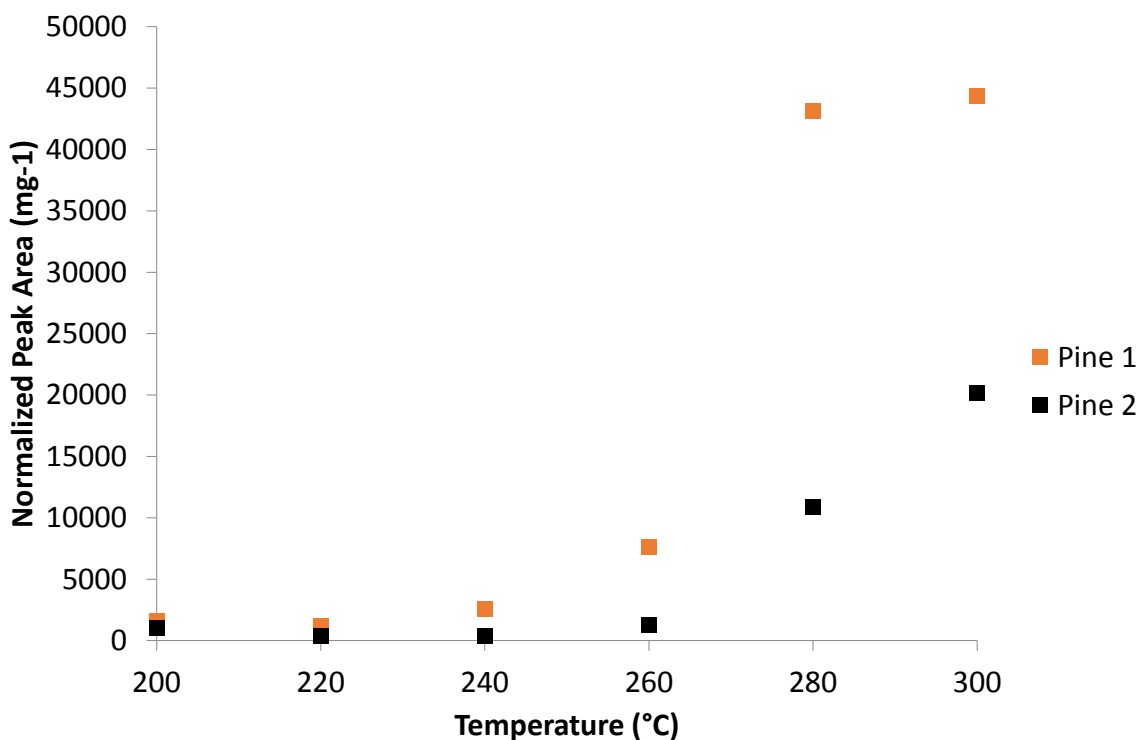


Fig. 40. Production of 2-methoxy-4-vinylphenol during torrefaction of pine.

The proportion of each semi-quantified and quantified species in the overall formation is calculated by integrating the formation of the condensable species within the interval of temperature. When the value of this integral is equal or higher than 10%, it is considered that formation of the species is significant.

The set of experiments carried out to investigate the condensable species formation during torrefaction of miscanthus turned out not to be exploitable for quantification and semi-quantification. Hence these data has only been exploited for qualitative analysis.

3. ^{13}C CP/MAS SOLID-STATE NMR

3.1. DEVICE DESCRIPTION

The study of the evolution of chemical composition in the solid phase was carried out using the ^{13}C Cross-Polarization/Magic Angle Spinning (CP/MAS) solid-state Nuclear Magnetic Resonance (NMR) technique. Experiments were performed with a Bruker Avance III 400 MHz spectrometer (see Fig. 41).



Fig. 41. Solid-state NMR device.

The spectrometer operated at 100.6 MHz for ^{13}C , using the combination of cross-polarization and magic angle spinning (CP/MAS) methods. The spinning speed was set at 12000 Hz. The ^1H radio frequency field strength was set to give a 90° -pulse duration at 2.5

μs , while the Hartman-Hahn conditions were obtained by matching the ^{13}C radio frequency field strength at 60 kHz. The standard conditions were defined by recording at least 2000 transients with a contact time of 2 ms and recycle delay of 2 s. The acquisition time was set at 30 ms and the sweep width at 29400 Hz.

The chemical shift of the carbonyl group of glycine was set at 176.03 ppm as an external standard. It was checked out that in these conditions the integrations were quantitative, taking into account a 1.1 correction for non-protonated carbons according to calibration experiments with glycine.

3.2. EXPERIMENTAL PROCEDURE

Samples investigated in solid-state NMR were raw and torrefied biomass. In order to be characterized in solid-state NMR, thermal-treated samples were previously torrefied in the TGA device with a heating rate of $5^{\circ}\text{C}/\text{min}$ until the final temperature of torrefaction (200, 220, 240, 260, 280 or 300°C). To carry out the solid-state NMR experiment, the raw or torrefied sample was packed inside the rotor and then analyzed without destruction of the sample.

In this work, the evolution of eight chemical shifts, shown in Table 14, is followed in order to study the evolution of cellulose, hemicellulose and lignin during torrefaction process. The choice of intervals has been made on the basis of chemical shifts reported in literature (Ben and Ragauskas, 2012; David et al., 2009; Holtman et al., 2010; Wikberg and Maunu, 2004; Zheng et al., 2013).

Table 14. Signal assignments for solid-state NMR spectra of biomasses.

Chemical shift (ppm)	Assignment
190-109	Aromatics in lignin
109-96	C1 of cellulose (signals for hemicellulose overlap)
92-87	C4 of crystalline cellulose
87-80	C4 of amorphous cellulose (signals for hemicellulose overlap)
68-64	C6 of crystalline cellulose
64-58	C6 of amorphous cellulose (signals for hemicellulose overlap)
58-50	Methoxyl groups (-O-CH ₃) in lignin
24-18	Acetyl groups (-CO-CH ₃) in hemicellulose

Three types of signals coexist in solid-state NMR spectra:

- Signals without overlapping from other functional groups: C4 of crystalline cellulose, C6 of crystalline cellulose and acetyl groups in hemicellulose.
- Signals overlapped by other functional groups during the whole interval of torrefaction temperatures: C1 of cellulose, C4 of amorphous cellulose and C6 of amorphous cellulose.
- Signals overlapped due to char formation: aromatics and methoxyl groups in lignin.

3.3. SOLID-STATE NMR DATA TREATMENT

Output spectra are firstly treated on two aspects:

- Corrections of phase are carried out in order to avoid dispersive components;
- Corrections of baseline aim to set the background noise to zero. This allows that an empty spectrum – carried out without sample – which only emits noise, can correspond to an area integral value of zero.

At the end of this first treatment, the areas of peak corresponding to each assignment of interest (A_p) are obtained. In the acquisition conditions used in this study, peak area is proportional to the number of carbons. These peak areas are further treated, so as to take into account the mass loss of the sample (ML) and thus compare spectra obtained at different temperatures. Thereby, the normalized peak area (NA_p) is obtained by dividing the peak area (A_p) by the total area of the spectrum (A_t), i.e. the relative abundance of each contribution, corrected by the mass loss suffered by the sample during torrefaction, as indicated in equation (2).

$$(2) NA_p = \frac{A_p}{A_t} \cdot ML$$

In the present work, the crystallinity index of cellulose is calculated for biomass samples, both raw and torrefied. It is defined as the ratio between the integrated area of the C4 peak of crystalline cellulose and the integrated total area of the two C4 peaks of cellulose – crystalline and amorphous (Heux et al., 1999).

CHAPTER IV: EXPERIMENTAL RESULTS

1. INTRODUCTION

In order to achieve the objectives exposed in section 4 of chapter I, three types of experiments have been carried out:

- Evolution of the **mass loss in the solid phase** and the **formation of condensable species in the gaseous phase**, versus temperature and biomass species, by the means of TGA-GC-MS;
- Evolution of the **functional groups in the solid phase**, versus temperature and biomass species, by the means of solid-state NMR.

Finally, a synergy of experimental results is discussed. This leads, in chapter V, to a proposition of some reaction mechanisms which take place during torrefaction.

2. MASS LOSS OF SOLID

Evolution of the mass loss of solid, followed by TGA-GC-MS, is discussed in this section. Mass loss of the four biomasses under dynamic conditions of torrefaction is shown in Fig. 42, and reaction rate is shown in Fig. 43.

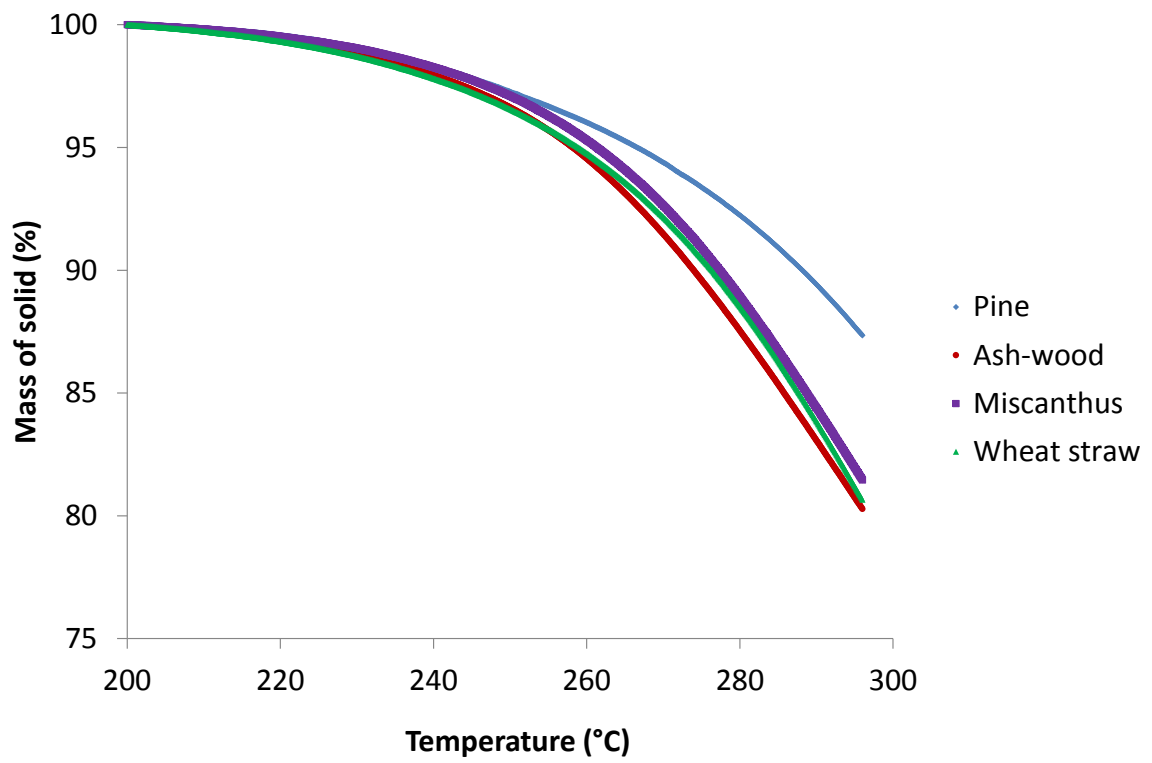


Fig. 42. Mass loss evolution of the four biomasses during dynamic torrefaction.

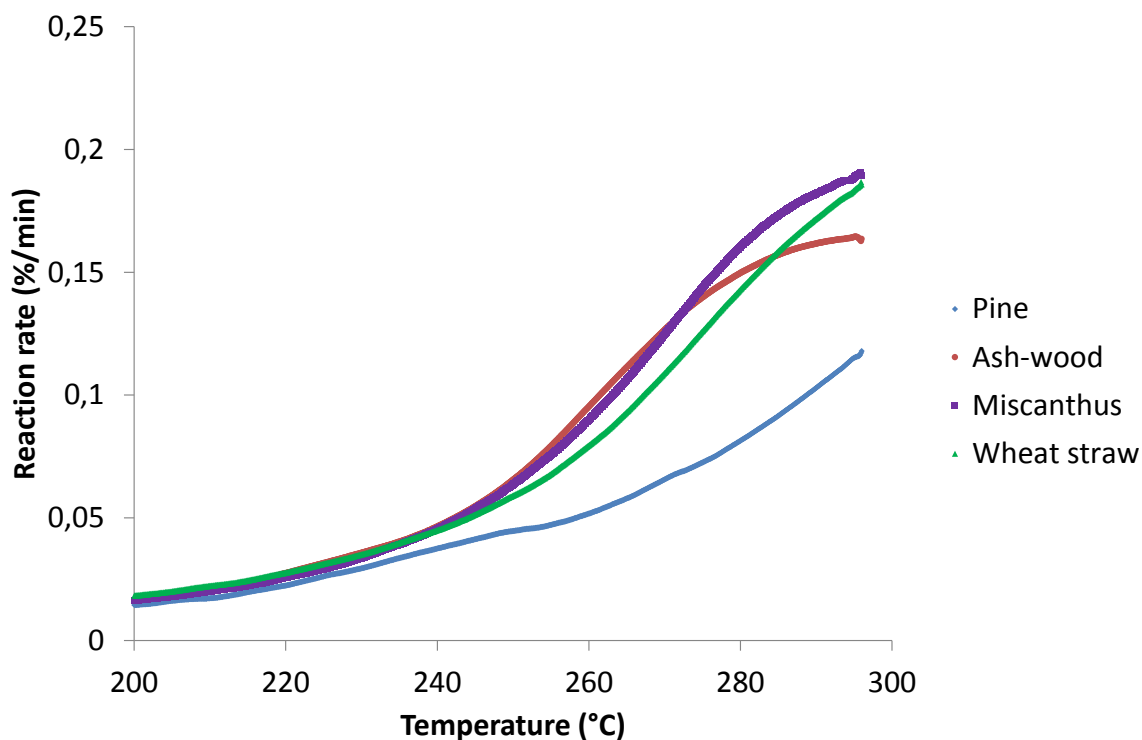


Fig. 43. Reaction rate evolution of the four biomasses during dynamic torrefaction.

Evolution of mass loss as a function of temperature during dynamic torrefaction could be divided into two stages. The first stage goes from 200 until 250°C, and corresponds to a slight increase in reaction rate, thus a slight acceleration of mass loss. The second stage goes from 250 until 300°C, and corresponds to a strong increase in reaction rate, thus a strong acceleration of mass loss.

Evolution of mass loss as a function of biomass species during dynamic torrefaction could also be divided into two stages. During the first stage of dynamic torrefaction (until 250°C), similar mass losses of 3%w take place for all biomasses. The maximal difference, in terms of mass loss, between two biomasses at the end of this first stage is lower than 1%w, which is not a significant difference. During the second stage of dynamic torrefaction, however, biomasses show different mass losses. Pine suffers mass loss of 13%w, miscanthus and wheat straw of 19%w, and ash-wood of 20%w. The maximal difference, in terms of mass loss, between two biomasses at the end of this second stage is 7%w, which is a significant difference. According to these observations, within this second stage, two families of biomasses can be differentiated. On the one

hand, pine exhibits the lowest mass loss, whereas on the other hand, miscanthus, wheat straw and ash-wood exhibit higher mass losses, and similar among them. Higher mass losses could be related to a higher content in xylan, as it is the most reactive sugar in hemicellulose. This would explain the observed trends, since ash-wood, miscanthus and wheat straw contain higher proportions of xylan than pine, and similar among them.

Dynamic torrefaction consists of increasing temperature on a ramp and then stopping thermal treatment. An alternative is to, instead of stopping the thermal treatment, add a plateau after this ramp of temperature, carrying out isothermal torrefaction. In this work, experiments under isothermal conditions of torrefaction are carried out in order to investigate the influence of residence time on solid mass loss during biomass torrefaction. A set of TGA experiments under isothermal conditions were carried out – after drying at 105°C for 1h – with a heating rate of 5°C/min, a torrefaction temperature of 280°C and 2h of residence time. These isothermal experiments are hereafter compared to the previous dynamic experiments – which had been carried out with a heating rate of 5°C/min and until a torrefaction temperature of 300°C. Mass loss of the four biomasses under isothermal conditions of torrefaction is shown in Fig. 44, and reaction rate is shown in Fig. 45.

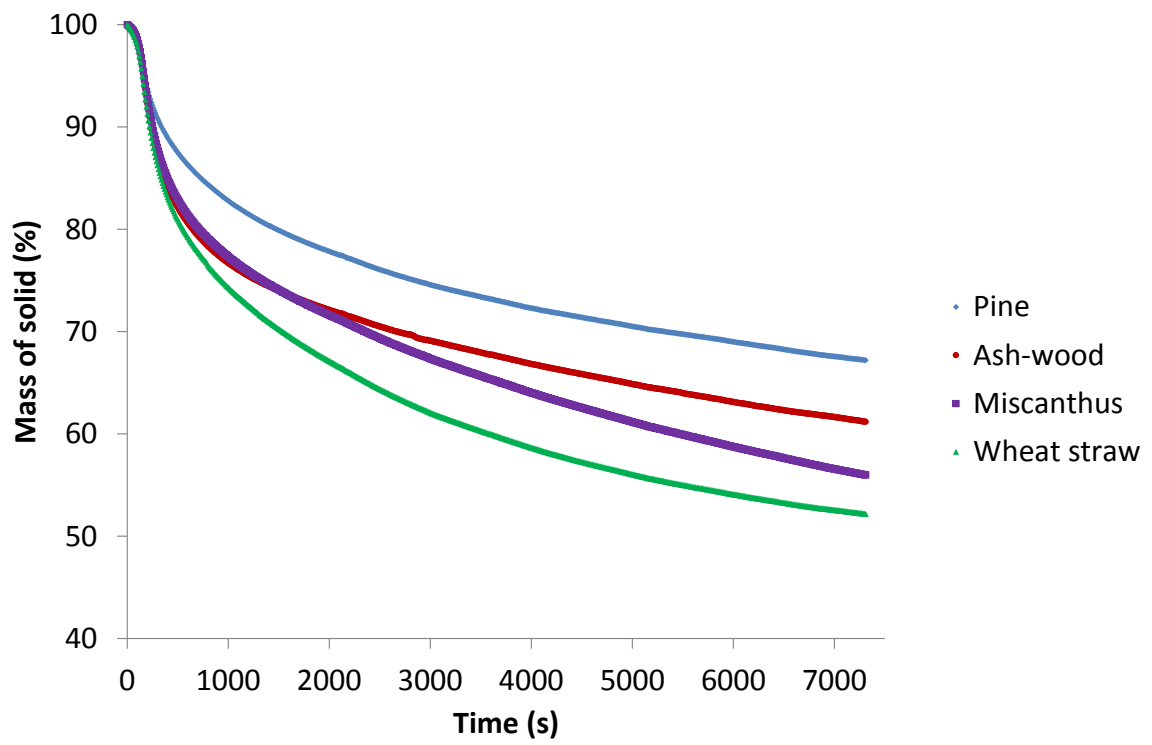


Fig. 44 Mass loss evolution of the four biomasses during isothermal torrefaction.

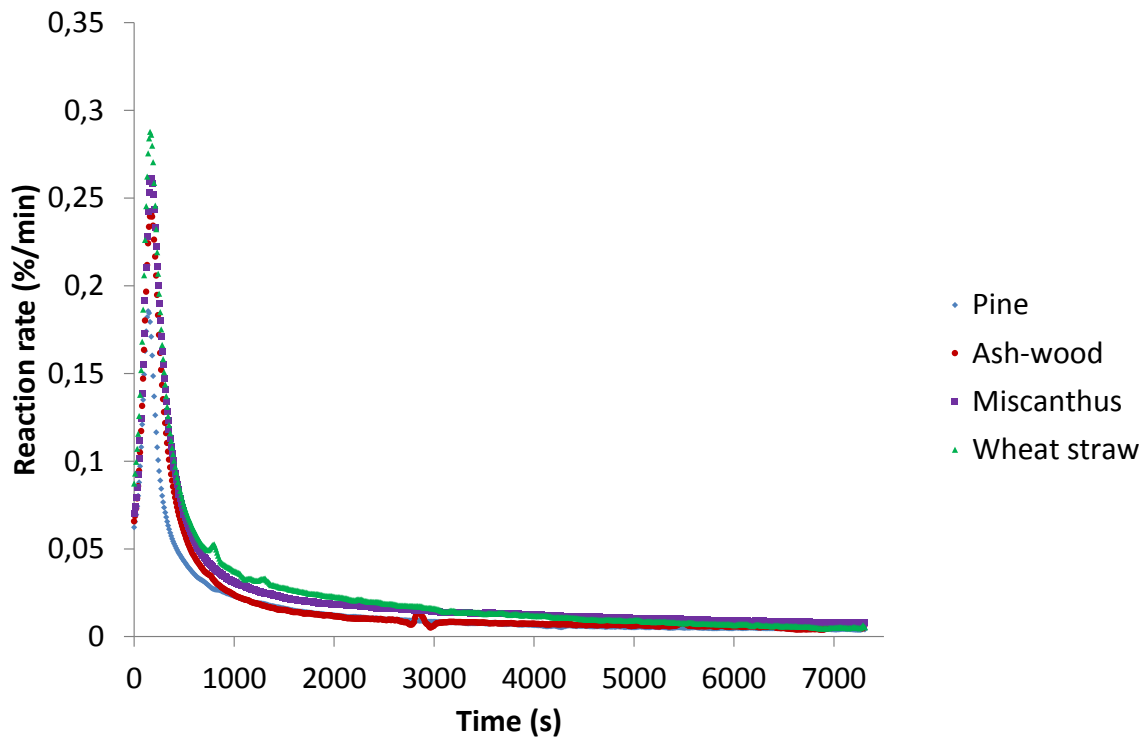


Fig. 45. Reaction rate evolution of the four biomasses during isothermal torrefaction.

Evolution of mass loss as a function of time during isothermal torrefaction could be divided into two stages, although the criterion is not the same as under dynamic conditions. The first stage corresponds to the ramp of increasing temperature, i.e. the dynamic conditions of torrefaction. During the first stage of isothermal torrefaction, reaction rate increases, thus mass loss accelerates. The second stage of isothermal torrefaction corresponds to the plateau of temperature. During this second stage, reaction rate strongly increases, afterwards it rapidly decreases and then decreases more slowly. Thus, mass loss strongly accelerates, afterwards it rapidly decelerates and then decelerates more softly.

Evolution of mass loss as a function of biomass species during isothermal torrefaction could also be divided into two stages. During the first stage of isothermal torrefaction, mass loss increases for all biomasses, reaching values of 4-6%w. The maximal difference, in terms of mass loss, between two biomasses at the end of this first stage is 1%w, which is not a significant difference. At the end of the first stage of isothermal torrefaction experiments, mass loss (4-6%w) is lower than at the end of

dynamic torrefaction experiments (13-20%w) for two reasons. The first reason is that isothermal torrefaction experiments include a drying step – at 105°C for 1h –, which is responsible for a fraction of the difference in mass loss. The second reason is that dynamic experiments reach 300°C, whereas isothermal experiments only reach 280°C, hence this would explain the other fraction of the difference in mass loss. During the second stage of isothermal torrefaction, pine suffers mass loss of 33%w, ash-wood of 39%w, miscanthus of 44%w and wheat straw of 48%w. The maximal difference, in terms of mass loss, between two biomasses at the end of this second stage is 15%w, which is a significant difference. Hence, during the second stage of isothermal torrefaction, biomasses present different mass loss behaviors. However, one does not find two families of behavior like during dynamic torrefaction, but it rather seems that each biomass represents a family of behavior. The least consumed biomass continues to be pine, like under dynamic conditions. The most consumed biomass under isothermal conditions is wheat straw, followed by miscanthus and ash-wood, as explained before. It can be concluded that the evolution of mass loss is related to the proportion and composition of the main constituents in biomass. During dynamic torrefaction, the most affected constituent is hemicellulose, thus differences in mass loss evolution may be mostly linked to the proportion and composition of hemicellulose in each biomass. During isothermal torrefaction, differences in mass loss evolution may be also linked to the proportion of cellulose and lignin in each biomass, as well as crystallinity of cellulose and lignin composition in each biomass.

These trends have been reported before under the same isothermal conditions of torrefaction – a torrefaction temperature of 280°C and 2h of residence time, although the heating rate was higher, 30°C/min (Dupont et al., 2011). These authors classified biomasses into three families, as shown in Fig. 46. Each biomass of the present work can be related to one of the families presented in their work. Thereby, pine belongs to softwood family, ash-wood to hardwood family, miscanthus to perennial crops family and wheat straw to cereal crops or agricultural by-products family. For Dupont et al. (2011), the hardwood tested is the least reactive biomass, followed by the softwood, the perennial crop and the cereal crop. Hence, they observed that, under isothermal

conditions at 280°C for 2h, non-woody biomasses are more reactive than woody biomasses.

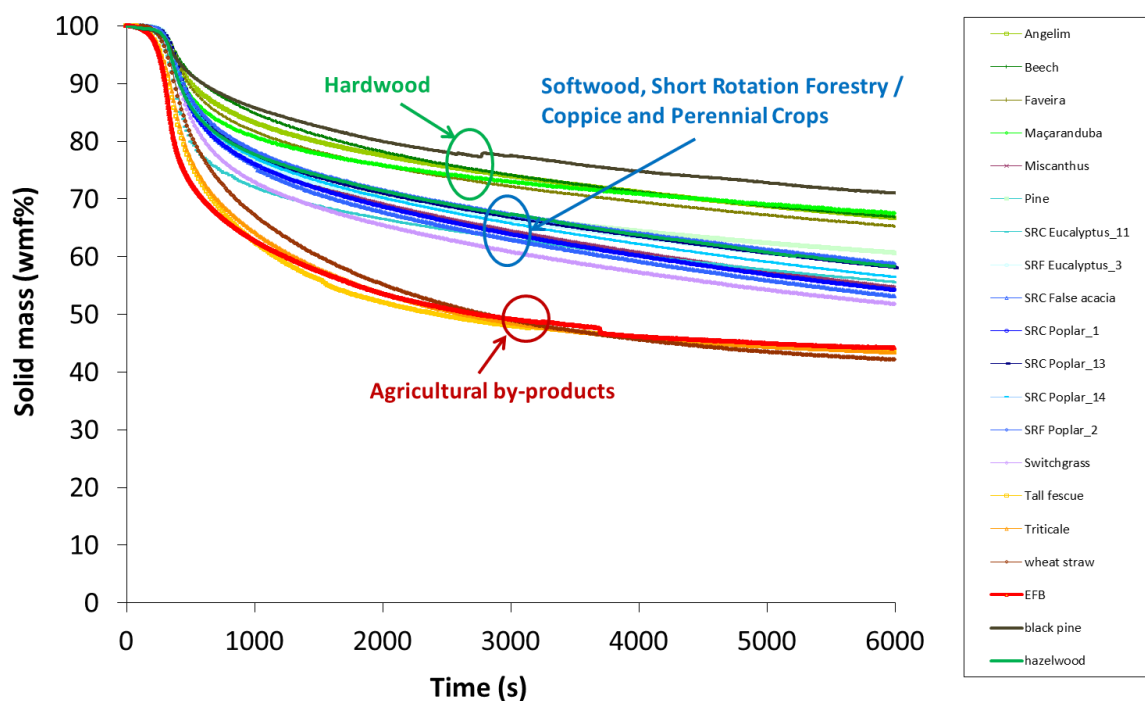


Fig. 46. Mass loss of several biomasses during torrefaction under isothermal conditions (T = 280°C, t = 2h, heating rate = 30°C/min) (Dupont et al., 2011).

3. FORMATION OF CONDENSABLE SPECIES

In this section, the evolution of the production of condensable species in the gaseous phase, followed by TGA-GC-MS, is discussed.

3.1. QUALITATIVE RESULTS

In Table 15, Table 16, Table 17 and Table 18, the thirty-two condensable species detected during torrefaction of the four biomasses are presented.

Two general families of condensable species can be identified:

- The first family of condensable species is constituted by extractive species which are mainly produced during the first half of torrefaction, from 200°C until 250-260°C. These species are α -pinene, camphene, β -pinene, D-limonene and cymene. These “classic” extractive species are only released by pine, whereas the other three biomasses do not emit these extractive species at any temperature.
- The second family of condensable species is constituted by those mainly produced either only during the second half of torrefaction, or during the whole interval of torrefaction temperatures:
 - The condensable species mainly produced during the second half of torrefaction, from 240-250°C until 300°C, are: 2-methylfuran, glycolaldehyde, propanoic acid, 2-butanone-1-hydroxy-, 2(5H)-furanone-5-methyl-, 2-cyclopenten-1-one-2-hydroxy-, phenol-2-methoxy-, eugenol and isoeugenol.
 - The condensable species mainly produced during the whole interval of torrefaction are: methanol, 2,3-butanedione, formic acid, acetic acid, hydroxyacetone, furfural, 2-furanmethanol, 2-propanone-1-(acetyloxy)-, 4-cyclopentene-1,3-dione, cymene – the only extractive species produced during the whole interval of torrefaction –, benzaldehyde, 2-furancarboxaldehyde-5-methyl-, butyrolactone, 2-methoxy-4-vinylphenol, 2(5H)-furanone, phenol, hydroxymethylfurfural (HMF) and vanillin.

The majority of condensable species included in this second family are formed during torrefaction of the four biomasses. Methanol, furfural, 2-furanmethanol, butyrolactone, 2-furancarboxaldehyde-5-methyl-, phenol, 2-methoxy-4-vinylphenol and vanillin are produced within the whole spectrum of temperatures from the four biomasses. 1-Hydroxy-2-butanone, 2-propanone-1-(acetyloxy)-, 2(5H)-furanone-5-methyl-, 2-cyclopenten-1-one-2-hydroxy-, phenol and phenol-2-methoxy- are produced from non-woody biomasses at low temperature (200°C), whereas they are formed from woody

biomasses at higher temperature (210-240°C). Some condensable species present a different evolution for one biomass in comparison with the others. Glycolaldehyde, formic acid, 2(5H)-furanone, 4-cyclopentene-1,3-dione and 2-methylfuran are formed at a different temperature for pine in comparison with ash-wood, miscanthus and wheat straw. Glycolaldehyde is produced from pine at 270°C, whereas at 220-230°C from the other three biomasses; formic acid is produced from pine at 230°C, whereas at 200-210°C from the other biomasses; 2(5H)-furanone is formed at 220°C from pine, but at 200°C from the other biomasses; 4-cyclopentene-1,3-dione is produced at 240°C from pine, but at 200°C from the others. However, 2-methylfuran is produced at 200°C from pine, whereas at 240-260°C from the other biomasses. 2,3-Butanedione is produced during the whole range of torrefaction temperatures from wheat straw, whereas it is formed only at 230-260°C from pine, ash-wood and miscanthus. Other condensable species show specific evolutions. Acetic acid, hydroxyacetone and isoeugenol are formed from all the biomasses but at a different temperature. Acetic acid is formed at 240°C from pine, at 220°C from ash-wood, at 230°C from miscanthus and at 200°C from wheat straw. Hydroxyacetone is formed at 260°C from pine, at 220°C from ash-wood, at 230°C from miscanthus and at 200°C from wheat straw. Isoeugenol is formed at 260°C from pine, miscanthus and wheat straw, whereas at 200°C from ash-wood. Hydroxymethylfurfural (HMF) is produced during the whole torrefaction of pine, ash-wood and wheat straw, but is barely formed during torrefaction of miscanthus – only from 200 to 230°C. Benzaldehyde is released from low temperatures for every biomass, but at high temperatures it disappears for miscanthus (260°C) and wheat straw (270°C). Eugenol is produced at 250°C from pine and at 260°C from ash-wood, however it is not produced from non-woody biomasses.

Lê Thành et al. (2015) identified condensable species formed during torrefaction of the same four biomasses. Some of the species that they identified are in common to the present work, while others are not. The common identified species are acetic acid, 2-propanone,1-hydroxy-, methanol, 2-furanmethanol, formic acid, 2-methoxy-4-vinylphenol, 2-butanone-1-hydroxy-, furfural, 1-acetyloxy-2-propanone, propanoic acid, isoeugenol and phenol-2-methoxy-.

They also identified some species which were not detected in the present work, such as formaldehyde, LAC – which stands for 3,6-dioxabicyclo[3.2.1]octan-2-one,1-hydroxy-,(1R) –, DGP – which stands for 1,4:3,6-dianhydro- α -D-glucopyranose – and levoglucosan. Several works in literature have detected formaldehyde during torrefaction (Anca-Couce et al., 2014; Bridgeman et al., 2008; Nocquet et al., 2014a), thus the reason for not detecting it in the present work could be that the quantity formed was below the detection limit. Lê Thành et al. (2015) measured significant quantities of formaldehyde from 250°C to 300°C, except for wheat straw at 250 and 280°C. The molecules LAC, DGP and levoglucosan are sugars which start to form at high temperatures of torrefaction, thus in the present work they were probably very diluted to reach the detection limit of the MS. Lê Thành et al. (2015) detected glycolaldehyde dimer, which is the dimeric state of the glycolaldehyde detected in the present work. The reason why they detected the dimer could be that glycolaldehyde is a reactive molecule, which becomes more stable after dimerization. In addition, some other molecules were detected in the present work, but not by Lê Thành et al. (2015), for instance, 3-butanedione and 2(5H)-furanone-5-methyl-.

Table 15. Condensable species produced during torrefaction of pine.

	Elution time (min)	Temperature (°C)										
		200	210	220	230	240	250	260	270	280	290	300
Methanol	4.80	X		X	X	X	X	X	X	X	X	X
2-Methylfuran	7.05	X						X	X	X	X	X
2,3-Butanedione	8.33				X	X	X	X	X	X	X	X
Glycolaldehyde	10.51								X	X	X	X
Formic acid	10.99				X	X	X	X	X	X	X	X
Acetic acid	12.88					X	X	X	X	X	X	X
Hydroxyacetone	14.82							X	X	X	X	X
Propanoic acid	18.09				?	X	X	X	X	X	X	X
2-Butanone-1-hydroxy-	20.13					X		X	X	X	X	X
α-Pinene	21.79	X		?								
Camphene	22.84	X		X	X	X	X	X	X			
Furfural	23.10	X		X	X	X	X	X	X	X	X	X
β-Pinene	24.24	X										
2-Furanmethanol	24.87	X		X	X	X	X	X	X	X	X	X
2-Propanone-1-(acetyloxy)-	25.27				X	X	X	X	X	X	X	X
2(5H)-Furanone-5-methyl-	25.91			?	?	X	X	X	X	X	X	X
D-Limonene	26.48	X		X	X	X	X	X	X			
4-Cyclopentene-1,3-dione	26.85	X		X	X	X	X	X	X	X	X	X
Cymene	27.19	X		X	X	X	X	X	X	X	X	
2-Cyclopenten-1-one-2-hydroxy-	27.61			?	?	X	X	X	X	X	X	X
Benzaldehyde	27.88	X		X	X	X	X	X	X		X	?
2-Furancarboxaldehyde-5-methyl-	28.78	X		X	X	X	X	X	X	X	X	X
Butyrolactone	29.70	X		X	X	X	X	X	X	X	X	X
2(5H)-Furanone	30.06			X	X	X	X	X	X	X	X	X
Cymenene	30.27	X				X	X	X	X			
Phenol	32.25	X		X	X	X	X	X	X	X	X	
Phenol-2-methoxy-	33.06					X	X	X	X	X	X	X
2-Methoxy-4-vinylphenol	40.70	X		X	X	X	X	X	X	X	X	X
Eugenol	41.37							X	X	X	X	X
Hydroxymethylfurfural (HMF)	41.69	X			X	X	X	X	X	X	X	X
Isoeugenol	44.41							X	X	X	X	X
Vanillin	45.16			X	X	X	X	X	X	X	X	X

Table 16. Condensable species produced during torrefaction of ash-wood.

	Elution time (min)	Temperature (°C)										
		200	210	220	230	240	250	260	270	280	290	300
Methanol	4.80	X	X	X	X	X	X	X	X	X	X	X
2-Methylfuran	7.05							X		X	X	X
2,3-Butanedione	8.33			?				X	X	X	X	X
Glycolaldehyde	10.51				X	X	X	X	X	X	X	X
Formic acid	10.99		X	X	X	X	X	X	X	X	X	X
Acetic acid	12.88			X	X	X	X	X	X	X	X	X
Hydroxyacetone	14.82			X	X	X	X	X	X	X	X	X
Propanoic acid	18.09											
2-Butanone-1-hydroxy	20.13			X	X	X	X	X	X	X	X	X
α-Pinene	21.79											
Camphene	22.84											
Furfural	23.10	X	X	X	X	X	X	X	X	X	X	X
β-Pinene	24.24											
2-Furanmethanol	24.87	X	X	X	X	X	X	X	X	X	X	X
2-Propanone-1-(acetyloxy)-	25.27		X	X	X	X	X	X	X	X	X	X
2(5H)-Furanone-5-methyl-	25.91					X	X	X	X	X	X	X
D-Limonene	26.48											
4-Cyclopentene-1,3-dione	26.85			X	X	X	X	X	X	X	X	X
Cymene	27.19											
2-Cyclopenten-1-one-2-hydroxy-	27.61			X	X	X	X	X	X		?	?
Benzaldehyde	27.88		X	X	X	X	X	X	X	X	X	X
2-Furancarboxaldehyde-5-methyl-	28.78	X	X	X	X	X	X	X	X	X	X	X
Butyrolactone	29.70	X	X	X	X	X	X	X	X	X	X	X
2(5H)-Furanone	30.06	X	X	X	X	X	X	X	X	X	X	X
Cymenene	30.27											
Phenol	32.25		X	X	X	X	X	X	X	X	X	X
Phenol, 2-methoxy-	33.06		X	X	X	X	X	X	X	X	X	X
2-Methoxy-4-vinylphenol	40.70	X	X	X	X	X	X	X	X	X	X	X
Eugenol	41.37						X	X	X	X	X	X
Hydroxymethylfurfural (HMF)	41.69	X	X	X	X	X	X	X	X	X	X	X
Isoeugenol	44.41	X		X	X	X	X	X	X	X	X	X
Vanillin	45.16	X	X	X	X	X	X	X	X	X	X	X

Table 17. Condensable species produced during torrefaction of miscanthus.

	Elution time (min)	Temperature (°C)										
		200	210	220	230	240	250	260	270	280	290	300
Methanol	4.80	X	X	X	X	X	X	X	X	X	X	X
2-Methylfuran	7.05						X		X	X	X	X
2,3-Butanedione	8.33		X			X	X	X	X	X	X	X
Glycolaldehyde	10.51			X	X	X		X	X	X	X	X
Formic acid	10.99	X	X	X	X	X	X	X	X	X	X	X
Acetic acid	12.88				X	X	X	X	X	X	X	X
Hydroxyacetone	14.82				X	X	X	X	X	X	X	X
Propanoic acid	18.09											
2-Butanone-1-hydroxy	20.13	X		X	X	X	X	X	X	X	X	X
α-Pinene	21.79											
Camphene	22.84											
Furfural	23.10	X	X	X	X	X	X	X	X	X	X	X
β-Pinene	24.24											
2-Furanmethanol	24.87	X	X	X	X	X	X	X	X	X	X	X
2-Propanone-1-(acetyloxy)-	25.27	X	X	X	X	X	X	X	X	X	X	X
2(5H)-Furanone-5-methyl-	25.91	X	X		X	X	X	X	X	X	X	X
D-Limonene	26.48											
4-Cyclopentene-1,3-dione	26.85	X	X	X	X	X	X	X	X	X	X	X
Cymene	27.19											
2-Cyclopenten-1-one-2-hydroxy-	27.61	X	X	X	X	X	X	X	X	?	?	X
Benzaldehyde	27.88		X	X	X	X	X					
2-Furancarboxaldehyde-5-methyl-	28.78	X	X	X	X	X	X	X	X	X	X	X
Butyrolactone	29.70	X	X	X	X	X	X	X	X	X	X	X
2(5H)-Furanone	30.06	X	X	X	X	X	X	X	X	X	X	X
Cymenene	30.27											
Phenol	32.25	X	X	X	X	X	X	X	X	X	X	X
Phenol, 2-methoxy-	33.06	X	X	X	X	X	X	X	X	X	X	X
2-Methoxy-4-vinylphenol	40.70	X	X	X	X	X	X	X	X	X	X	X
Eugenol	41.37											
Hydroxymethylfurfural (HMF)	41.69	X		X	X							
Isoeugenol	44.41							X	X	X	X	X
Vanillin	45.16	X	X	X	X	X	X	X	X	X	X	X

Table 18. Condensable species produced during torrefaction of wheat straw.

	Elution time (min)	Temperature (°C)										
		200	210	220	230	240	250	260	270	280	290	300
Methanol	4.80	X	X	X	X	X	X	X	X	X	X	X
2-Methylfuran	7.05			X		X	X	X	X	X	X	X
2,3-Butanedione	8.33	X	X	X	X	X	X	X	X	X	X	X
Glycolaldehyde	10.51			X	X	X		X	X	X	X	X
Formic acid	10.99	X	X	X	X	X	X	X	X	X	X	X
Acetic acid	12.88	X	X	X	X	X	X	X	X	X	X	X
Hydroxyacetone	14.82	X	X	X	X	X	X	X	X	X	X	X
Propanoic acid	18.09											
2-Butanone-1-hydroxy	20.13	X	X	X	X	X	X	X	X	X	X	X
α -Pinene	21.79											
Camphene	22.84											
Furfural	23.10	X	X	X	X	X	X	X	X	X	X	X
β -Pinene	24.24											
2-Furanmethanol	24.87	X	X	X	X	X	X	X	X	X	X	X
2-Propanone-1-(acetyloxy)-	25.27	X	X	X	X	X	X	X	X	X	X	X
2(5H)-Furanone-5-methyl-	25.91	X	X	X	X	X		X	X	X	X	X
D-Limonene	26.48											
4-Cyclopentene-1,3-dione	26.85	X	X	X	X	X	X	X	X		X	X
Cymene	27.19											
2-Cyclopenten-1-one-2-hydroxy-	27.61	X	X	X	X	X	X	?	?	X	X	X
Benzaldehyde	27.88	X	X	X	X	X	X	X			X	?
2-Furancarboxaldehyde-5-methyl-	28.78	X	X	X	X	X	X	X	X	X	X	X
Butyrolactone	29.70	X	X	X	X	X	X	X	X	X	X	X
2(5H)-Furanone	30.06	X	X	X	X		X	X	X	X	X	X
Cymenene	30.27											
Phenol	32.25	X	X	X	X	X	X	X	X	X	X	X
Phenol, 2-methoxy-	33.06	X	X	X	X	X	X	X	X	X	X	X
2-Methoxy-4-vinylphenol	40.70	X	X	X	X	X	X	X	X	X	X	X
Eugenol	41.37											
Hydroxymethylfurfural (HMF)	41.69	X	X	X	X	X	X	X	X	X		
Isoeugenol	44.41							X	X	X	X	X
Vanillin	45.16	X	X	X	X	X	X	X	X	X	X	X

From the qualitative analysis of these thirty-two condensable species produced during torrefaction, it was found that:

- One can find formation of condensable species within the whole range of torrefaction temperatures;
- Fourteen (out of thirty-two) condensable species were produced within the whole interval of torrefaction temperatures, seven species were formed during the first half of the interval of torrefaction temperatures, and nine species were formed during the second half;
- Twenty-two (out of thirty-two) condensable species were produced from all biomass species;
- Five extractive species were only measured during torrefaction of pine (softwood).

Based on these results, quantification has been carried out for condensable species abundantly produced during torrefaction and for which external standards were available in laboratory. Semi-quantification has been carried out for condensable species abundantly produced during torrefaction and for which external standards were not available.

3.2. QUANTITATIVE RESULTS

3.2.1. Hydroxyacetone

The formation of hydroxyacetone shows similar trends, whatever biomass (see Fig. 47). Hydroxyacetone is produced mainly from 250°C. At this temperature, the increase in its production accelerates, and then it tends to decelerate at higher temperatures, between 280 and 300°C. Wheat straw and ash-wood form more hydroxyacetone (7 and 3 times more, respectively) than pine in the overall torrefaction.

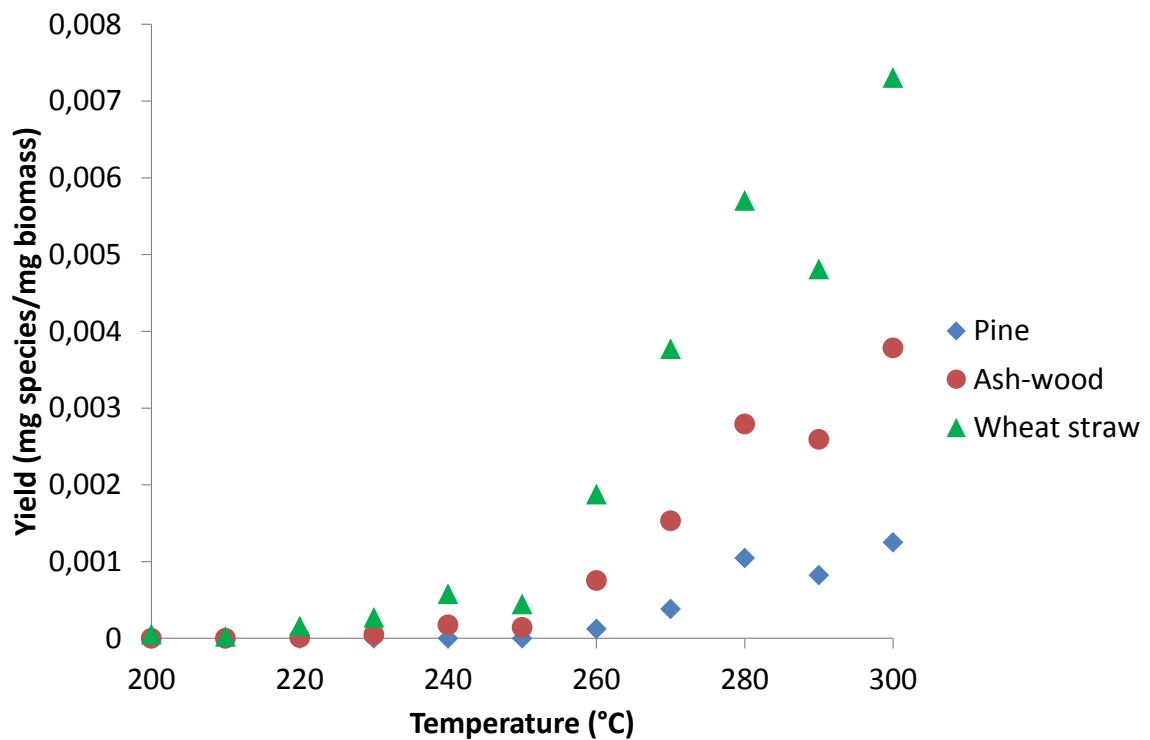


Fig. 47. Production of hydroxyacetone during torrefaction.

Table 19 shows the proportion of hydroxyacetone in the overall formation at each temperature for each biomass. It can be observed that hydroxyacetone is significantly formed from 270°C for every biomass. More precisely, from 270 until 300°C, 97% of the hydroxyacetone formed from pine is produced, 91% of the formed from ash-wood and 65% of the formed from wheat straw.

Table 19. Proportion of hydroxyacetone in the overall formation at each temperature.

T (°C)	Proportion in the overall formation (%)		
	Pine	Ash-wood	Wheat straw
200	---	---	---
210	---	---	0.2
220	---	0.1	0.1
230	---	0.4	0.6
240	---	1.5	1.1
250	---	1.2	2.3
260	3.4	6.4	1.8
270	10.6	13.0	7.5
280	28.8	23.6	15.1
290	22.7	21.9	22.9
300	34.5	32.0	19.3

In literature, Lê Thành et al. (2015) also detected hydroxyacetone during isothermal torrefaction of pine, ash-wood, miscanthus and wheat straw. Isothermal conditions consisted of a heating rate of 10°C/min, final temperatures of torrefaction of 250, 280 and 300°C, and 45 min of residence time (see Table 20). The proportions of hydroxyacetone in the overall formation at 250, 280 and 300 °C, have been compared between the work of Lê Thành et al. (2015) and the present work. However, the difference between their isothermal and our dynamic conditions of torrefaction has to be taken into account. Firstly, values in the present work are lower in comparison with Lê Thành et al. (2015). The reason could be that their value includes the formation of the condensable species during the temperature ramp of 10°C/min plus the residence time of 45 min, whereas, in the present work, only the formation during the temperature ramp is considered. Thus a higher amount of the condensable species would be accumulated in their case. Regarding the influence of temperature, values in the present work increase as temperature increases, and this observation agrees with Lê Thành et al. (2015). In the present work, only in one case it has not been possible to measure hydroxyacetone, probably because its quantity was lower than the detection limit. Regarding the influence of biomass species, values in the present work are far from those of Lê Thành et al. (2015) for all biomasses.

Table 20. Comparative formation of hydroxyacetone (mg/g initial biomass).

Biomass	Lê Thành et al. (2015) Isothermal profile			Our work Dynamic profile		
	250°C	280°C	300°C	250°C	280°C	300°C
Pine	1.1	6.3	12.2	---	1.0	1.2
Ash-wood	1.9	5.9	12.1	0.1	2.8	3.8
Wheat straw	3.1	12.6	18.2	0.4	5.7	7.3

Hydroxyacetone would be mainly formed from cellulose degradation. One hypothesis is that lignin may protect cellulose fibrils, thus a higher content in lignin would mean higher protection of cellulose from thermal degradation. Ash-wood and pine – woody biomasses – contain higher proportions of lignin, whereas wheat straw – non-woody biomass – contains lower proportions. Hence cellulose in ash-wood and pine would be more protected from thermal degradation than in wheat straw, which would result in lower quantities of hydroxyacetone formed during ash-wood and pine torrefaction.

3.2.2. Acetic acid

The production of acetic acid shows different trends among biomasses (see Fig. 48). Acetic acid is slightly produced from 200°C. The increase in its production accelerates from 240°C, and then it decelerates from 280°C. For ash-wood, production decreases from 280°C. In the overall torrefaction, ash-wood and wheat straw form more acetic acid (8 and 6 times more, respectively) than pine.

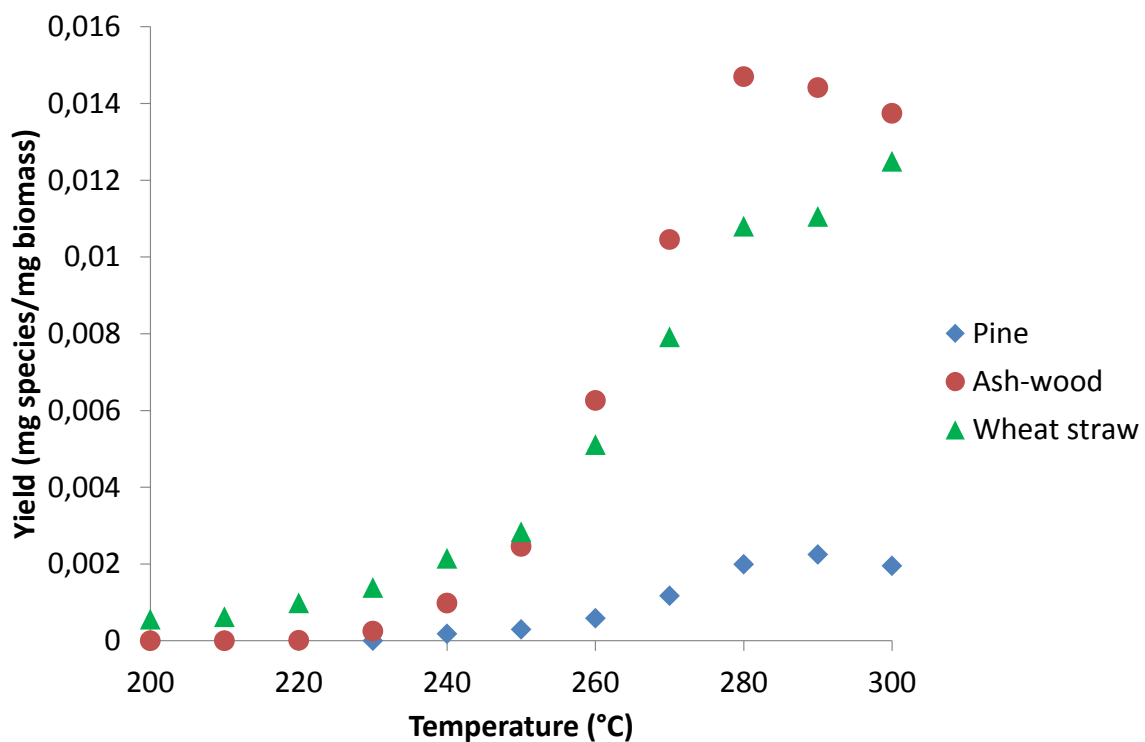


Fig. 48. Production of acetic acid during torrefaction.

Table 21 shows the proportion of acetic acid in the overall formation at each temperature for each biomass. Despite the fact that ash-wood and wheat straw start to produce acetic acid before pine, this species is significantly formed from 270°C for the three biomasses. Within the short interval of temperatures between 270 and 300°C, 87% of the acetic acid from pine is formed, 84% of the formed from ash-wood and 76% of the formed from wheat straw.

Table 21. Proportion of acetic acid in the overall formation at each temperature.

T (°C)	Proportion in the overall formation (%)		
	Pine	Ash-wood	Wheat straw
200	---	---	---
210	---	---	1.1
220	---	0.0	1.8
230	---	0.4	2.5
240	2.2	1.6	3.9
250	3.5	3.9	5.1
260	7.0	9.9	9.2
270	13.9	16.5	14.3
280	23.7	23.2	19.5
290	26.7	22.8	20.0
300	23.1	21.7	22.6

Lê Thành et al. (2015) have also measured acetic acid formation during isothermal torrefaction for 45 min (see Table 22). Values obtained in the present work are lower than those of Lê Thành et al. (2015), like in the case of hydroxyacetone, and probably for the same reason. Regarding the influence of temperature, values in the present work do not completely agree with those of Lê Thành et al. (2015). In their work, values rise as temperature increases. In the present work, only half of the values follow this trend. The other half of the values – formation from pine at all temperatures, and formation from ash-wood at 300°C – decrease as temperature increases. Regarding the influence of biomass species, values in the present work are far from those of Lê Thành et al. (2015) for all biomasses, like in the case of hydroxyacetone.

Table 22. Comparative formation of acetic acid (mg/g initial biomass).

Biomass	Lê Thành et al. (2015)			Our work		
	Isothermal profile			Dynamic profile		
	250°C	280°C	300°C	250°C	280°C	300°C
Pine	4.5	14.2	19.4	0.3	2.0	2.0
Ash-wood	27.1	40.8	47.2	2.5	14.7	13.7
Wheat straw	18.6	31.9	39.1	2.8	10.8	12.5

Acetic acid is said to be formed from the release of acetyl groups contained in hemicellulose, mainly in xylan (Nocquet et al., 2014a; Prins et al., 2006a). Moreover, xylan is known to be the most reactive sugar in hemicellulose, as mentioned before. Hence, the

higher proportion of xylan in ash-wood and wheat straw in comparison with that in pine, could explain the fact that ash-wood and wheat straw produce higher quantities of acetic acid during torrefaction than pine.

3.2.3. 2-Furanmethanol

The formation of 2-furanmethanol shows different trends among biomasses (see Fig. 49). 2-Furanmethanol is produced from approximately 240°C. The increase in its formation accelerates up to 280°C, and then decelerates. Ash-wood and wheat straw form more 2-furanmethanol than pine (3 and 3.5 times more, respectively) in the overall torrefaction.

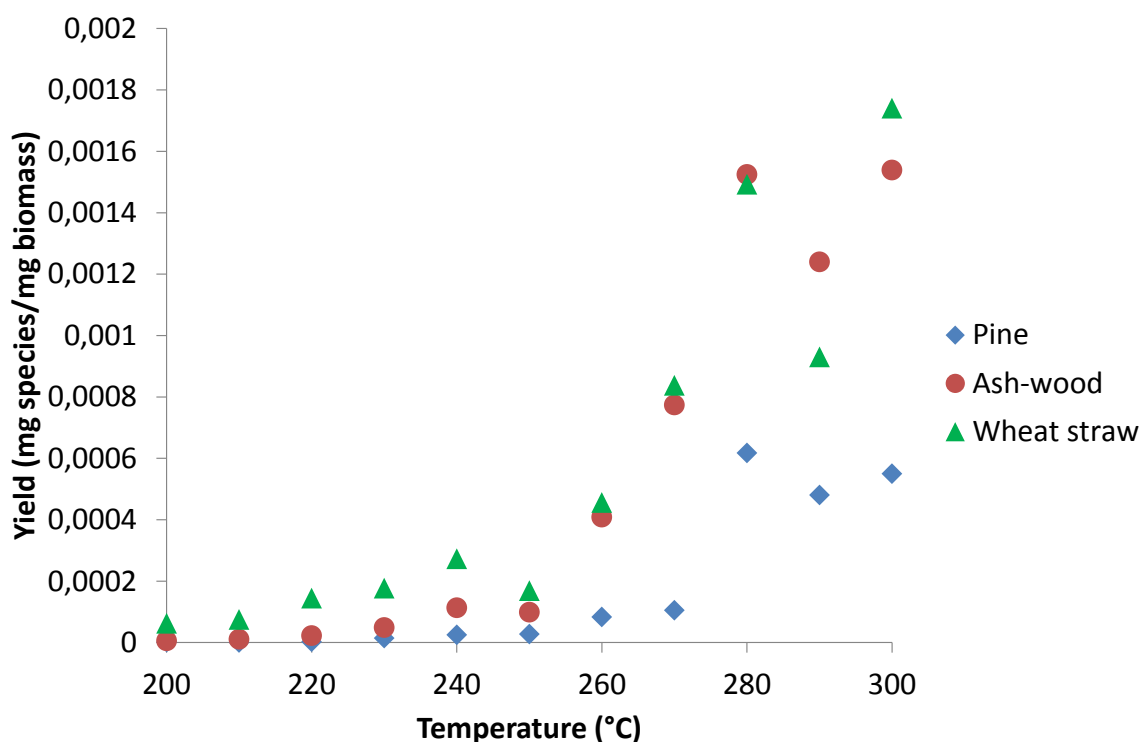


Fig. 49. Production of 2-furanmethanol during torrefaction.

Table 23 shows the proportion of 2-furanmethanol in the overall formation at each temperature for each biomass. Like in the case of hydroxyacetone and acetic acid, 2-

furanmethanol is significantly formed from the same temperature for all biomasses. Within the interval of temperature from 270 until 300°C, 92% of the total 2-furanmenthanol from pine is formed, 88% of that from ash-wood and 80% of that from wheat straw.

Table 23. Proportion of 2-furanmethanol in the overall formation at each temperature.

T (°C)	Proportion in the overall formation (%)		
	Pine	Ash-wood	Wheat straw
200	---	---	---
210	0.0	0.2	1.2
220	0.1	0.4	2.3
230	0.8	0.8	2.8
240	1.3	2.0	4.3
250	1.4	1.7	2.7
260	4.4	7.1	7.2
270	5.5	13.4	13.3
280	32.4	26.4	23.7
290	25.2	21.5	14.8
300	28.9	26.6	27.7

Lê Thành et al. (2015) have measured the quantity of 2-furanmethanol formed under isothermal torrefaction for 45 min (see Table 24). Values in the present work are lower in comparison with those of Lê Thành et al. (2015), like in the case of hydroxyacetone and acetic acid, thus the comments are similar to the previous ones. Regarding the influence of temperature, values in the present work increase with temperature, the same as in their work. Regarding the influence of biomass species, values in the present work are, far from those of Lê Thành et al. (2015) for all biomasses, like in the cases of hydroxyacetone and acetic acid.

Table 24. Comparative formation of 2-furanmethanol (mg/g initial biomass).

Biomass	Lê Thành et al. (2015)			Our work		
	Isothermal profile			Dynamic profile		
	250°C	280°C	300°C	250°C	280°C	300°C
Pine	1.1	3.2	5.9	0.03	0.6	0.6
Ash-wood	2.1	3.4	5.7	0.1	1.5	1.5
Wheat straw	1.3	4.4	6.2	0.2	1.5	1.7

In literature, the origin of 2-furanmethanol is not as well-known as the origin of hydroxyacetone or acetic acid. As mentioned before, ash-wood and wheat straw form more acetic acid than pine within the same interval of temperatures. Acetic acid may catalyze the production of 2-furanmethanol, thus a higher content in xylan could lead to the formation of a higher quantity of 2-furanmethanol.

3.2.4. Eugenol

The formation of eugenol shows different trends among biomasses (see Fig. 50). Eugenol is produced from 250°C. From 250 and until 280°C, the increase in its production accelerates, then decelerates; it also reaccelerates for pine between 290 and 300°C. In the overall torrefaction, ash-wood and pine form more eugenol (12 and 6 times more, respectively) than wheat straw.

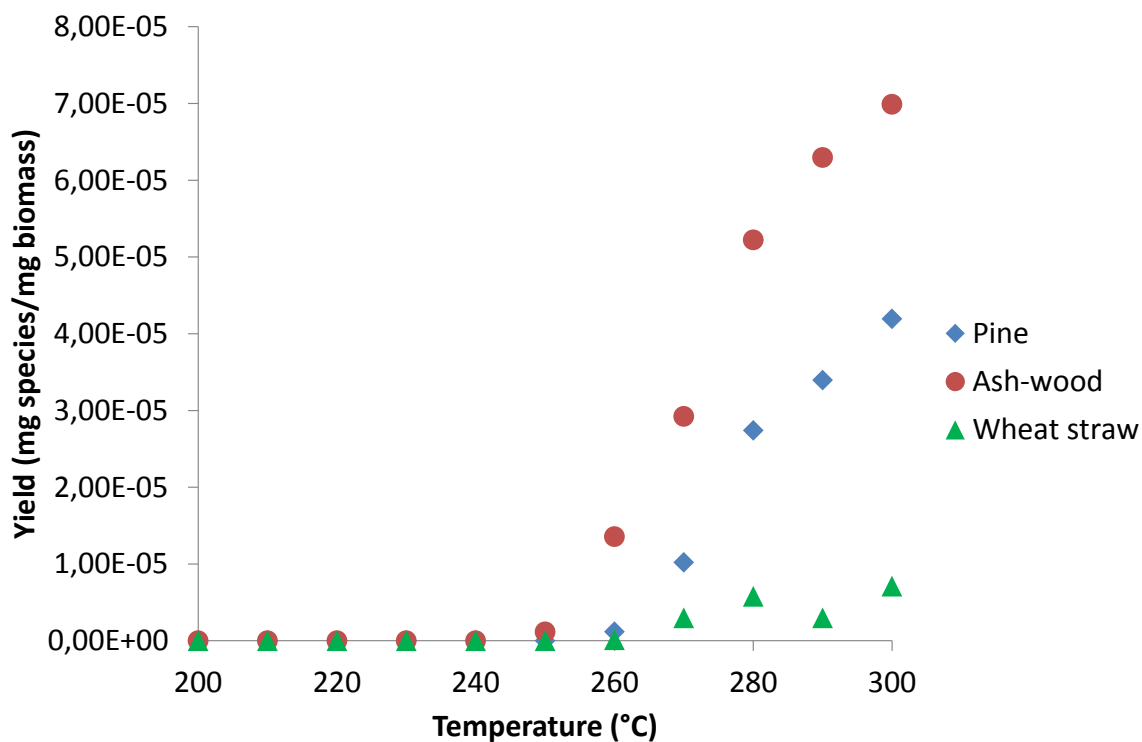


Fig. 50. Production of eugenol during torrefaction.

Table 25 shows the proportion of eugenol in the overall formation at each temperature for each biomass. As in the previous cases, eugenol is produced from a different temperature among biomasses, however this species is significantly formed from the same temperature for all biomasses. More precisely, between 270 and 300°C, 99% of the total eugenol from pine is formed, 94% of the total eugenol from ash-wood and 99% of the total eugenol from wheat straw.

Table 25. Proportion of eugenol in the overall formation at each temperature.

T (°C)	Proportion in the overall formation (%)		
	Pine	Ash-wood	Wheat straw
200	---	---	---
210	---	---	---
220	---	---	---
230	---	---	---
240	---	---	---
250	---	0.5	---
260	1.0	5.9	0.6
270	8.9	12.8	15.7
280	23.9	22.8	30.5
290	29.6	27.5	15.7
300	36.6	30.5	37.5

In the case of eugenol, the results of Lê Thành et al. (2015) could not be compared to ours, since no quantification of this condensable species is available in their work.

Eugenol is an aromatic species which would come from lignin degradation. As ash-wood and pine contain more lignin – they are woody biomasses – than wheat straw – it is a non-woody biomass –, this would lead to the production of higher quantities of eugenol during torrefaction of these biomasses.

3.2.5. Isoeugenol

The formation of isoeugenol shows similar trends, whatever biomass (see Fig. 51). Isoeugenol is formed from 250°C, and the increase in its production suffers an acceleration from 250 until 280°C, and then a deceleration from 280°C. Pine and ash-wood form more isoeugenol (3 and 9 times more, respectively) than wheat straw in the overall torrefaction.

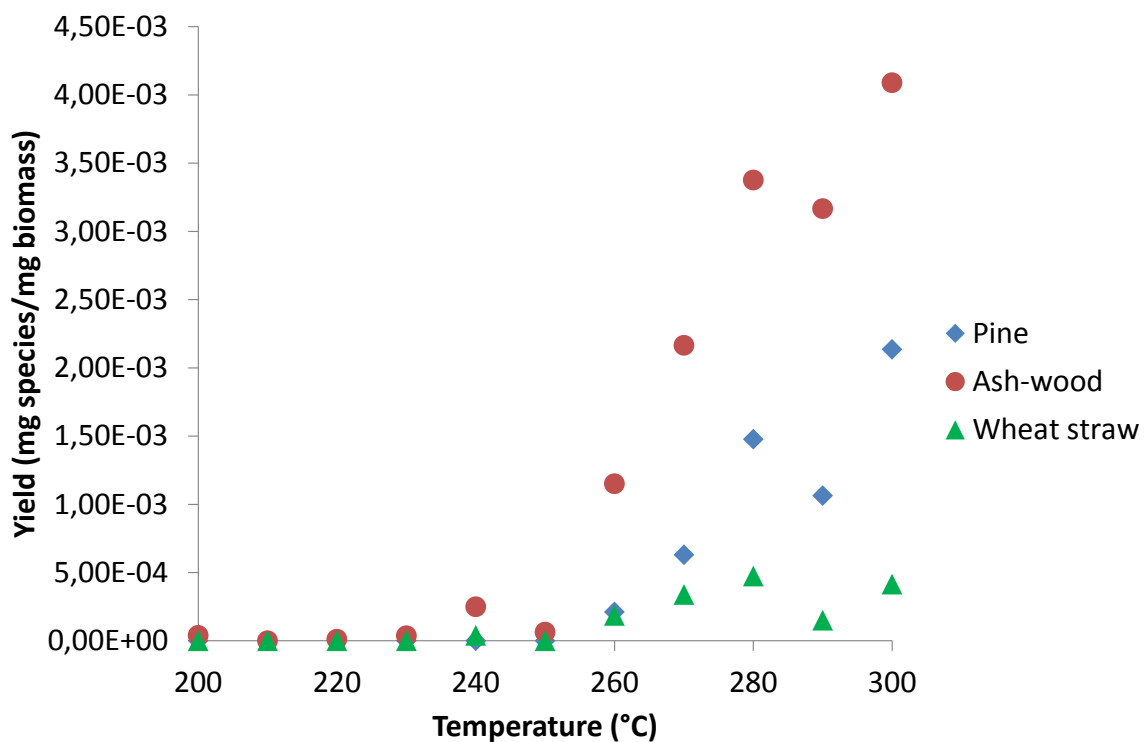


Fig. 51. Production of isoeugenol during torrefaction.

Table 26 shows the proportion of isoeugenol in the overall formation at each temperature for each biomass. Like in the cases of the previous condensable species, isoeugenol is significantly formed from 270 until 300°C: 96% of the total isoeugenol from pine is released within this interval, 89% of that from ash-wood and 86% of that from wheat straw.

Table 26. Proportion of isoeugenol in the overall formation at each temperature.

T (°C)	Proportion in the overall formation (%)		
	Pine	Ash-wood	Wheat straw
200	---	---	---
210	---	---	---
220	---	0.1	---
230	---	0.3	---
240	---	1.7	2.5
250	---	0.4	---
260	3.8	8.0	11.6
270	11.4	15.1	21.1
280	26.8	23.6	29.6
290	19.3	22.1	9.4
300	38.7	28.6	25.9

Lê Thành et al. (2015) measured, for most conditions, lower quantities of isoeugenol during torrefaction of the four biomasses (see Table 27). In the present work, in two cases it has not been possible to measure isoeugenol, probably because its quantity was lower than the detection limit. Regarding influence of temperature, it can be observed that quantities rise as temperature increases, except the value corresponding to wheat straw at 300°C. Regarding influence of biomass species, values in the present work for pine and wheat straw are closer to those of Lê Thành et al. (2015) than in the cases of hydroxyacetone, acetic acid and 2-furanmethanol.

Table 27. Comparative formation of isoeugenol (mg/g initial biomass).

Biomass	Lê Thành et al. (2015)			Our work		
	Isothermal profile			Dynamic profile		
	250°C	280°C	300°C	250°C	280°C	300°C
Pine	0.3	1.2	1.8	---	1.5	2.1
Ash-wood	0.6	0.9	1.1	0.06	3.4	4.1
Wheat straw	0.1	0.2	0.2	---	0.5	0.4

As mentioned before, ash-wood and pine contain more lignin than wheat straw. As isoeugenol is an aromatic compound, its production could come from the degradation of lignin. Hence a higher content in lignin would give rise to higher quantities of isoeugenol.

Table 28 synthesizes this quantitative analysis of condensable species formation. The normal font corresponds to appearance of the species, and the bold font corresponds to significant appearance.

Table 28. Synthesis of the quantitative analysis of condensable species formation.

	200°C	240°C	250°C	270°C
Pine	acetic acid	2-furanmethanol	hydroxyacetone eugenol isoeugenol	hydroxyacetone acetic acid 2-furanmethanol eugenol isoeugenol
Ash-wood	acetic acid	2-furanmethanol	hydroxyacetone eugenol isoeugenol	hydroxyacetone acetic acid 2-furanmethanol eugenol isoeugenol
Wheat straw	acetic acid	2-furanmethanol	hydroxyacetone eugenol isoeugenol	hydroxyacetone acetic acid 2-furanmethanol eugenol isoeugenol

3.3. SEMI-QUANTITATIVE RESULTS

3.3.1. Glycolaldehyde

The formation of glycolaldehyde shows similar trends, whatever biomass (see Fig. 52). Glycolaldehyde is formed from 250°C. Its production increases from 250 until 280°C, and then it strongly decreases. Wheat straw and ash-wood form more glycolaldehyde than pine (4 and 7 times more) in the overall torrefaction.

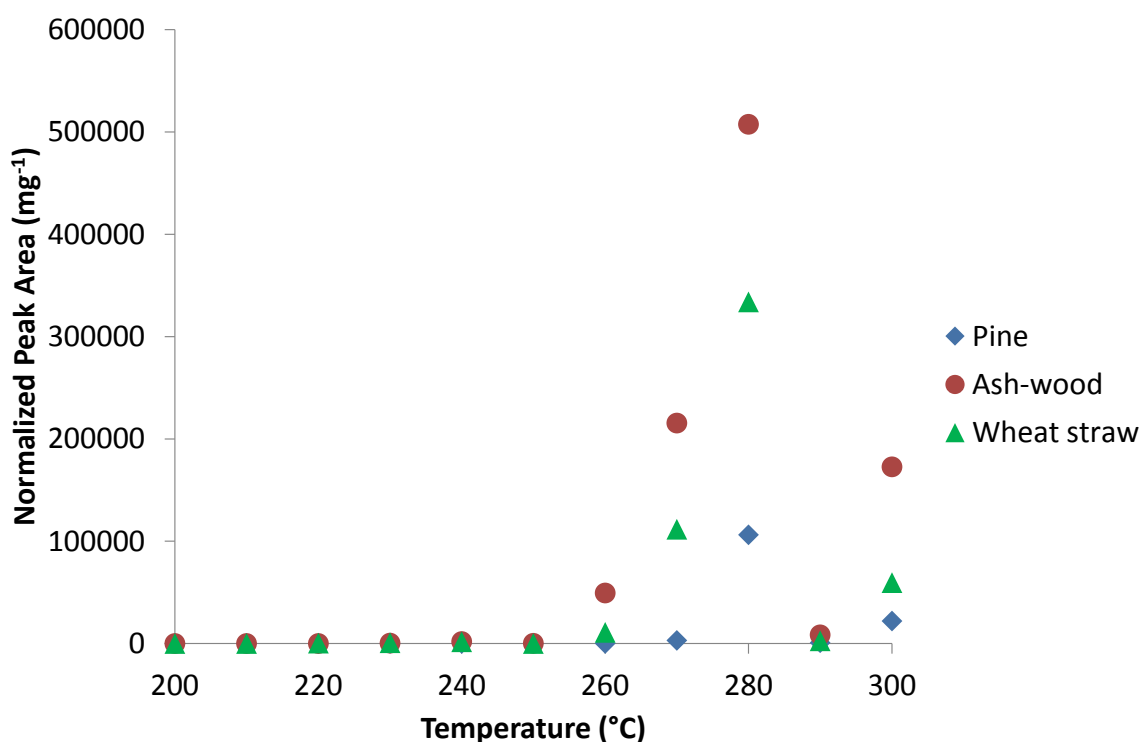


Fig. 52. Production of glycolaldehyde during torrefaction.

Table 29 shows the proportion of glycolaldehyde in the overall formation at each temperature for each biomass. Ash-wood and wheat straw significantly produce glycolaldehyde between 270 and 300°C, whereas pine significantly produces

glycolaldehyde between 280 and 300°C. Ash-wood and wheat straw produce 95% and 97% of glycolaldehyde, respectively, in the interval of 270-300°C, while pine produces 98% in the interval of 280-300°C.

Table 29. Proportion of glycolaldehyde in the overall formation at each temperature.

T (°C)	Proportion in the overall formation (%)		
	Pine	Ash-wood	Wheat straw
200	---	---	---
210	---	---	---
220	---	---	0.1
230	---	0.0	0.1
240	---	0.2	0.3
250	---	0.0	0.0
260	---	5.2	2.1
270	2.4	22.5	21.4
280	80.4	53.1	64.0
290	0.7	0.9	0.5
300	16.6	18.1	11.4

Lê Thành et al. (2015) observed glycolaldehyde formation during torrefaction of the four biomasses, under the form of glycolaldehyde dimer. They observed that glycolaldehyde dimer quantity rises with temperature, although they did not observe the drop between 280 and 300°C.

Glycolaldehyde could come from the degradation of hemicellulose sugars of five and six carbons. Hemicellulose degradation would be accelerated in a catalytic acid medium created, for instance, by the presence of acetic acid. Since ash-wood and wheat straw form more acetic acid than pine within the same interval of temperature, this would lead to higher production of glycolaldehyde.

3.3.2. Formic acid

The formation of formic acid shows different trends among biomasses (see Fig. 53). Formic acid is produced from 220°C. The increase in its formation accelerates until 280-290°C, and then it decelerates. Pine and wheat straw produce approximately as much formic acid, whereas ash-wood forms more formic acid (3 times more).

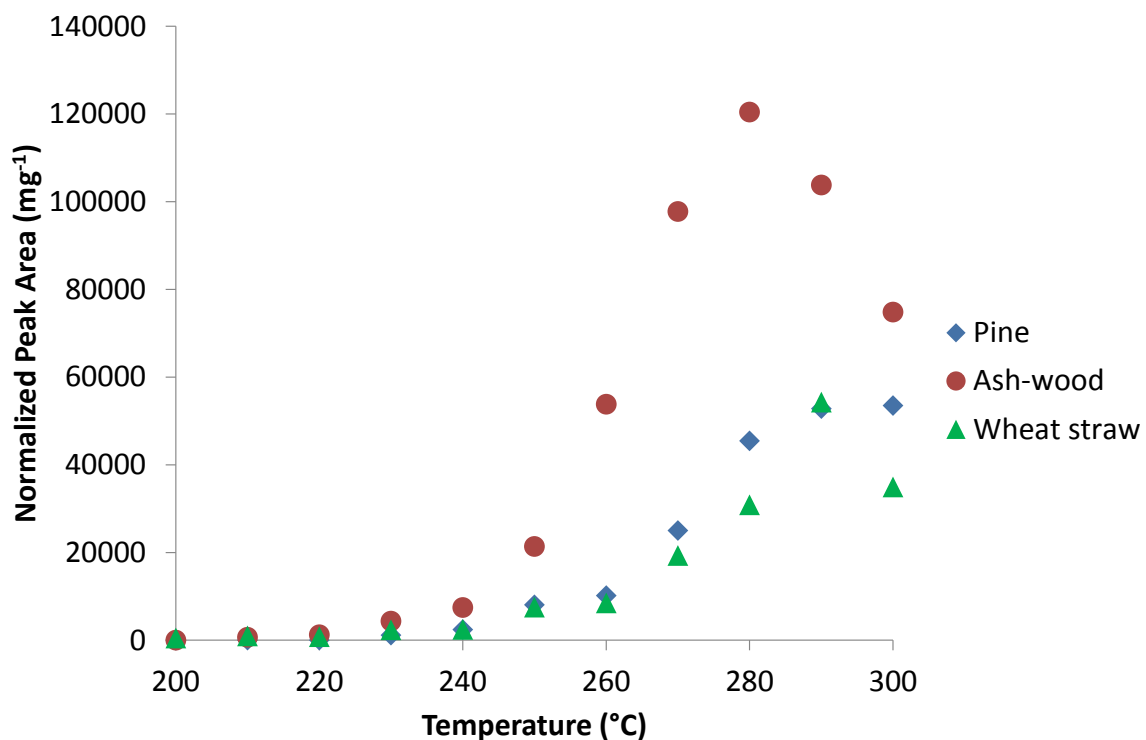


Fig. 53. Production of formic acid during torrefaction.

Table 30 shows the proportion of formic acid in the overall formation at each temperature for each biomass. Ash-wood significantly produces formic acid from 260 to 300°C, whereas pine and wheat straw significantly produce formic acid from 270 to 300°C. Thereby, ash-wood forms 93% of formic acid in the interval of 260-300°C, while pine and wheat straw form 89% and 86%, respectively, in the interval of 270-300°C.

Table 30. Proportion of formic acid in the overall formation at each temperature.

T (°C)	Proportion in the overall formation (%)		
	Pine	Ash-wood	Wheat straw
200	---	---	0.3
210	---	0.1	0.6
220	---	0.3	0.5
230	0.6	0.9	1.5
240	1.2	1.5	1.5
250	4.1	4.4	4.7
260	5.1	11.1	5.2
270	12.6	20.1	11.9
280	22.9	24.8	19.0
290	26.6	21.4	33.5
300	27.0	15.4	21.6

Lê Thành et al. (2015) also observed the formation of formic acid during torrefaction of all biomasses. They noticed that formation rises with temperature, but they did not observe the final drop between 280 and 300°C.

Formic acid would be mainly originated during degradation of hemicellulose sugars of five carbons. Hemicellulose degradation may be accelerated by the presence of acetic acid, thus biomasses which form more acetic acid would be expected to produce more formic acid. Since ash-wood and wheat straw produce more acetic acid than pine, it could be expected that ash-wood and wheat straw form more formic acid. This is true for ash-wood, whereas wheat straw forms less formic acid than expected, reaching proportions similar to those produced from pine.

3.3.3. Furfural

The formation of furfural shows different trends among biomasses (see Fig. 54). Furfural is formed from the beginning of torrefaction, i.e. at 200°C. The increase in its production suffers an acceleration from 200 until 280°C, then its production starts to decrease for all biomasses, except production for wheat straw, which continues to increase. In the overall torrefaction, wheat straw and ash-wood produce approximately 2 times more furfural than pine.

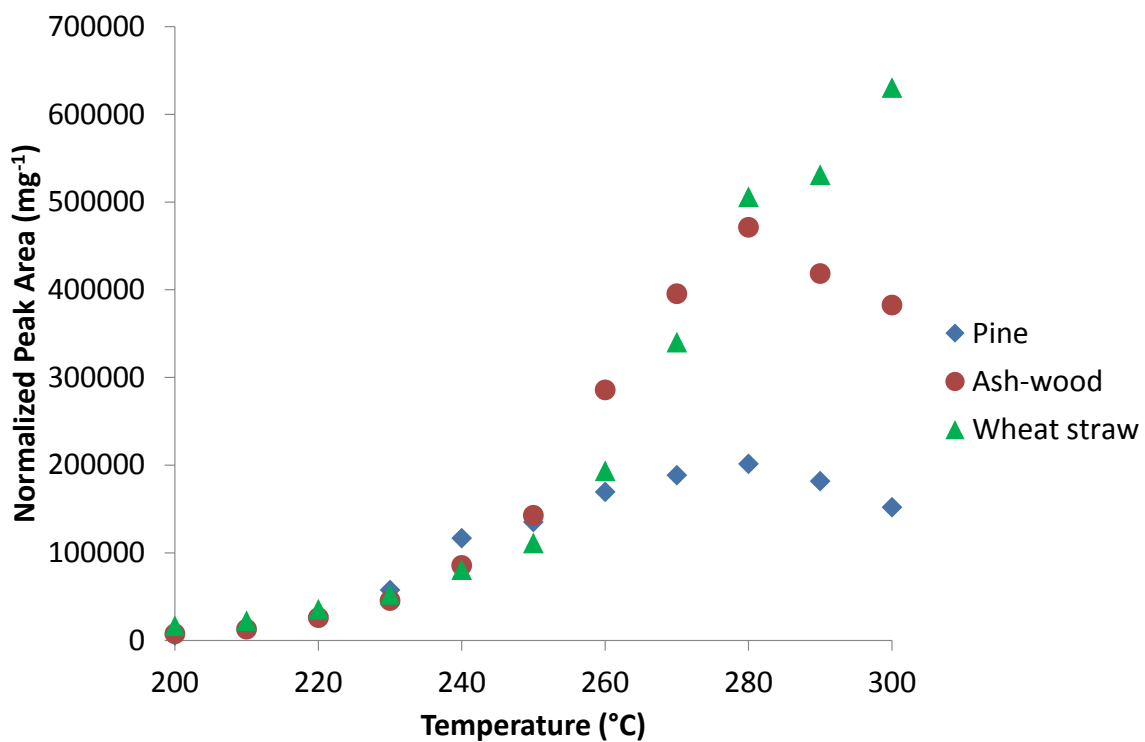


Fig. 54. Production of furfural during torrefaction.

Table 31 shows the proportion of furfural in the overall formation at each temperature for each biomass. Furfural is significantly produced from pine at 250-300°C from ash-wood at 260-300°C and from wheat straw at 270-300°C. Within their respective intervals, pine forms 84% of the total furfural, ash-wood forms 86% and wheat straw forms 80%.

Table 31. Proportion of furfural in the overall formation at each temperature.

T (°C)	Proportion in the overall formation (%)		
	Pine	Ash-wood	Wheat straw
200	0.5	0.3	0.7
210	---	0.6	0.9
220	2.3	1.1	1.4
230	4.7	2.0	2.1
240	9.5	3.8	3.2
250	11.0	6.3	4.4
260	13.8	12.6	7.7
270	15.3	17.4	13.6
280	16.4	20.8	20.2
290	14.8	18.5	21.2
300	12.3	16.9	25.2

Lê Thành et al. (2015) observed production of furfural during torrefaction of the four biomasses. Its quantity rises with temperature in their work, whereas in the present work the quantity drops between 280 and 300°C for ash-wood and pine.

Furfural would come from the degradation of cellulose and hemicellulose. The presence of acetic acid may accelerate the degradation of these polysaccharides. Ash-wood and wheat straw produce more acetic acid than pine within the same interval of temperature; therefore the pH becomes lower throughout their torrefaction. This would explain the fact that cellulose and hemicellulose are degraded faster for these two biomasses and, consequently, they produce more furfural.

3.3.4. 2-Methoxy-4-vinylphenol

The formation of 2-methoxy-4-vinylphenol shows different trends among biomasses (see Fig. 55). 2-Methoxy-4-vinylphenol is formed mainly from 250°C. The increase in its production accelerates from 250 until 280°C, and then its production decreases. More 2-methoxy-4-vinylphenol is formed from ash-wood and wheat straw (4 and 12 times more, respectively) than from pine.

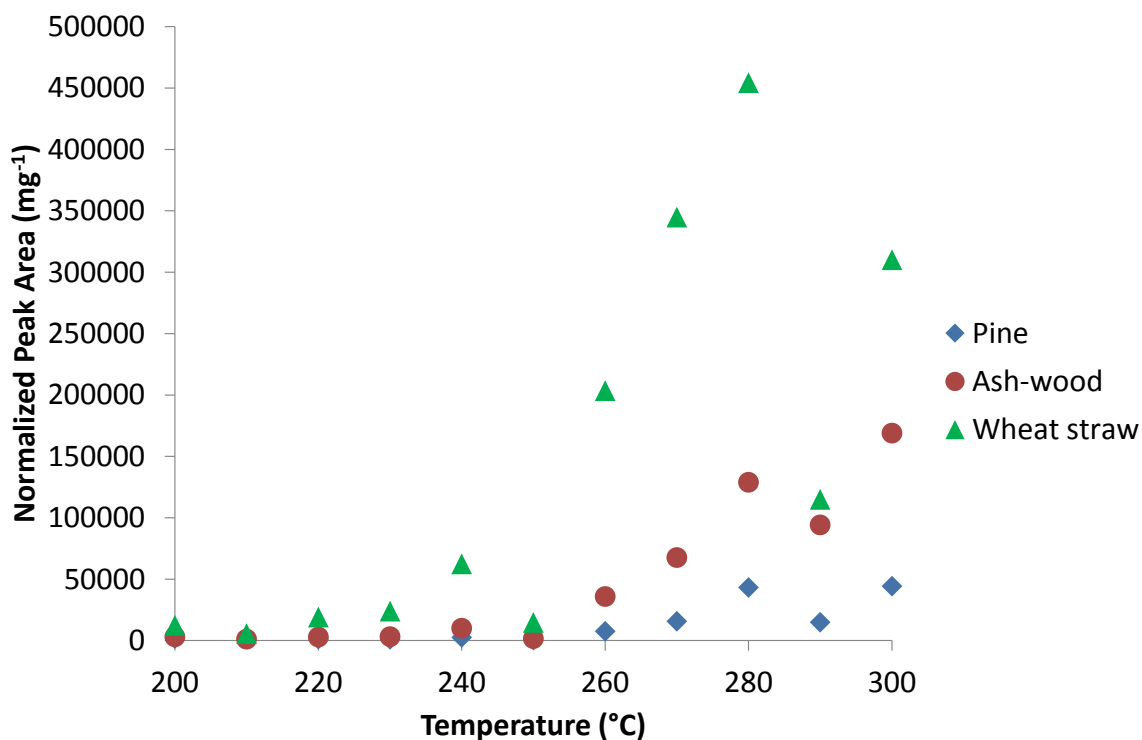


Fig. 55. Production of 2-methoxy-4-vinylphenol during torrefaction.

Table 32 shows the proportion of 2-methoxy-4-vinylphenol in the overall formation at each temperature for each biomass. Wheat straw significantly forms 2-methoxy-4-vinylphenol between 260 and 300°C, whereas pine and ash-wood significantly form this species between 270 and 300°C. Within their respective intervals, wheat straw forms 92% of 2-methoxy-4-vinylphenol, pine forms 90% and ash-wood forms 89%.

Table 32. Proportion of 2-methoxy-4-vinylphenol in the overall formation at each temperature.

T (°C)	Proportion in the overall formation (%)		
	Pine	Ash-wood	Wheat straw
200	1.2	0.6	0.8
210	---	0.2	0.4
220	0.9	0.5	1.2
230	0.7	0.6	1.5
240	2.0	1.9	4.0
250	0.3	0.3	0.9
260	5.8	7.0	13.1
270	11.9	13.1	22.2
280	33.0	25.1	29.2
290	11.4	18.3	7.4
300	33.9	32.9	20.0

Lê Thành et al. (2015) have also measured the formation of 2-methoxy-4-vinylphenol. They observed that formation rises with temperature for all biomasses, while, in the present work, it decreases for wheat straw between 280 and 300°C.

2-Methoxy-4-vinylphenol is an aromatic molecule whose origin could be in the degradation of lignin. It is known that lignin composition varies from one type of biomass to another, with the predominance of different phenylpropanoid monomers in the lignin skeleton – H, G or S units. As mentioned in section 1.4.3 of chapter I, softwood lignin contains mainly G and H units, where G ones prevail, and hardwood lignin is a mixture of S and G units, where S ones predominate. Lignin of cereal crops is constituted by equivalent amounts of G and S units, and perennial crops are mostly made up of H units. As the 2-methoxy-4-vinylphenol is thought to be formed from the degradation of S and G units of lignin, it would be expected that biomasses which contain these units – ash-wood and wheat straw – form more 2-methoxy-4-vinylphenol.

3.3.5. Vanillin

The formation of vanillin shows different trends among biomasses (see Fig. 56). Vanillin is formed from early torrefaction, i.e. at 200°C. The increase in its production accelerates until 250°C, and then it evolves differently depending on the biomass species. The production increases – with the same acceleration –, then decreases for pine; the

increase in production decelerates, then accelerates for ash-wood; and the production decreases, then increases and decreases for wheat straw. Pine and wheat straw form more vanillin than ash-wood in the overall torrefaction (2 and 3 times more, respectively).

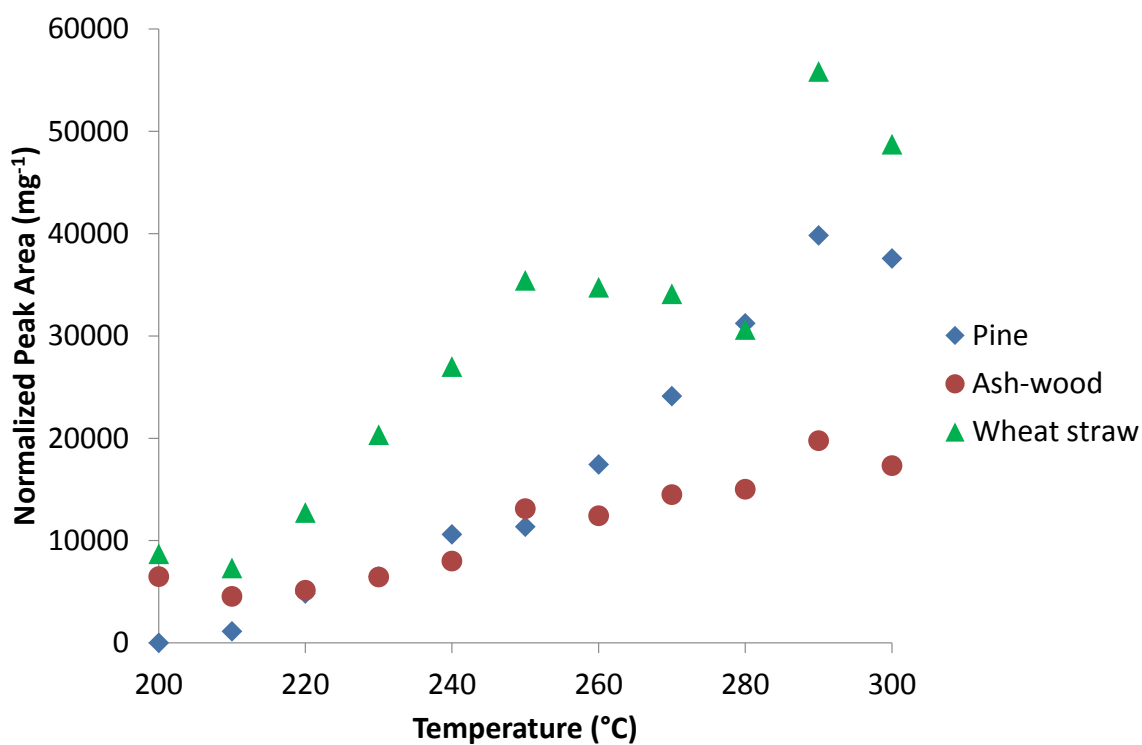


Fig. 56. Production of vanillin during torrefaction.

Table 33 shows the proportion of vanillin in the overall formation at each temperature for each biomass. Ash-wood and wheat straw significantly form vanillin before pine does. Between 250 and 300°C, ash-wood forms 79% out of the total vanillin, and wheat straw forms 78%. Between 270°C and 300°C, pine forms 72%.

Table 33. Proportion of vanillin in the overall formation at each temperature.

T (°C)	Proportion in the overall formation (%)		
	Pine	Ash-wood	Wheat straw
200	---	5.6	2.8
210	0.6	3.9	2.4
220	2.6	4.4	4.2
230	3.5	5.5	6.6
240	5.8	6.9	8.8
250	6.2	11.3	11.5
260	9.4	10.7	11.3
270	13.1	12.5	11.1
280	16.9	12.9	10.0
290	21.6	17.0	18.2
300	20.4	14.9	15.9

Vanillin could arise from the degradation of G and S units of lignin. As mentioned before, pine lignin mainly contains G and H units (G units predominate), ash-wood lignin contains a mixture of S and G units (S units predominate), and wheat straw lignin contains equivalent amounts of G and S units. This leads to think that kinetics of degradation might be faster for G units than for S units to form vanillin. Thereby, wheat straw would form vanillin due to the contribution of half of G “fast” units and half of S “slow” units, pine would form vanillin due to the contribution of a major proportion of G “fast” units, and ash-wood would form vanillin due to the contribution of a minor proportion of G “fast” units and a major proportion of S “slow” units.

Table 34 synthesizes this semi-quantitative analysis of condensable species formation. The normal font corresponds to appearance of the species, and the bold font corresponds to significant appearance.

Table 34. Synthesis of the semi-quantitative analysis of condensable species formation.

	200°C	220°C	250°C	260°C	270°C	280°C
Pine	furfural vanillin	formic acid	glycolaldehyde furfural 2-methoxy-4-vinylphenol vanillin		formic acid 2-methoxy-4-vinylphenol	glycolaldehyde
Ash-wood	furfural vanillin	formic acid	glycolaldehyde 2-methoxy-4-vinylphenol vanillin	formic acid furfural	glycolaldehyde 2-methoxy-4-vinylphenol	
Wheat straw	furfural vanillin	formic acid	glycolaldehyde 2-methoxy-4-vinylphenol vanillin	2-methoxy-4-vinylphenol	glycolaldehyde formic acid furfural	

4. CHEMICAL EVOLUTION OF SOLID

The gaseous phase produced during torrefaction has been analyzed in the previous section. In the present section, the chemical evolution of the solid phase, which has been followed by solid-state NMR, is characterized as a function of temperature and biomass species.

4.1. QUALITATIVE RESULTS

In Fig. 57, Fig. 58, Fig. 59 and Fig. 60, one can observe a strong change of spectra characteristics versus torrefaction temperature, thus a strong solid chemical transformation. Interestingly, this transformation takes place for the four biomasses but at different temperatures for each one. Disappearance of spectrum peaks related to polysaccharides – hemicellulose and cellulose – for non-woody biomasses indicates the complete degradation of the polysaccharides: in wheat straw they completely degrade at 280°C and in miscanthus, at 300°C. Strong flattening of spectrum peaks related to polysaccharides for woody biomasses indicates that these biomasses suffer major structural transformation of polysaccharides: around 300°C polysaccharides in the two woody biomasses degrade, although those in pine degrade slightly before than those in ash-wood.

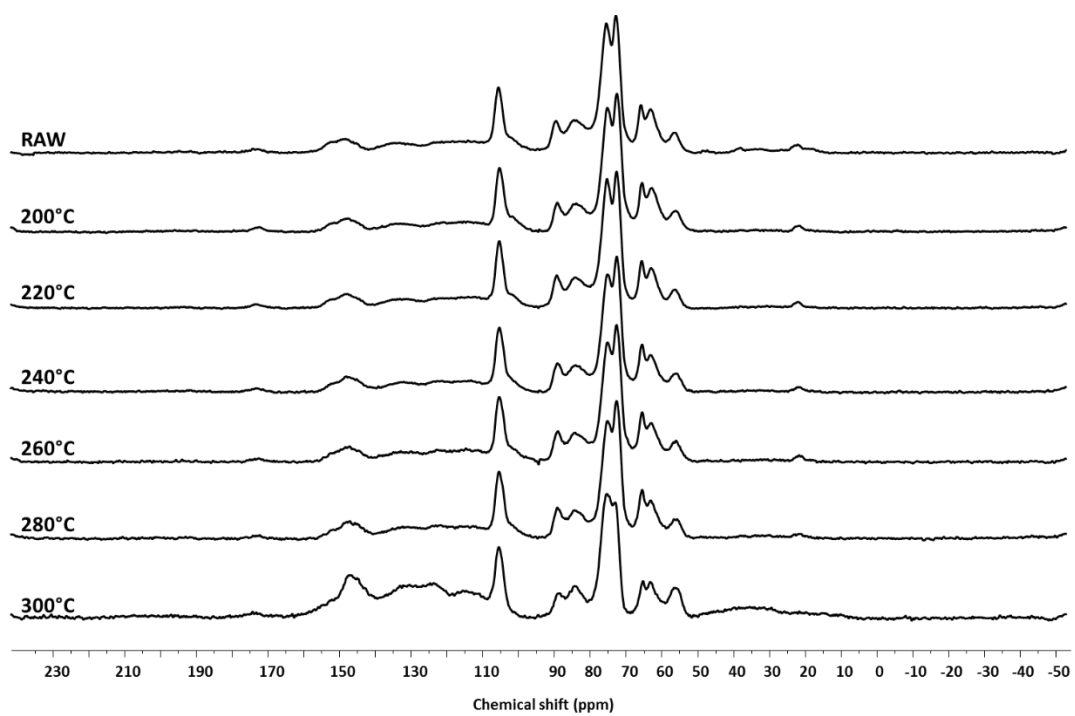


Fig. 57. Solid-state NMR spectra of pine samples: raw and torrefied at 200, 220, 240, 260, 280 and-300°C.

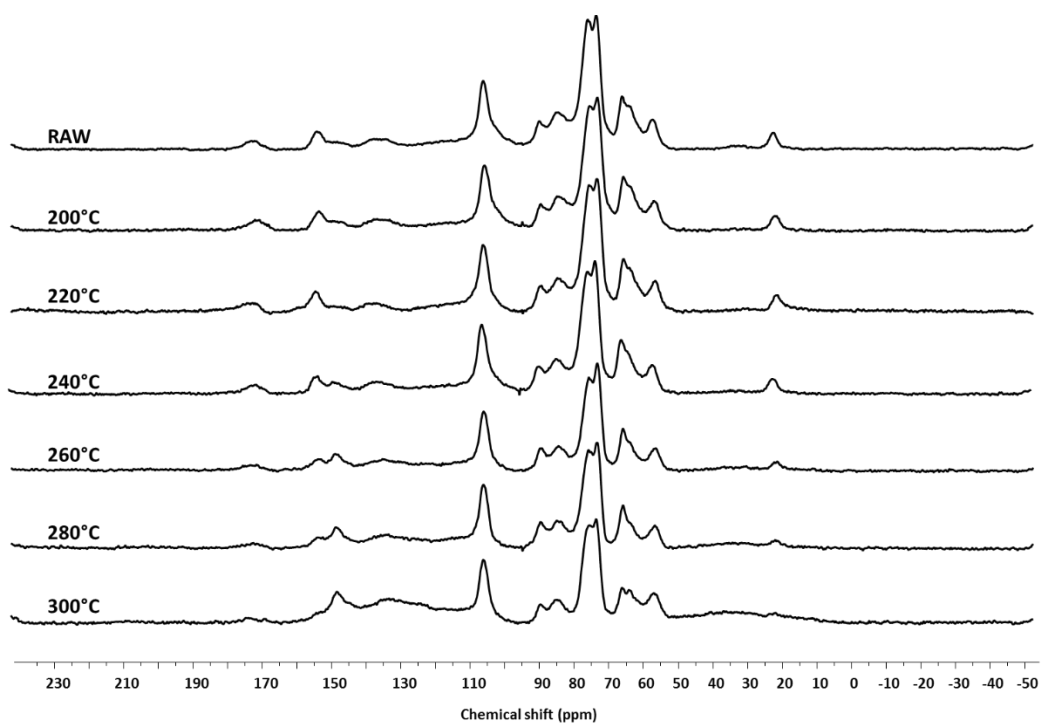


Fig. 58. Solid-state NMR spectra of ash-wood samples: raw and torrefied at 200, 220, 240, 260, 280 and-300°C.

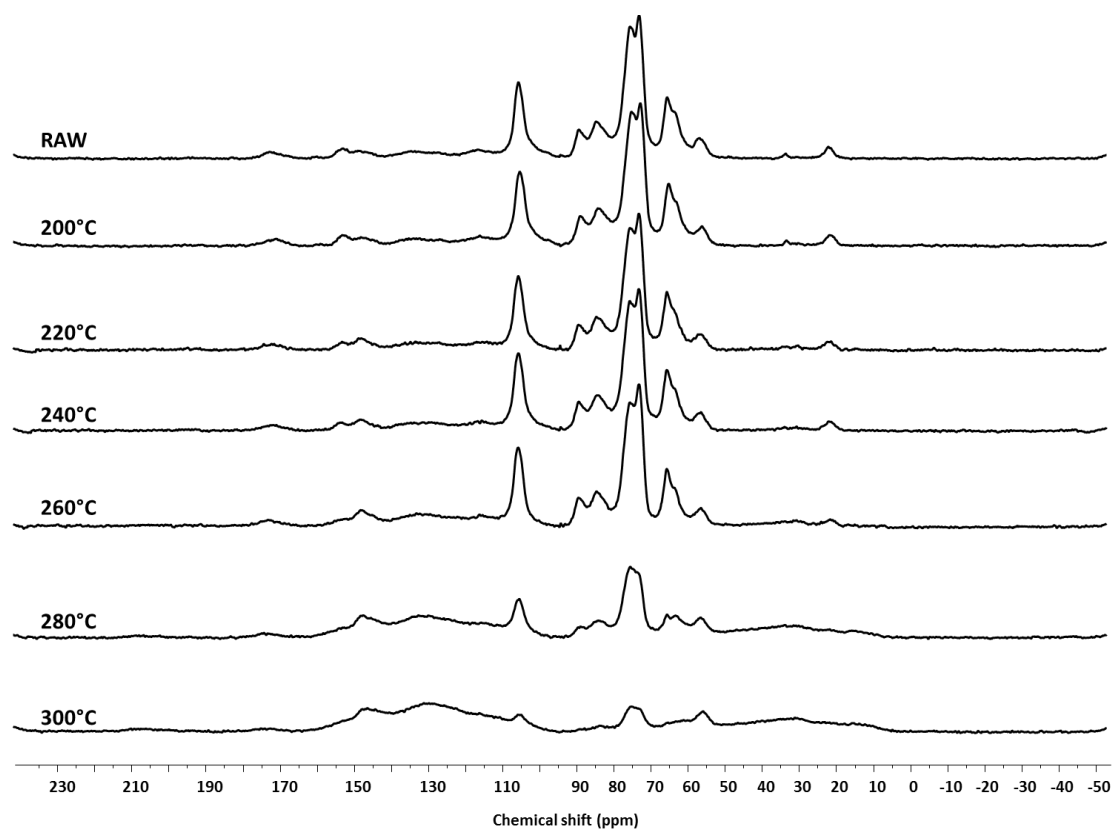


Fig. 59. Solid-state NMR spectra of miscanthus samples: raw and torrefied at 200, 220, 240, 260, 280 and 300°C.

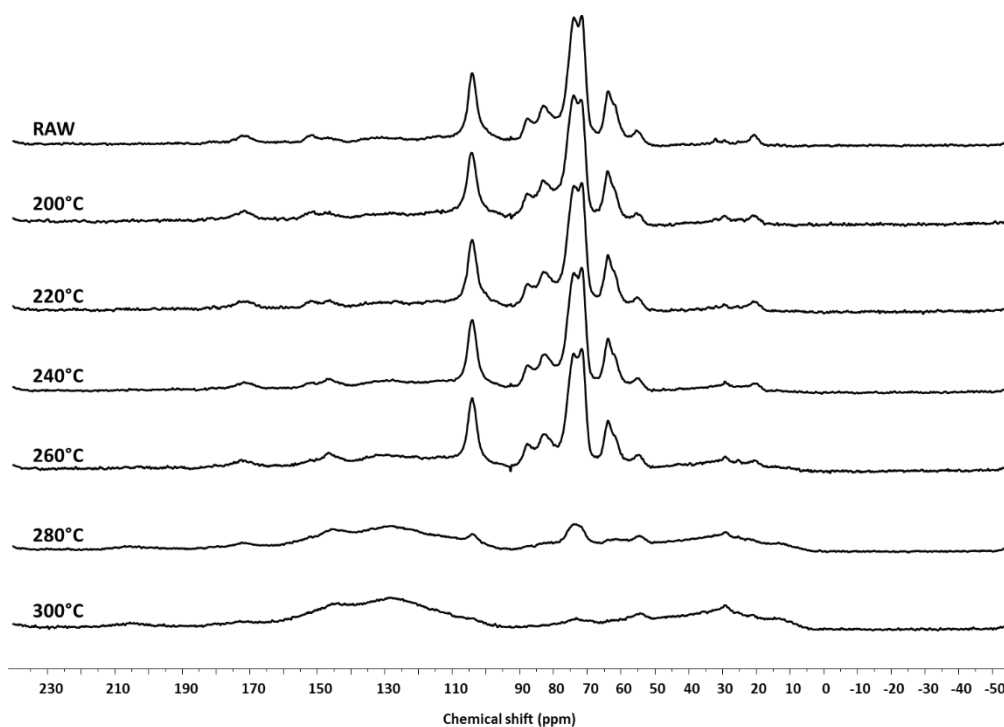


Fig. 60. Solid-state NMR spectra of wheat straw samples: raw and torrefied at 200, 220, 240, 260, 280 and-300°C.

4.2. QUANTITATIVE RESULTS

A quantitative analysis of the evolution of each representative spectral region versus temperature has been carried out, in order to follow the transformation during torrefaction of functional groups listed in section 3.2 of chapter III. The eight functional groups – aromatics in lignin, C1 of cellulose, C4 and C6 of crystalline cellulose, C4 and C6 of amorphous cellulose, methoxyl groups in lignin and acetyl groups in hemicellulose – have been quantified on raw and torrefied biomasses.

4.2.1. Aromatics in lignin

The evolution of the proportion of aromatics in lignin shows different trends among biomasses (see Fig. 61). Aromatic structures in lignin appear to be conserved until 260°C, and from this temperature the proportion of aromatics in lignin increases in all

biomasses, except in ash-wood. At 280°C, the increase in aromatics continues: this increase accelerates for ash-wood and miscanthus, and it decelerates for pine and wheat straw. At the end of the torrefaction experiments, the evolution of the proportion of aromatics in lignin is, from more to less abundancy, as follows: wheat straw, miscanthus, pine and ash-wood.

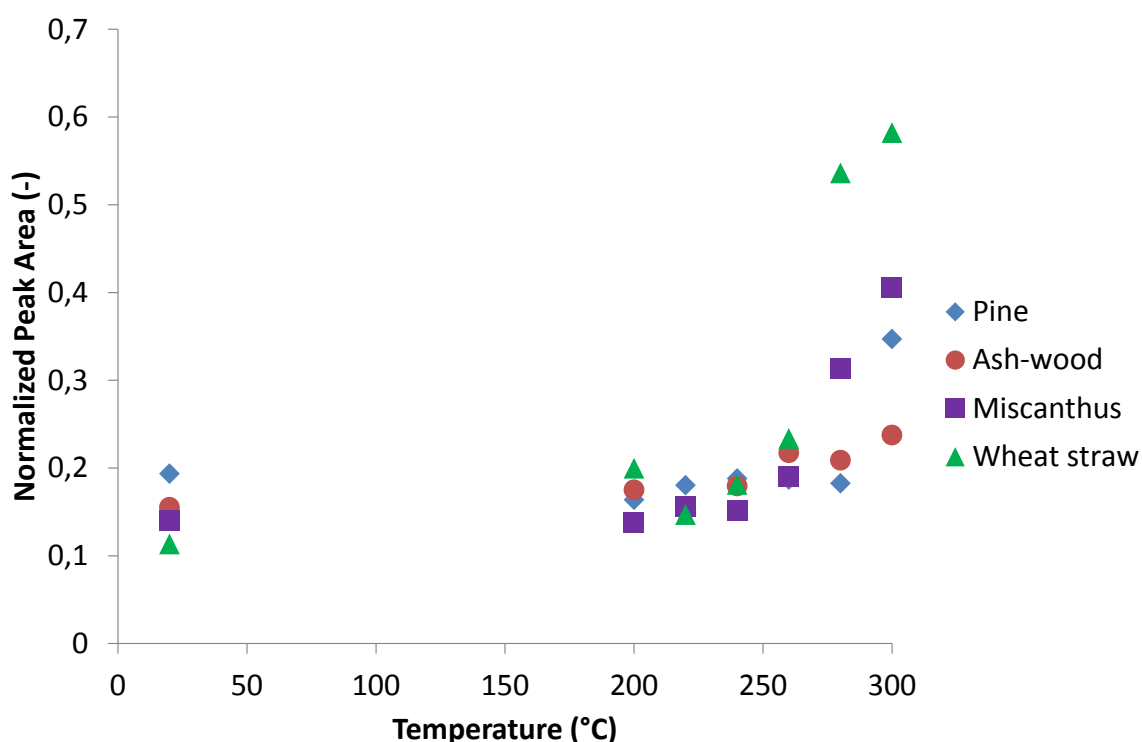


Fig. 61. Evolution of the proportion of aromatics in lignin during torrefaction.

Hence it seems that aromatic structures in lignin are not affected by torrefaction until 260°C. Above this temperature, the aromatic structures in lignin of wheat straw are the most affected by torrefaction, followed by those of miscanthus and pine, and those in ash-wood are the least affected. The reason could be related to the cellulose crystallinity of each biomass, shown in Table 35. Wheat straw presents a lower initial crystallinity index than the other three biomasses. As amorphous cellulose is more reactive than crystalline cellulose, a higher initial proportion of amorphous cellulose would lead to a higher proportion of char coming from cellulose, hence more abundant aromatics.

Table 35. Crystallinity index of the four biomasses.

Temperature (°C)	Pine	Ash-wood	Miscanthus	Wheat straw
Raw	34	30	29	26
200	33	28	30	27
220	35	29	28	26
240	34	30	30	26
260	35	33	31	27
280	35	34	25	6
300	30	28	13	---

In literature, the increase in aromatic carbon content due to charring of the three major components has been reported (Wen et al., 2014). These features seem to be correlated with the degradation of polysaccharides, discussed in the previous section. Polysaccharides would be completely degraded at 280°C for wheat straw, at 300°C for miscanthus, and above 300°C for pine and ash-wood. In parallel of polysaccharides degradation, the contribution linked to charring increases. The two non-woody biomasses, miscanthus and wheat straw, are the most affected by the polysaccharides degradation already at 260°C. For ash-wood and pine, the two woody biomasses, charring is not negligible at 300°C, whereas polysaccharides still resist at this temperature, with however a small decrease in crystallinity. This may mean that charring becomes a predominant mechanism of solid conversion at high temperatures of torrefaction. In addition, the increase in abundance of aromatics while polysaccharides are still not degraded, and also after they degrade, might prove that char initially comes from lignin degradation, then also from polysaccharides.

4.2.2. C1 of cellulose

The evolution of the proportion of C1 of cellulose shows different trends among biomasses (see Fig. 62). C1 of cellulose signal is conserved until it starts to decrease: at 200°C for wheat straw, at 260°C for miscanthus, and at 280°C for pine and ash-wood. Thus agricultural by-products, represented by wheat straw, seem to start degrading before other biomasses.

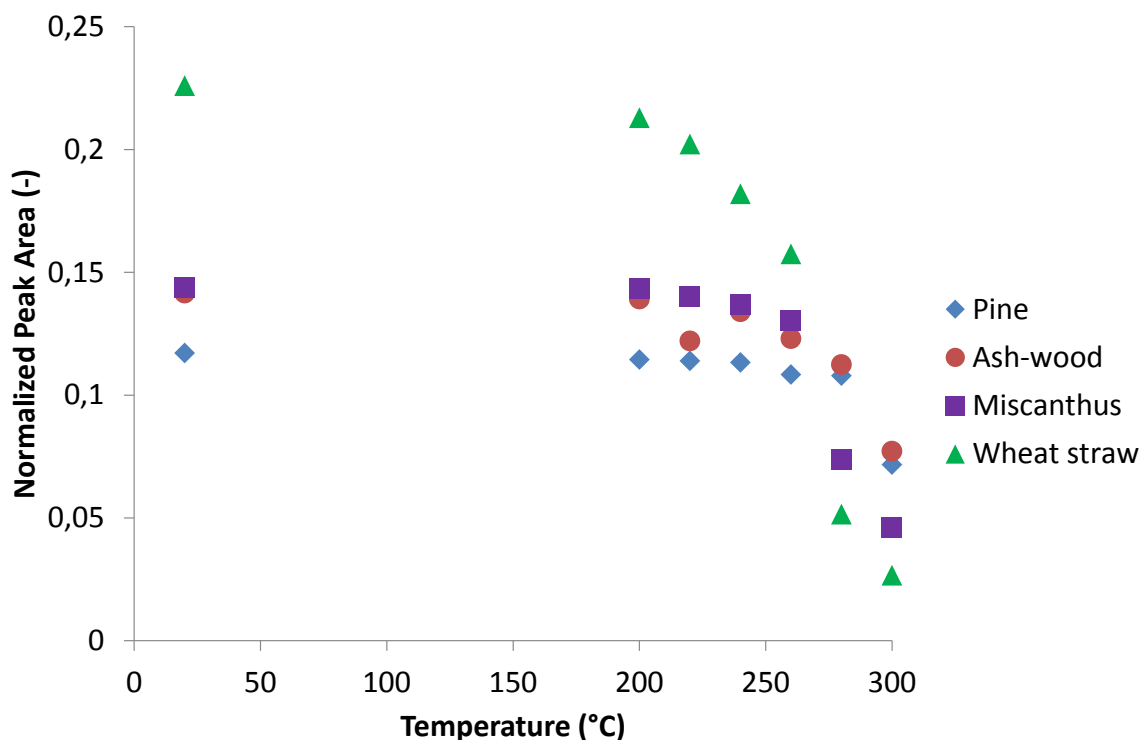


Fig. 62. Evolution of the proportion of C1 of cellulose during torrefaction.

The reason for this difference in C1 of cellulose evolution during torrefaction could lie in crystallinity of cellulose, which is initially lower for wheat straw than for the other three biomasses, as already mentioned. As amorphous cellulose is the most reactive fraction of cellulose, a higher initial proportion of amorphous cellulose would imply a faster degradation of cellulose.

4.2.3. C4 and C6 of crystalline cellulose

The evolution of the proportions of C4 and C6 of crystalline cellulose shows different trends among biomasses (see Fig. 63 and Fig. 64). C4 and C6 peaks of crystalline cellulose are conserved until they start to decrease at 200°C for wheat straw, at 260°C for miscanthus, and at 280°C for pine and ash-wood. Like in the case of C1 of cellulose, it would mean that agricultural by-products start to degrade before the other biomasses.

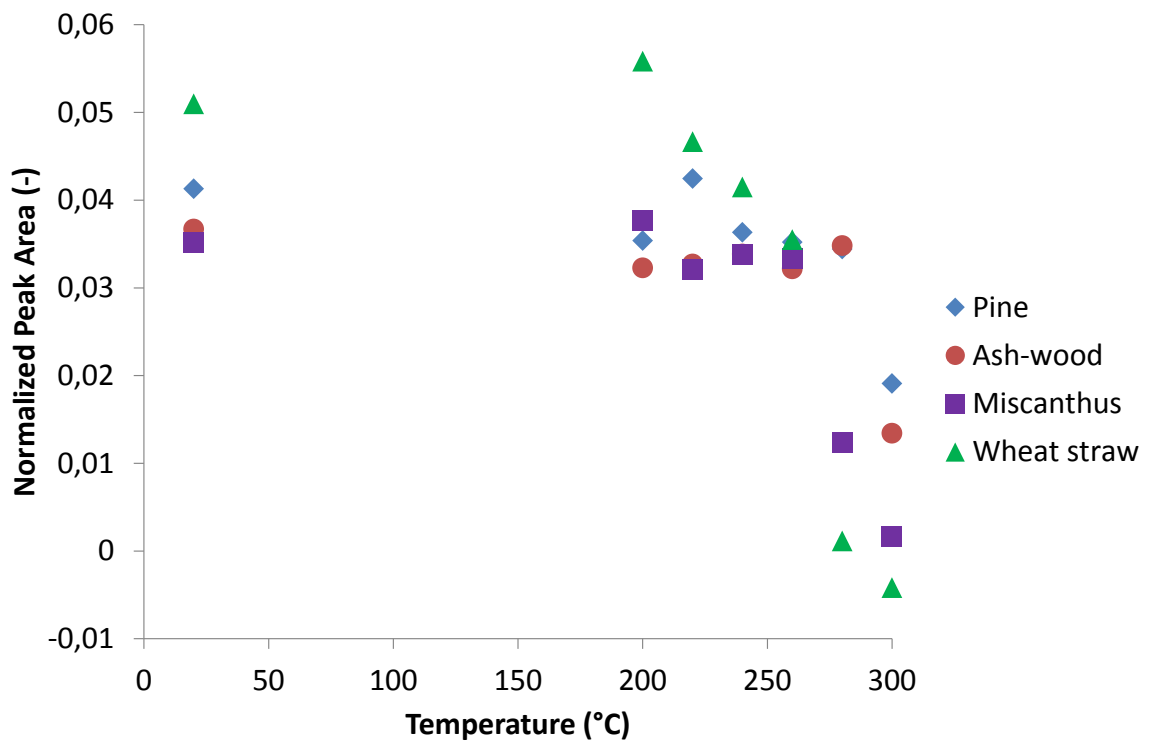


Fig. 63. Evolution of the proportion of C4 of crystalline cellulose during torrefaction.

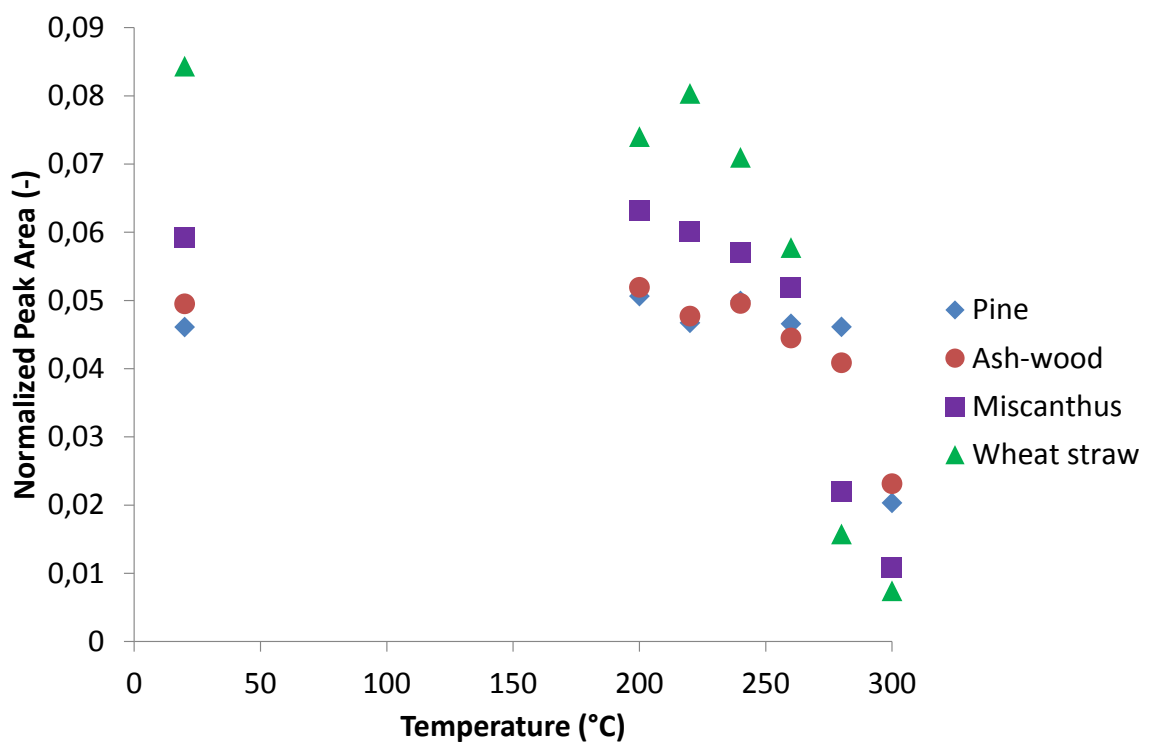


Fig. 64. Evolution of the proportion of C6 of crystalline cellulose during torrefaction.

The reason for the differences in evolution of crystalline cellulose during torrefaction may again lie in crystallinity index of cellulose. This index is initially lower for wheat straw than for the other three biomasses, which means that wheat straw has a higher initial proportion of amorphous cellulose. This could lead to a faster degradation of cellulose in wheat straw in comparison with the other biomasses.

A slight increase of crystallinity index can be observed for ash-wood at 260 and 280°C. In some studies, this phenomenon has been attributed to cellulose partial recrystallization before degradation at high temperatures (Melkior et al., 2012; Wen et al., 2014). However, it could be more simply due to the initial mass loss in ash-wood. Indeed, as amorphous contribution comprises contribution from amorphous cellulose and hemicellulose, this signal slightly decreases when hemicelluloses are degraded and then the crystalline ratio is logically higher, even if cellulose crystallinity remains unchanged.

As mentioned in section 4.1, there is a significant difference between spectra profiles of the woody and the non-woody biomasses. The whole structure is totally modified for wheat straw at 280°C and for miscanthus at 300°C, whereas at 300°C the structure is partly but not totally modified for ash-wood and pine. These characteristics would have a strong correlation with the lignin content of biomasses. The fact that cellulose in pine and ash-tree is less degraded than in miscanthus and wheat straw, could be due to the fact that woody biomasses contain more lignin than non-woody biomasses. Thus, lignin may play a protecting role forwards cellulose during thermal treatment.

4.2.4. C4 and C6 of amorphous cellulose

The evolution of the proportions of C4 and C6 of amorphous cellulose shows different trends among biomasses (see Fig. 65 and Fig. 66). The proportions of C4 and C6 of amorphous cellulose are conserved, until they start to decrease at 200°C for wheat straw, at 260°C for miscanthus, and at 280°C for pine and ash-wood. As for the other carbons of cellulose, the evolution of the proportions of C4 and C6 of amorphous cellulose tends to show that agricultural by-products start to degrade before other biomasses. Thus degradation trends of crystalline cellulose – discussed in the previous section – and those of amorphous cellulose seem to be quite similar.

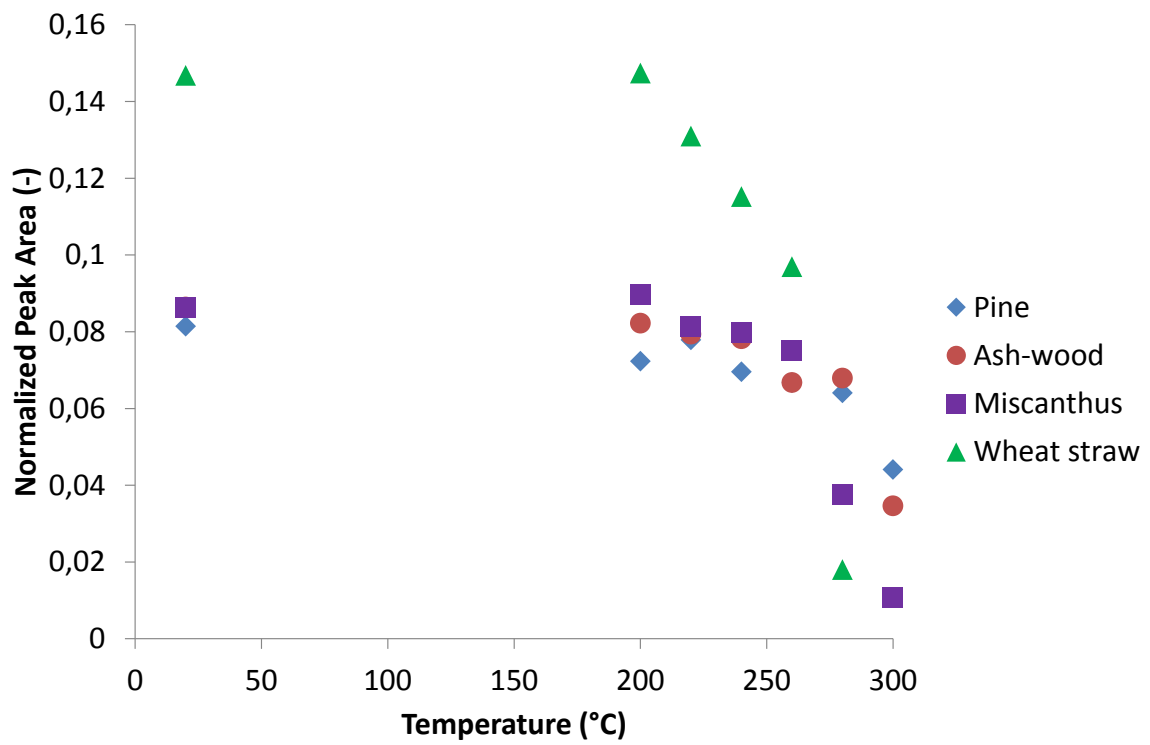


Fig. 65. Evolution of the proportion of C4 of amorphous cellulose during torrefaction.

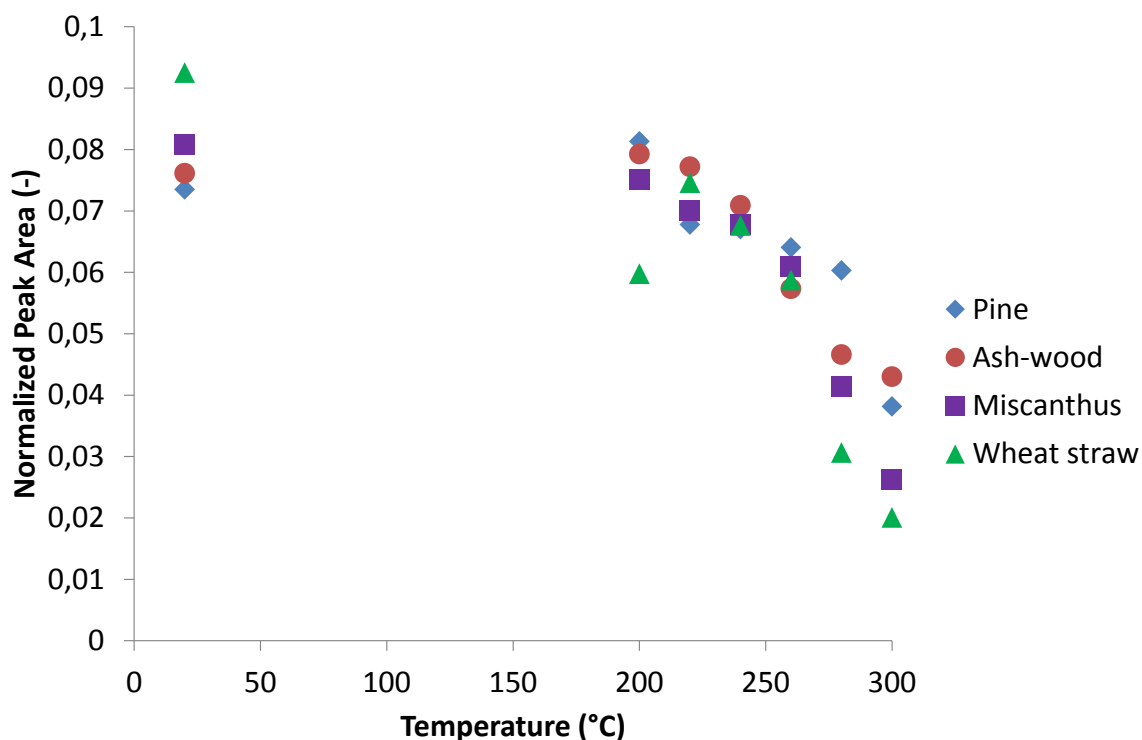


Fig. 66. Evolution of the proportion of C6 of amorphous cellulose during torrefaction.

As for C4 and C6 of crystalline cellulose, the behavior of C4 and C6 of amorphous cellulose may be related to crystallinity index of cellulose. This index is initially lower for wheat straw than for the other three biomasses, which could lead to a faster degradation of cellulose in wheat straw in comparison with cellulose in the other biomasses.

4.2.5. Methoxyl groups in lignin

The evolution of the proportion of methoxyl groups in lignin shows different trends among biomasses (see Fig. 67). Methoxyl groups in lignin of pine and ash-wood are conserved during torrefaction, whereas methoxyl groups in lignin of miscanthus and, especially, wheat straw increase from 260°C.

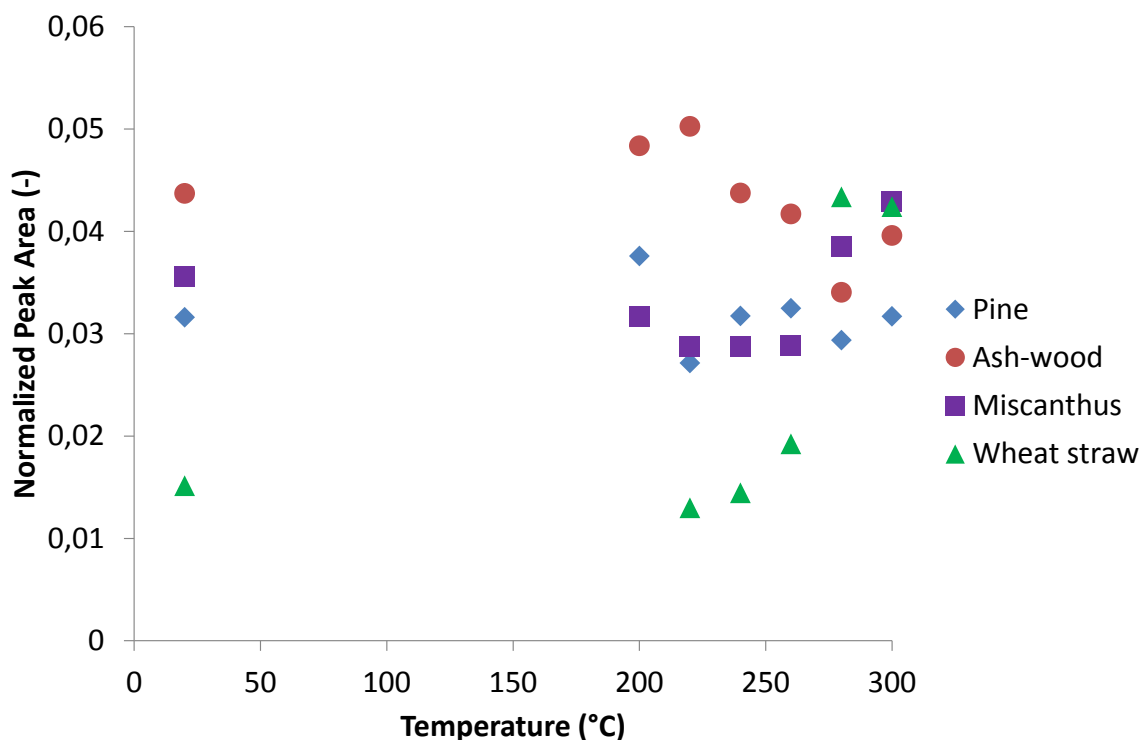


Fig. 67. Evolution of the proportion of methoxyl groups in lignin during torrefaction.

The key to understand this evolution could be in the overall degradation of lignin, not only methoxyl groups. Miscanthus and wheat straw contain lower proportion of lignin than pine and ash-wood. As discussed in section 4.2.1, aromatics in lignin degrade during torrefaction; however, it could be possible that methoxyl groups in lignin either slightly react or do not react during torrefaction. This would lead to an increase in the proportion of methoxyls in the total lignin upon torrefaction. Lignin in miscanthus and wheat straw degrades faster than lignin in pine and ash-wood, as already mentioned. Hence, the faster decrease of aromatics in lignin could provoke the apparent increase in methoxyl groups, which would actually not be degraded during torrefaction.

In literature, some works have attributed the increase in methoxyls signal during torrefaction to an enrichment of this functional group, such as Ben and Ragauskas (2012). However, the increase of methoxyl peak intensity with temperature would not necessarily imply that methoxyl groups are created during torrefaction. It might come from a bias in the calibration with the C1 peak of cellulose, since some works have assumed that the C1 of cellulose signal does not evolve under the torrefaction conditions

tested, such as Melkior et al. (2012). However, this aspect of spectra treatment is not commented in the work of Ben and Ragauskas (2012). Hence, this bias in the calibration would lead to think that concentration of methoxyl groups is higher, whereas they may simply slightly degrade, in comparison with other functional groups, during torrefaction.

4.2.6. Acetyl groups in hemicellulose

The evolution of the proportion of acetyl groups in hemicellulose shows different trends among biomasses (see Fig. 68). Acetyl groups signals begin to decrease at 260°C for ash-wood, miscanthus and wheat straw, whereas acetyl groups of pine are conserved during torrefaction. After reaching a minimum, values for miscanthus and wheat straw increase from 280°C, which might be due to the fact that acetyls have been completely released, and new structures with the same chemical shift as acetyls are being formed. Thus it can be considered that acetyl groups of miscanthus and wheat straw are completely degraded at 280°C.

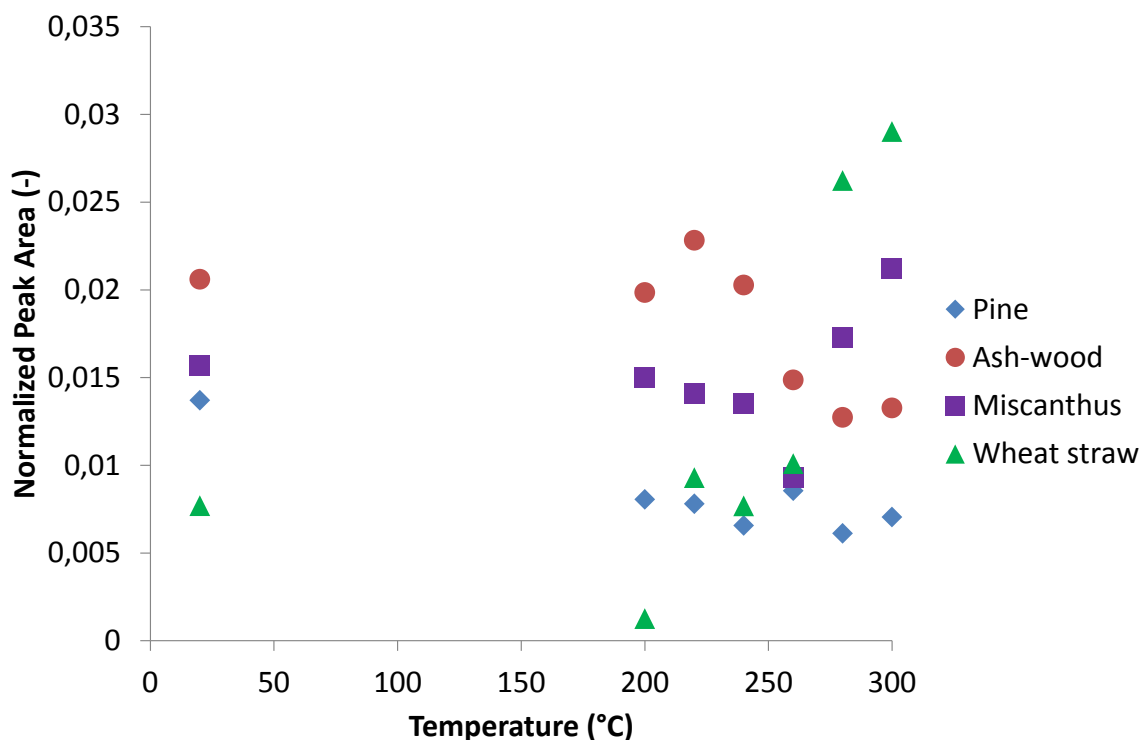


Fig. 68. Evolution of the proportion of acetyl groups in hemicellulose during torrefaction.

The differences in degradation of acetyl groups could be explained by the xylan content in biomasses. As mentioned in section 3.2.2, acetyl groups are mainly contained in xylan, which is the most reactive sugar in hemicellulose. Ash-wood, miscanthus and wheat straw contain higher proportions of xylan than pine, which would lead to a faster release of acetyl groups.

This result confirms the lability of this group, reported before in literature by several works (Ben and Ragauskas, 2012; Melkior et al., 2012; Sivonen et al., 2002).

Table 36 synthesizes the quantitative characterization of the solid phase during torrefaction of pine, ash-wood, miscanthus and wheat straw. The green font indicates the increase of the functional group, the red font indicates its decrease, and the strikethrough font indicates its disappearance.

Table 36. Synthesis of quantitative characterization of the solid phase.

	200°C	260°C	280°C
Pine		aromatics in lignin	C1 of cellulose C4 and C6 of crystalline cellulose C4 and C6 of amorphous cellulose
Ash-wood		acetyl groups in hemicellulose	aromatics in lignin C1 of cellulose C4 and C6 of crystalline cellulose C4 and C6 of amorphous cellulose
Miscanthus		aromatics in lignin C1 of cellulose C4 and C6 of crystalline cellulose C4 and C6 of amorphous cellulose methoxyl groups in lignin acetyl groups in hemicellulose	acetyl groups in hemicellulose
Wheat straw	C1 of cellulose C4 and C6 of crystalline cellulose C4 and C6 of amorphous cellulose	aromatics in lignin methoxyl groups in lignin acetyl groups in hemicellulose	acetyl groups in hemicellulose

5. SYNERGY OF RESULTS

The three types of data presented in section 2 – mass loss of the solid obtained by TGA –, section 3 – formation of condensable species obtained by TGA-GC-MS –, and section 4 – chemical evolution of the solid obtained by solid-state NMR – have been individually analyzed.

5.1. MASS LOSS AND CHEMICAL EVOLUTION OF THE SOLID

TGA results showed two families of biomasses when considering mass loss evolution versus temperature. One family is constituted by pine, and the other family is constituted by miscanthus, wheat straw and ash-wood.

At 300°C, pine suffered the lowest mass loss in TGA and was also the least chemically transformed biomass in solid-state NMR. The other three biomasses – ash-wood, miscanthus and wheat straw – suffered similar mass losses, but exhibited different trends regarding chemical evolution of the solid phase. This means that, for the same mass loss, chemical evolution of the solid may change from one biomass to another. In other words, a similar overall mass loss may hide different chemical evolutions within the solid.

Results of the present work imply that mass loss criterion alone would not be sufficient to characterize the quality of the torrefied solid. Several works in literature have claimed that mass loss would be the only indicator needed to describe the degree of torrefaction intensity, i.e. products quality and properties, at least for samples from the same type of biomass (Englisch M., 2011; Sabil et al., 2013; Grigante and Antolini, 2015; Almeida et al., 2010). Other works have claimed that both mass loss and chemical transformation criteria would be needed to describe the degree of torrefaction intensity (Boonstra et al., 2007; Rutherford et al., 2012; Windeisen et al., 2009).

5.2. PRODUCTION OF GASEOUS SPECIES AND CHEMICAL EVOLUTION OF THE SOLID

TGA-GC-MS results can be coupled with solid-state NMR results. In particular, the synergy of the case acetic acid-acetyl groups is presented. In literature, it has been reported that, under torrefaction conditions, the release of acetyl groups leads to the formation of acetic acid (Nocquet et al., 2014a; Prins et al., 2006a).

Fig. 69, Fig. 70 and Fig. 71 show the synergy of: the production of acetic acid in the gaseous phase, and the degradation of acetyl groups and the mass loss of the solid phase, for pine, ash-wood and wheat straw, respectively. The yield of acetic acid and the solid mass loss have been obtained by TGA-GC-MS, and the proportion of acetyl groups has been obtained by solid-state NMR.

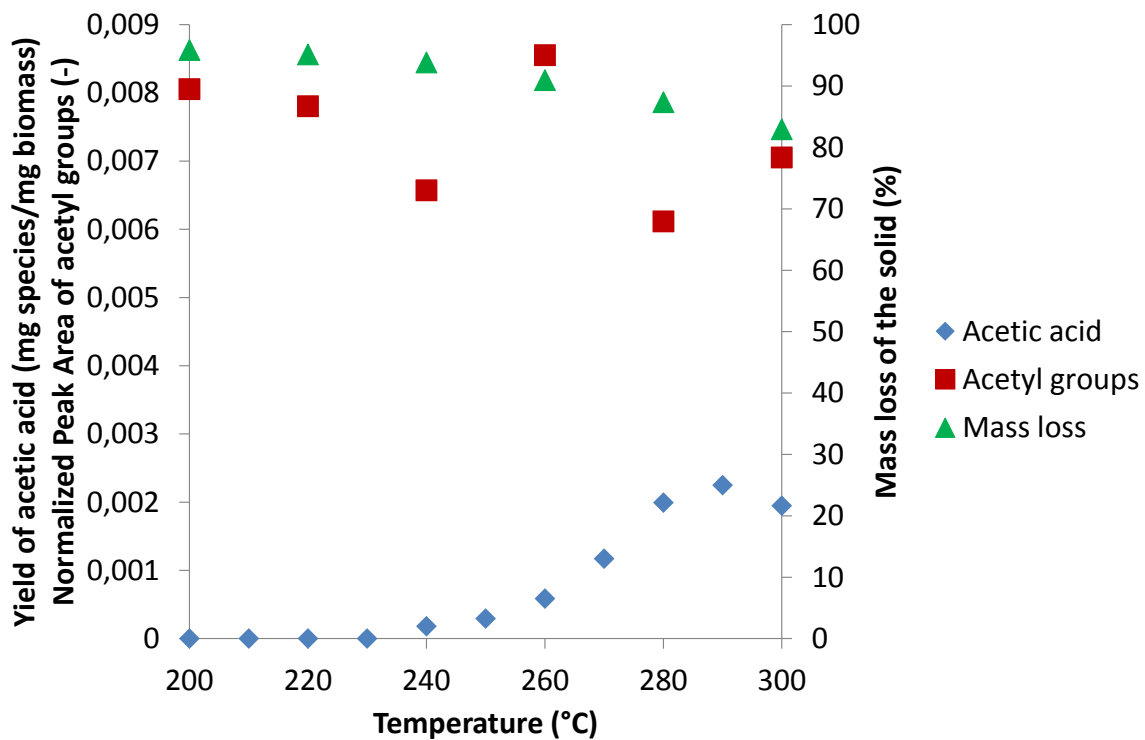


Fig. 69. TGA-GC-MS and solid-state NMR synergy for pine.

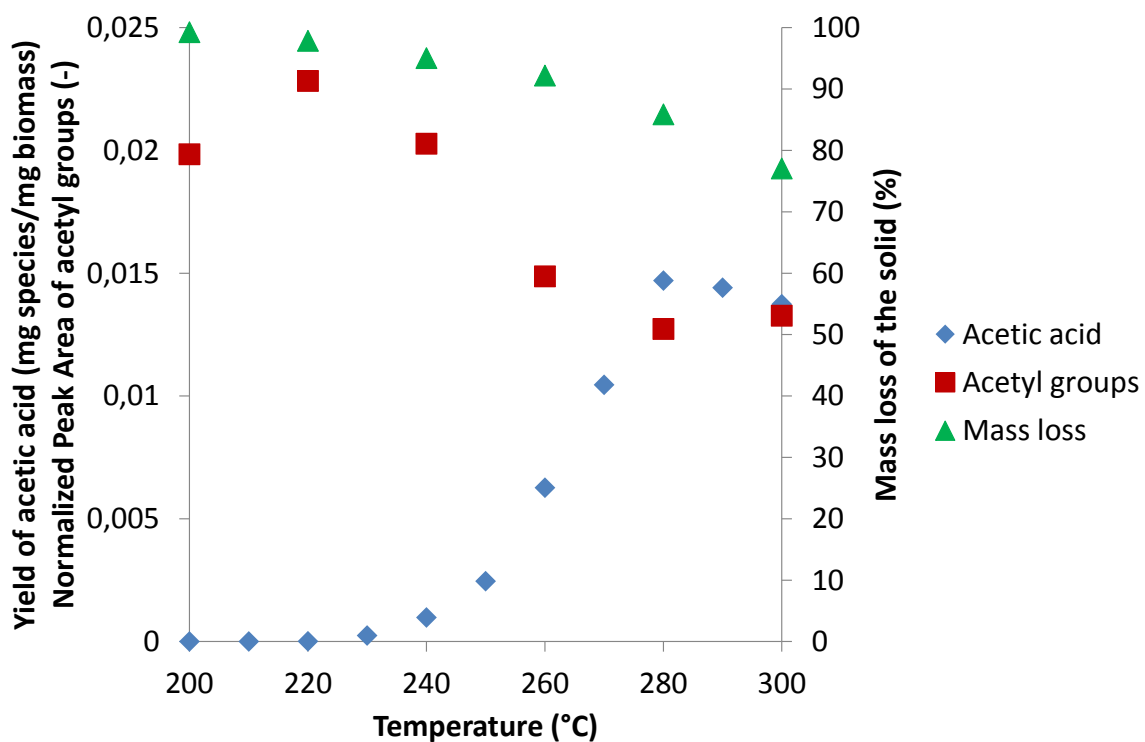


Fig. 70. TGA-GC-MS and solid-state NMR synergy for ash-wood.

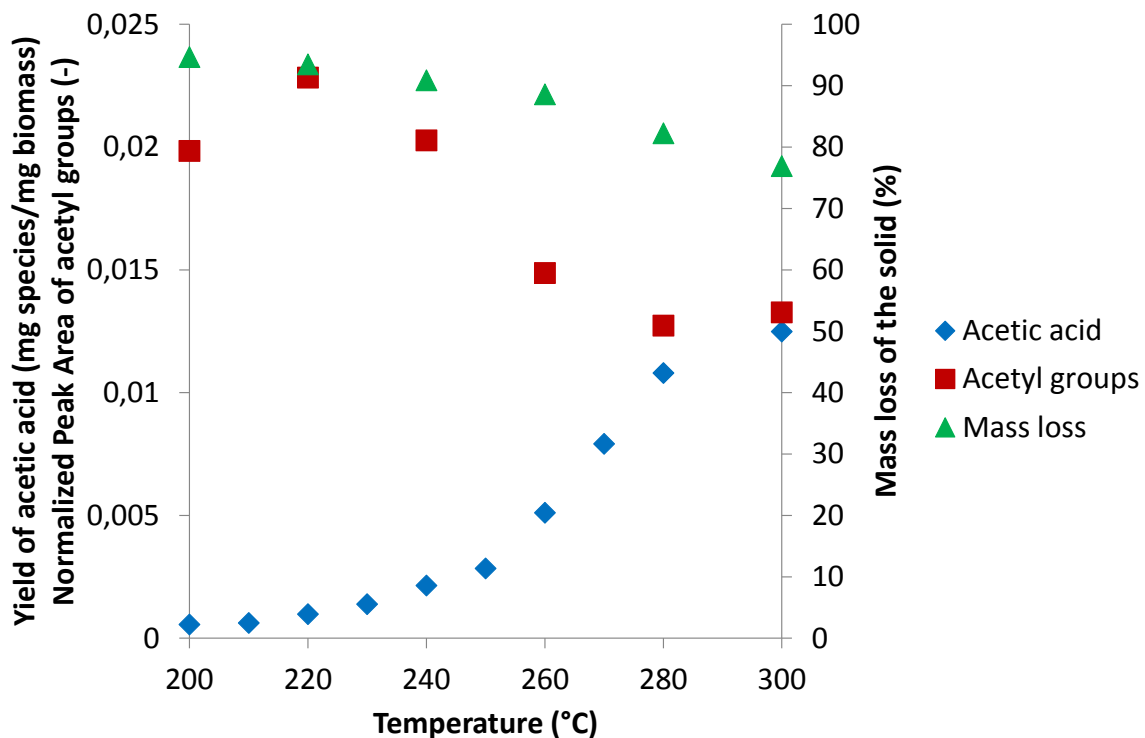


Fig. 71. TGA-GC-MS and solid-state NMR synergy for wheat straw.

For ash-wood and wheat straw, the production of acetic acid increases and, in parallel, the proportion of acetyl groups decreases. This leads to think that the production of acetic acid and the degradation of acetyl groups would be correlated for ash-wood and wheat straw. However, for pine, the production of acetic acid increases whereas, in parallel, the proportion of acetyl groups remains stable. This leads to think that the production of acetic acid and the degradation of acetyl groups would not be correlated for pine.

6. CONCLUSION

Table 37 synthesizes all the original experimental results, obtained by TGA-TG-MS and solid-state NMR. For results on the formation of condensable species, the normal font corresponds to appearance of the species, and the bold font corresponds to significant appearance. For results on the characterization of functional groups within the

solid, the green font indicates the increase of the functional group, the red font indicates its decrease, and the strikethrough font indicates its disappearance.

Table 37. Synthesis of original experimental results from TGA-GC-MS and solid-state NMR.

	200°C	220°C	240°C	250°C	260°C	270°C	280°C
Pine	acetic acid furfural vanillin	formic acid	2-furanmethanol	hydroxyacetone eugenol isoeugenol glycolaldehyde furfural 2-methoxy-4-vinylphenol vanillin	aromatics in lignin	hydroxyacetone acetic acid 2-furanmethanol eugenol isoeugenol formic acid 2-methoxy-4-vinylphenol	C1 of cellulose C4 and C6 of crystalline cellulose C4 and C6 of amorphous cellulose glycolaldehyde
Ash-wood	acetic acid furfural vanillin	formic acid	2-furanmethanol	hydroxyacetone eugenol isoeugenol glycolaldehyde 2-methoxy-4-vinylphenol vanillin	acetyl groups in hemicellulose formic acid furfural	hydroxyacetone acetic acid 2-furanmethanol eugenol isoeugenol glycolaldehyde 2-methoxy-4-vinylphenol	aromatics in lignin C1 of cellulose C4 and C6 of crystalline cellulose C4 and C6 of amorphous cellulose
Miscanthus					aromatics in lignin C1 of cellulose C4 and C6 of crystalline cellulose C4 and C6 of amorphous cellulose methoxyl groups in lignin acetyl groups in hemicellulose		acetyl groups in hemicellulose
Wheat straw	C1 of cellulose C4 and C6 of crystalline cellulose C4 and C6 of amorphous cellulose acetic acid furfural vanillin	formic acid	2-furanmethanol	hydroxyacetone eugenol isoeugenol glycolaldehyde 2-methoxy-4-vinylphenol vanillin	aromatics in lignin methoxyl groups in lignin acetyl groups in hemicellulose 2-methoxy-4-vinylphenol	hydroxyacetone acetic acid 2-furanmethanol eugenol isoeugenol glycolaldehyde formic acid furfural	acetyl groups in hemicellulose

CHAPTER V: MODELLING

1. INTRODUCTION

In the present chapter, a conceptual model of torrefaction reaction mechanisms is proposed, based on the set of experimental results and their associated synergy exposed in chapter IV.

2. APPROACH

As already mentioned, biomass is mainly constituted of the macro-polymers cellulose, hemicellulose and lignin, and to a less extent of extractives and ashes. There is at the moment no consensus on the role of these minor constituents during torrefaction. However, several authors claim that their role would not be significant within the torrefaction interval of temperatures (Collard and Blin, 2014; Sebio-Puñal et al., 2012). Moreover, kinetic models discussed in section 4.2 of chapter II did not consider neither extractives nor ashes in reactivity of biomass. Based on these facts, the conceptual model of the present work considers biomass reactivity only on the basis of cellulose, hemicellulose and lignin reactivity.

Significant interactions between certain constituents of biomass have been reported in literature during torrefaction (Nocquet, 2012). However, in the present work, these interactions are not considered. The reason is that our model aims to give a first approach to detailed mechanisms of torrefaction, thus it has been chosen to simplify the model and focus on detailed individual degradation of the three macro-constituents.

In the present work, a more detailed approach of biomass constituents composition is proposed, in order to explain the differences in cellulose, hemicellulose and lignin – and thus of the whole biomass – reactivity during torrefaction of different species of biomass:

- Cellulose is considered as composed only of glucose monomers (see section 1.4.1 of chapter I), thus cellulose is described with the same chemical formula for all biomasses. Crystalline and amorphous cellulose coexist, as shown by calculation of crystalline index shown in section 4.2.1 of chapter IV. Crystalline and amorphous cellulose do not suffer the same reaction mechanisms of degradation during torrefaction. Amorphous cellulose gives rise to chemical

species in the gaseous phase, whereas crystalline cellulose gives rise to amorphous cellulose.

- Hemicellulose is considered as a blend of C5 and C6 sugars – with different average chemical formulae, shown in Table 38 –, and the proportion of these sugars varies as a function of biomass type, as indicated by chemical analysis shown in section 1.4.2 of chapter I. Some mechanisms affect only C5 sugars, others affect only C6 sugars, and the remaining affect both C5 and C6 sugars.
- Lignin is considered as a blend of H, S and G units– with different chemical formulae, shown in Table 38 –, and the proportion of these units also varies as a function of biomass species (see section 1.4.3 in chapter I). In the present work, no chemical analysis of lignin units has been carried out. Reaction mechanisms of lignin degradation affect either all units, or only G and S units.

Table 38 shows the reactants considered in torrefaction mechanisms of the present works, and their chemical formulae.

Table 38. Reactants in torrefaction mechanisms.

Constituent	Approach	Chemical formula	Bibliographic reference
Cellulose	Crystalline cellulose	$C_6H_{10}O_5$	Sjostrom (1993)
	Amorphous cellulose		
Hemicellulose	C5 sugars	$C_5H_{10}O_6$	Wang et al. (2013)
	C6 sugars	$C_6H_{10.5}O_5$	
Lignin	H unit	$C_9H_{10}O_2$	Lupoi et al. (2015)
	G unit	$C_{10}H_{12}O_3$	
	S unit	$C_{11}H_{14}O_4$	

Our model has a validated chemical meaning, however, it has not been developed mathematically. For this reason, in next sections, the model proposed is referred to as a conceptual model.

In addition, the adjustment of stoichiometric coefficients in reactions has been carried out on the basis of the elemental composition of reactants and products.

3. PRODUCTS CONSIDERED

In the present work, twenty-six species are considered to be involved in the reaction mechanisms proposed. The choice of mechanisms has been done on the basis of the condensable species of interest defined in the framework of the INVERTO project.

The case of propanoic acid deserves special mention. In literature, this species has been considered a product of torrefaction mechanisms (Lê Thành et al., 2015). However, in the present work propanoic acid has been considered to come from extractive matter in biomass, and it would be directly released from biomass, without transformation, during torrefaction. For this reason, its production has not been considered in the present proposition of reaction mechanisms.

Table 39 and Table 40 show the name of each species as well as its abbreviation in the present work, chemical formula and representation.

Table 39. Gaseous species considered as products in reaction mechanisms.

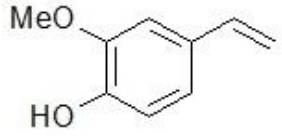
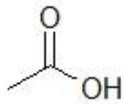
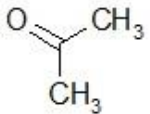
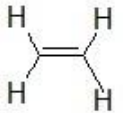
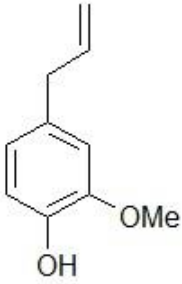
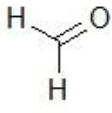
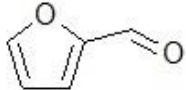
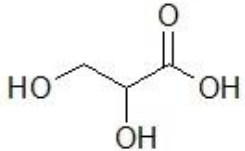
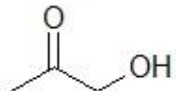
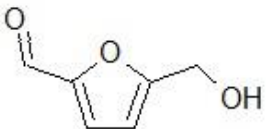
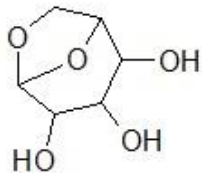
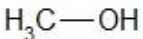
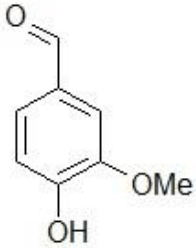
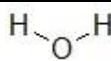
Name	Abbreviation	Chemical formula	Representation
2-methoxy-4-vinylphenol	2M4V	$C_9H_{10}O_2$	
Acetic acid	AA	$C_2H_4O_2$	
Acetone	Ac	C_3H_6O	
Carbon dioxide	---	CO_2	$O=O$
Carbon monoxide	---	CO	$=O$
Char	Ch	$C_5H_{8.5}O_3$ (reaction H7 and H12) $C_4H_8O_4$ (reaction H8) $C_4H_{6.5}O_3$ (reaction H9) $C_4H_8O_3$ (reaction H11) C_8H_8O (reaction L4)	?
Ethylene	Et	C_2H_4	
Eugenol	Eu	$C_{10}H_{12}O_2$	
Formaldehyde	Fo	CH_2O	
Formic acid	FA	CH_2O_2	

Table 40. Gaseous species considered as products in reaction mechanisms (continued).

Name	Abbreviation	Chemical formula	Representation
Furfural	FF	$C_5H_4O_2$	
Glyceric acid	GAc	$C_3H_6O_4$	
Glycolaldehyde	GA	$C_2H_4O_2$	
Hydrogen	---	H_2	
Hydroxyacetone	HA	$C_3H_6O_2$	
Hydroxymethylfurfural	HMF	$C_6H_6O_3$	
Levogluconan	LG	$C_6H_{10}O_5$	
Methanol	M	CH_4O	
Oxygen	---	O_2	
Propanal	Pr	C_3H_6O	
Vanillin	V	$C_8H_8O_3$	
Water	---	H_2O	

4. REACTION MECHANISMS

For each biomass constituent, a different number of reaction mechanisms take place. Cellulose presents six degradation mechanisms, while hemicellulose and lignin present twelve degradation mechanisms.

The reaction mechanisms of cellulose degradation are decrystallization, dehydration, transglycosylation, depolymerization, and fragmentations with formation of glycolaldehyde and hydroxyacetone. The reaction mechanisms of hemicellulose degradation are dehydration of alkyl chains, depolymerization, fragmentation of acetyl groups and methoxyl groups, fragmentation with formation of formic acid and glycolaldehyde, fragmentation of carboxyl groups and cracking of carbonyl groups. Finally, the reaction mechanisms of lignin degradation are dehydration of alkyl chains, fragmentation of C_{β} - C_{γ} bonds, and fragmentation with formation of eugenol, 2-methoxy-4-vinylphenol and vanillin. The thirty reaction mechanisms are detailed in the next sections.

The majority of chars come from the degradation of hemicellulose, only one comes from lignin and no char comes from cellulose. As explained in section 3, these chars do not present the same chemical formula among them. Their atomic H/C and O/C ratios are shown in Fig. 72. The torrefaction chars of the present work have H/C and O/C ratios slightly higher than torrefied biomass reported in literature (Prins, 2005).

Stoichiometric coefficients in reactions have been adjusted according to the elemental composition of reactants and products. However, they do not include thermodynamic considerations, like the enthalpy and the Gibbs free energy of formation.

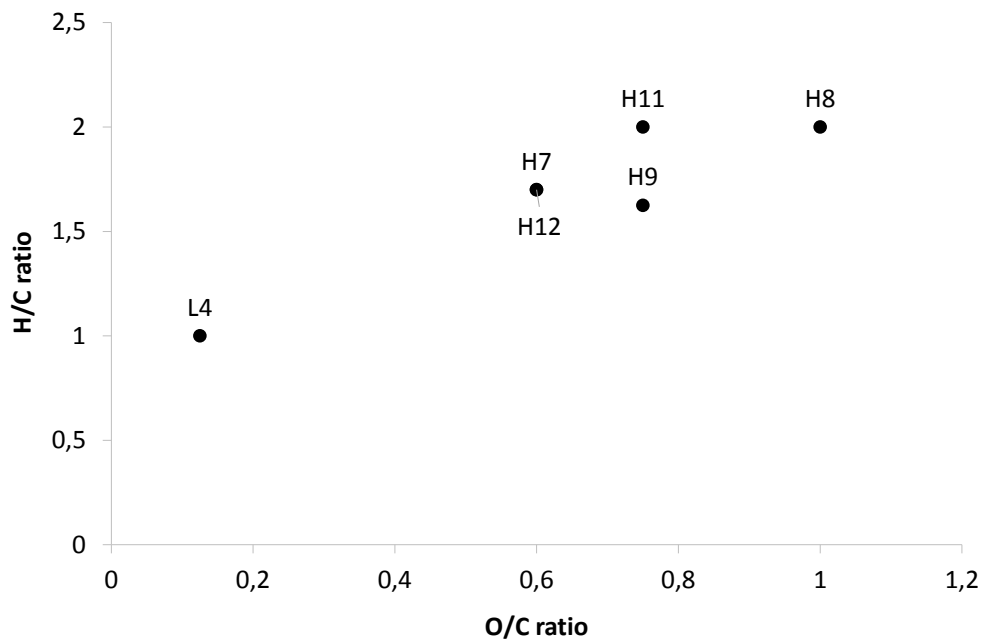


Fig. 72. Van Krevelen diagram of chars.

4.1. CELLULOSE REACTIVITY

Cellulose is proposed to be degraded through six reaction mechanisms during torrefaction. These reaction mechanisms are shown in Table 41.

Table 41. Reaction mechanisms of cellulose degradation.

No.	Name	Reactions	Phase	Range of temperature / Observations
C1	Decrystallization	$C_6H_{10}O_5$ crystalline \rightarrow $C_6H_{10}O_5$ amorphous	S \rightarrow S	200-325°C?
C2	Dehydration	$C_6H_{10}O_5$ amorphous \rightarrow $C_6H_8O_4$ + H_2O	S \rightarrow S + G	200-550°C?
C3	Transglycosylation	$C_6H_{10}O_5$ amorphous \rightarrow $C_6H_{10}O_5$ (LG)	S \rightarrow G	200-500°C?
C4	Depolymerization	$2 C_6H_{10}O_5$ amorphous \rightarrow $C_6H_{10}O_5$ (LG) + $C_5H_4O_2$ (FF) + CH_2O (Fo) + $2 H_2O$	S \rightarrow G	200-390°C?
C5	Fragmentation to form glycolaldehyde	$C_6H_{10}O_5$ amorphous + H_2O \rightarrow $3 C_2H_4O_2$ (GA)	S + G \rightarrow G	250°C-?
C6	Fragmentation to form hydroxyacetone	$C_6H_{10}O_5$ amorphous + H_2O \rightarrow $C_3H_6O_2$ (HA) + $C_3H_6O_4$ (GAc)	S + G \rightarrow G	250°C-?

4.1.1. Decrystallization

Reaction C1 is the decrystallization mechanism which transforms crystalline cellulose into amorphous cellulose.

Experimental results on chemical evolution of the solid phase have shown that decrystallization begins at 280°C for pine and ash-wood, at 260°C for miscanthus and at 200°C for wheat straw. At 300°C, crystalline cellulose of miscanthus and wheat straw have almost completely disappeared, whereas crystalline cellulose of pine and ash-wood have not completely disappeared. This would lead to think that decrystallization takes place from 200°C. This hypothesis is quite far from literature, where it has been reported that decrystallization takes place from 270°C. However, our hypothesis agrees with the reported fact that complete disappearance of crystalline structure takes place at high temperatures of torrefaction (Pastorova et al., 1994; Yu et al., 2012). Some works have stated the presence of a partial recrystallization before complete degradation of crystalline cellulose, as mentioned in section 4.2.3 of chapter IV. However, experimental results of the present work have not shown any cellulose recrystallization, thus recrystallization is not considered in the reaction mechanisms proposed here.

4.1.2. Dehydration

Reaction C2 shows the dehydration which leads from amorphous cellulose to anhydrocellulose and release of water.

Water has not been detected in the present work, yet the evolution of amorphous cellulose in the solid phase has been quantified. It has been observed that, during torrefaction, amorphous cellulose (and also hemicellulose) is conserved until 280°C for pine and ash-wood, whereas it degrades from 260°C for miscanthus, and from 200°C for wheat straw. This would mean that agricultural by-products start to degrade before other biomasses do. Besides, at 300°C, amorphous cellulose of miscanthus and wheat straw have almost completely disappeared, whereas at this temperature amorphous cellulose of pine and ash-wood have not completely disappeared. This could mean that dehydration of amorphous cellulose begins at 200°C. This hypothesis agrees with

literature, where reaction of cellulose dehydration has been reported to start at 220°C. According to the present work, dehydration finishes at 300°C or even above, which is also in agreement with literature, where it has been reported that dehydration continues beyond torrefaction interval of temperatures (Scheirs et al., 2001).

According to previous works, dehydration reaction would be responsible for most of the mass loss of cellulose during torrefaction, promoted by low temperatures and slow heating rates, as well as for being at the origin of charring formation. The dehydration can be originated either intra-ring (within a glucopyranose moiety) or inter-ring (between two chains). On the one hand, intra-ring dehydration gives rise to a keto-enol tautomerization equilibrium (see Fig. 73). This leads to the formation of C=C bonds, which promotes the formation of benzene rings composing char. On the other hand, inter-ring dehydration gives rise to stable ether bonds (see Fig. 73). This leads to the formation of covalent bonds, which means higher thermal stability. Within the torrefaction interval, dehydration reactions would be mainly inter-ring ones (Collard and Blin, 2014; Scheirs et al., 2001).

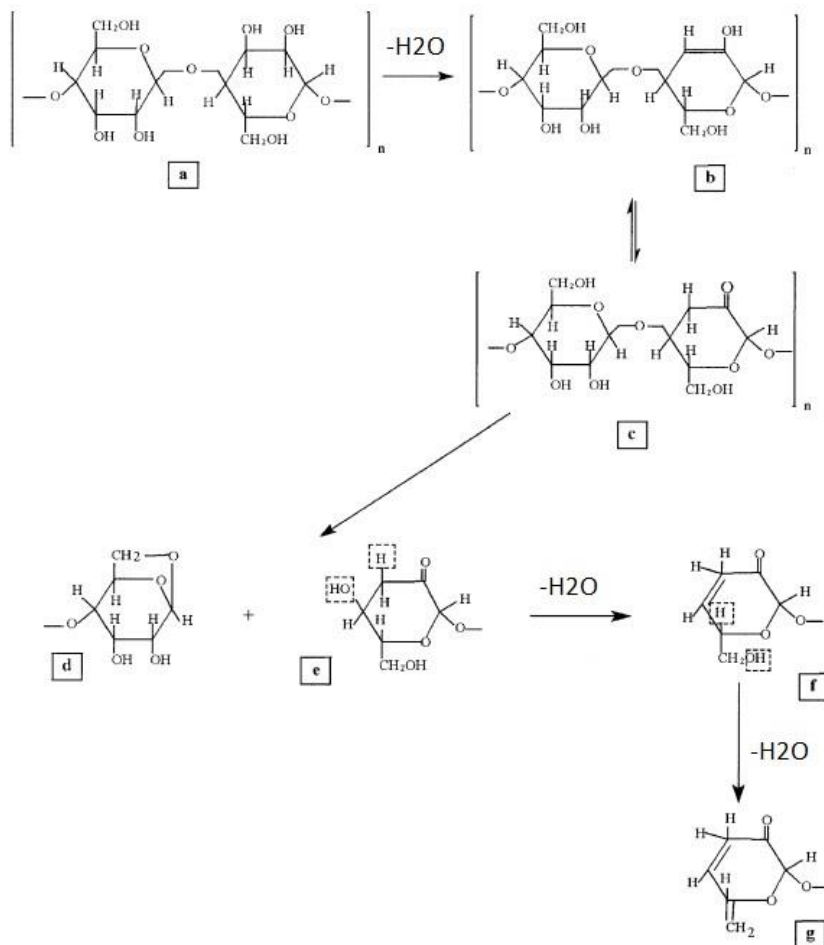


Fig. 73. Intra-ring dehydration of cellulose: (a) enol form of anhydrocellulose, (b) keto form of anhydrocellulose, (c) transglycosylation to form a levoglucosan chain-end, (d) hydroxyl glucosidic chain-end, (e) unsaturation on the glucosidic chain-end, (f) elimination of water on C6, (g) formation of a vinylene group (Scheirs et al., 2001).

4.1.3. Transglycosylation

Reaction C3 describes the mechanism of transglycosylation, which leads to formation of levoglucosan from amorphous cellulose (see Fig. 73).

Since levoglucosan has not been detected in the present work – probably due to the fact that its production did not reach the detection limit –, experimental measures are not available. However, the evolution of amorphous cellulose in the solid has been quantified. As already said, amorphous cellulose (and also hemicellulose) is conserved until 280°C for pine and ash-wood, whereas it degrades from 260°C for miscanthus, and

from 200°C for wheat straw. Besides, at 300°C, amorphous cellulose of miscanthus and wheat straw have almost completely disappeared, whereas at this temperature amorphous cellulose of pine and ash-wood have not completely disappeared. These observations might lead to think that transglycosylation starts at 200°C, although it is probable that the degradation of amorphous cellulose is caused by other mechanisms and not transglycosylation, at low temperatures. In literature, the reaction of transglycosylation has been reported to take place from 300°C (Wang et al., 2013), which would confirm that transglycosylation do not start at low torrefaction temperatures.

According to literature, transglycosylation consists of the rupture of glycosidic bonds between glucopyranoses. This type of depolymerization has a relatively slow kinetics within torrefaction interval, however it seems that water catalyzes this reaction. Therefore, the presence of water (partly released by dehydration mechanisms) would accelerate the transglycosylation (Collard and Blin, 2014; Wang et al., 2011, 2013).

4.1.4. Depolymerization

Reaction C4 describes the mechanism of further depolymerization of amorphous cellulose, which forms levoglucosan in the solid phase and light condensable species in the gaseous phase. These condensable species are furfural, formaldehyde and water.

Levoglucosan, formaldehyde and water have not been detected in the present work, however furfural has been semi-quantified. Experimental results have shown that formation of furfural increases with temperature, and is present from 200°C although starts to be significant from 250-270°C. Furfural is formed during torrefaction of pine, ash-wood and wheat straw (no data available for miscanthus). In parallel, evolution of amorphous cellulose in the solid has been quantified (see previous sections). These observations lead to think that depolymerization of amorphous cellulose would start at 200°C, although become significant from 250°C. In literature, depolymerization of amorphous cellulose has been reported to start at 300°C and to accelerate until 390°C (Scheirs et al., 1998). Thus, temperature for the start of depolymerization in the present work is much lower than the one reported in literature.

Several works in literature have claimed that depolymerization of cellulose is very fast, contrary to transglycosylation. At 300°C, glycosidic bonds become very reactive,

leading to a high yield of condensable species (Collard and Blin, 2014; Scheirs et al., 1998). In general, cellulose with a low crystallinity index would lead to less levoglucosan and more furans, whereas cellulose with a high crystallinity index would lead to more levoglucosan and less furans (Wang et al., 2013).

4.1.5. Fragmentation to form glycolaldehyde

Reaction C5 describes the mechanisms of amorphous cellulose fragmentation which leads to the formation of glycolaldehyde.

In the present work, glycolaldehyde has been semi-quantified. Results have shown that glycolaldehyde production increases with temperature, being present from 250°C and becoming significant from 270-280°C. Glycolaldehyde is produced by pine, ash-wood and wheat straw (no data available for miscanthus). In parallel, in the solid phase, it has to be remembered that amorphous cellulose (and also hemicellulose) is conserved until 280°C for pine and ash-wood, whereas it degrades from 260°C for miscanthus, and from 200°C for wheat straw. This could lead to think that the reaction of fragmentation to form glycolaldehyde takes place from 250°C, although it becomes significant from 270°C. However, in literature, this reaction has been observed only at 530°C (Shen and Gu, 2009; Wooten et al., 2004), thus our hypothesis is in disagreement with bibliography.

According to literature, fragmentation of amorphous cellulose to form glycolaldehyde would be a secondary mechanism, present to a very little extent during torrefaction interval of temperatures (Shen and Gu, 2009; Wooten et al., 2004).

4.1.6. Fragmentation to form hydroxyacetone

Reaction C6 describes the mechanism of amorphous cellulose fragmentation which leads to the formation of hydroxyacetone.

In the present work, hydroxyacetone has been quantified. Results have shown that hydroxyacetone production starts at 250°C, increases with temperature, and becomes significant from 270°C. Hydroxyacetone is produced by pine, ash-wood and wheat straw (no data available for miscanthus). Besides, and taking into account the evolution of amorphous cellulose in the solid phase, our results lead to think that the

fragmentation of amorphous cellulose to form hydroxyacetone could start at 250°C, then become significant at 270°C. Like in the case of fragmentation to form glycolaldehyde, in literature, this reaction has been observed only at 530°C (Shen and Gu, 2009; Wooten et al., 2004). Hence, our hypothesis is in disagreement with bibliography.

Like in the case of fragmentation to form glycolaldehyde, these bibliographic works claim that fragmentation of amorphous cellulose to form hydroxyacetone would be a secondary mechanism, present to a very little extent during torrefaction interval of temperatures (Shen and Gu, 2009; Wooten et al., 2004).

Finally, our hypothesis proposes that glyceric acid could be formed as a by-product during this reaction. To our knowledge, no formation of glyceric acid has been reported in literature during fragmentation of amorphous cellulose to form hydroxyacetone.

4.2. HEMICELLULOSE REACTIVITY

Hemicellulose is proposed to be degraded through twelve mechanisms. In the present work, the difference in reactivity for C5 and C6 sugars is considered. When the same reaction takes place from C5 and C6 sugars, it has been reported that C5 sugars react at a lower temperature, around 20-30°C lower, than C6 sugars (Collard and Blin, 2014). Table 42 shows the reaction mechanisms responsible for the degradation of hemicellulose sugars.

Table 42. Reaction mechanisms of hemicellulose degradation.

No.	Name	Reactions	Phase	Range of temperature / Observations
H1	Dehydration of C6 sugars	$C_6H_{10.5}O_5 \rightarrow C_6H_{8.5}O_4 + H_2O$	S → S + G	C6 sugars: 150?-270°C?
H2	Dehydration of C5 sugars	$C_5H_{10}O_6 \rightarrow C_5H_8O_5 + H_2O$	S → S + G	C5 sugars: 150?-240°C?
H3	Depolymerization of C6 sugars	$2 C_6H_{10.5}O_5 \rightarrow 2 C_6H_6O_3 \text{ (HMF)} + 4 H_2O + \frac{1}{2} H_2$	S → G	C6 sugars: 200-350°C?
H4	Depolymerization of C5 sugars	$2 C_5H_{10}O_6 \rightarrow 2 C_5H_4O_2 \text{ (FF)} + 6 H_2O + O_2$	S → G	C5 sugars: 200-320°C?
H5	Fragmentation of acetyls (-CO-CH3) of C5 sugars	$C_5H_{10}O_6 \rightarrow 2 C_2H_4O_2 \text{ (AA)} + CH_2O_2 \text{ (FA)}$	S → G	C5 sugars: 200-700°C?
		$C_5H_{10}O_6 \rightarrow 2 C_2H_4O_2 \text{ (AA)} + CO + H_2O$	S → G	
H6	Fragmentation of methoxyls (-O-CH3) of C5 sugars	$C_5H_{10}O_6 \rightarrow 2 CH_4O \text{ (M)} + CH_2O_2 \text{ (FA)}$	S → G	Hemicellulose: 200°C-?
		$C_5H_{10}O_6 \rightarrow 2 CH_4O \text{ (M)} + CO + H_2O$	S → G	
H7	Fragmentation and formation of formic acid from C6 sugars	$C_6H_{10.5}O_5 \rightarrow CH_2O_2 \text{ (FA)} + C_5H_{8.5}O_3 \text{ (Ch)}$	S → S + G	Hemicellulose: 220-300°C?
H8	Fragmentation and formation of formic acid from C5 sugars	$C_5H_{10}O_6 \rightarrow CH_2O_2 \text{ (FA)} + C_4H_8O_4 \text{ (Ch)}$	S → S + G	Hemicellulose: 220-300°C?
H9	Fragmentation and formation of glycolaldehyde from C6 sugars	$C_6H_{10.5}O_5 \rightarrow C_2H_4O_2 \text{ (GA)} + C_4H_{6.5}O_3 \text{ (Ch)}$	S → S + G	C6 sugars: 250-270°C?
H10	Fragmentation and formation of glycolaldehyde from C5 sugars	$C_5H_{10}O_6 \rightarrow 2 C_2H_4O_2 \text{ (GA)} + CH_2O_2 \text{ (FA)}$	S → G	C5 sugars: 250-320°C?
		$C_5H_{10}O_6 \rightarrow 2 C_2H_4O_2 \text{ (GA)} + CO + H_2O$	S → G	
H11	Fragmentation of carboxyls (-COOH) of C5 sugars	$C_5H_{10}O_6 \rightarrow CO_2 + H_2O + C_4H_8O_3 \text{ (Ch)}$	S → S + G	C5 sugars: 180?-900°C?
H12	Cracking of carbonyls (-CO-) of C6 sugars	$C_6H_{10.5}O_5 \rightarrow CO + H_2O + C_5H_{8.5}O_3 \text{ (Ch)}$	S → S + G	Hemicellulose: 210?-900°C?

4.2.1. Dehydration of C6 and C5 sugars

Reactions H1 and H2 consist of dehydration of C6 and C5 sugars of hemicellulose, respectively, to produce anhydrosugars and water.

In the present work, water formation during torrefaction has not been measured, thus no experimental data are available. In literature, dehydration of hemicellulose has been reported to start at 150°C for both C6 and C5 sugars. It would become significant from 200°C, and continue to take place until 270°C for C6 sugars and 240°C for C5 sugars (Worasuwannarak et al., 2007).

4.2.2. Depolymerization of C6 and C5 sugars

Reactions H3 and H4 represent the depolymerization of C6 and C5 sugars, which lead to formation of hydroxymethylfurfural and furfural, respectively, and water.

Water has not been detected in the present work, hydroxymethylfurfural has been detected and furfural has been semi-quantified in the present work. Experimental results have shown that hydroxymethylfurfural production increases with temperature from 200°C. This species is formed in torrefaction of pine, ash-wood and wheat straw, but barely formed during torrefaction of miscanthus – only from 200 to 230°C. Experimental results have shown that furfural production increases with temperature, and is present from 200°C, although formation starts to be significant from 250-270°C. Furfural is formed during torrefaction of pine, ash-wood and wheat straw (no data available for miscanthus). As there is no peak which purely corresponds to hemicellulose evolution, a direct relationship with hydroxymethylfurfural and furfural production cannot be established. However, from results on condensable species production, it could be derived that reactions H3 and H4 take place from 200°C and are significant from 250°C. In literature, reaction H3 for C6 sugars is reported to take place between 270 and 350°C, whereas reaction H4 for C5 sugars is reported to take place between 240 and 320°C (Alén et al., 1996; Boonstra et al., 2007; Branca et al., 2013). Thus, our hypothesis is quite in agreement with literature.

Finally, these reactions also formed by-products. Reaction H3 forms hydrogen, whereas reaction H4 forms oxygen. Neither of these by-products have been detected in the present work.

4.2.3. Fragmentation of acetyl groups

Reaction H5 consists of the fragmentation of acetyl groups mainly contained in xylan of C5 sugars, which produces acetic acid.

Acetic acid production has been quantified in the present work. The quantity of acetic acid formed increases with temperature, since it is detected from 200°C although formation starts to be significant from 270°C. Acetic acid is formed during torrefaction of pine, ash-wood and wheat straw (no data available for miscanthus). In parallel, degradation of acetyl groups in hemicellulose is measured from 260°C. According to results on chemical evolution of the solid during torrefaction, acetyl groups in hemicellulose begin to degrade at 260°C for ash-wood, miscanthus and wheat straw, whereas for pine they remain quite stable. Moreover, acetyl groups of miscanthus and wheat straw are completely degraded at 280°C. This could lead to think that reaction H5 takes place from 200°C at a relatively slow kinetics, knowing that from 260°C kinetics becomes faster. This hypothesis agrees with literature, which assumes the start temperature of reaction H5 at 200°C (Peng and Wu, 2010; Prins et al., 2006a).

In the present work, two hypotheses are proposed to explain the formation of the other products of this reaction. In addition of acetic acid formation, this reaction could form either formic acid (AF), or carbon monoxide plus water. In literature, it has been reported that acetic acid may be secondary decomposed into carbon monoxide and dioxide at high temperatures of torrefaction (Peng and Wu, 2010).

4.2.4. Fragmentation of methoxyl groups

Reaction H6 consists of the fragmentation of methoxyl groups mainly contained in xylan of C5 sugars to form methanol.

Methanol production has been detected in the present work. Formation of methanol is present from 200°C for pine, ash-wood, miscanthus and wheat straw. As there is no peak which purely corresponds to hemicellulose evolution, a direct relationship with methanol production cannot be established. Methanol production data may suggest that reaction H6 takes place from 200°C. This is in agreement with literature, where fragmentation of methoxyl groups in hemicellulose was reported to start at 200°C (Prins et al., 2006a).

Moreover, two hypotheses are proposed to explain the formation of the other products of this reaction. Reaction H6 could either form formic acid, or carbon monoxide plus water.

4.2.5. Fragmentation of side chains to form formic acid

Reactions H7 and H8 consist of fragmentation of side chains to form formic acid from C6 and C5 sugars, respectively.

Formic acid has been semi-quantified in the present work. Production of formic acid increases with temperature, is detected from 220°C and starts to be significant from 260-270°C. Moreover, formic acid is produced by pine, ash-wood and wheat straw (no data available for miscanthus). As usual, there is no peak which purely corresponds to hemicellulose evolution, a direct relationship with formic acid production cannot be established. Results for production of formic acid may suggest that reaction H5 takes place from 220°C at a relatively slow kinetics, and then acquires a faster kinetics from 260°C. This hypothesis is in agreement with literature, where formation of formic acid from hemicellulose is reported to take place from 230°C (Prins et al., 2006a).

Regarding formation of by-products, both reactions would lead to production of char. However, chemical formulae of these two chars are different: reaction H7 produces $C_5H_{8.5}O_3$, whereas reaction H8 produces $C_4H_8O_4$.

4.2.6. Fragmentation of C6 and C5 sugars to form glycolaldehyde

Reactions H9 and H10 are fragmentation mechanisms for C6 and C5 sugars, respectively, to form glycolaldehyde.

Glycolaldehyde has been semi-quantified in the present work. Results have shown that glycolaldehyde production increases with temperature, being present from 250°C although significant from 270-280°C. Glycolaldehyde is produced by pine, ash-wood and wheat straw (no data available for miscanthus). Again, because there is no peak which purely corresponds to hemicellulose evolution, a direct relationship with glycolaldehyde production cannot be established. However, with results on production of glycolaldehyde, it could be derived that reactions H9 and H10 take place from 250°C with a slow kinetics, then from 270°C with a faster kinetics. This contrasts with literature, where formation of glycolaldehyde is reported to begin at a lower temperature, around 220°C. Besides, reactions H9 and H10 have been reported to be secondary mechanisms, present in little extent within the torrefaction interval of temperatures (Wu et al., 2009).

Fragmentation of C6 sugars would also produce a form of char, whose chemical formula is $C_4H_{6.5}O_3$. Fragmentation of C5 sugars presents two hypotheses: it might form either formic acid, or carbon monoxide plus water.

4.2.7. Fragmentation of carboxyl groups in C5 sugars

Reaction H11 describes the fragmentation of carboxyl groups in C5 sugars. This reaction would form a gaseous phase composed of carbon dioxide and water, as well as a form of char in the solid phase – whose formula is $C_4H_8O_3$. As carbon dioxide and water formation during torrefaction have not been measured in the present work, no hypothesis could be emitted about this reaction. In literature, fragmentation of carboxyl groups has been reported to start at 180°C (Yang et al., 2007).

4.2.8. Fragmentation of carbonyl groups in C6 sugars

Reaction H12 presents the fragmentation of carbonyl groups in C6 sugars. This reaction would produce carbon monoxide and water in the gaseous phase, and a form of

char in the solid phase – whose formula is $C_5H_{8.5}O_3$. Again, since carbon monoxide and water formation during torrefaction have not been measured in the present work, no hypothesis could be emitted about this reaction. Previous works have reported the beginning of this reaction at 210°C (Yang et al., 2007).

4.3. LIGNIN REACTIVITY

Lignin is proposed to be degraded through twelve mechanisms. Table 43 shows the reaction mechanisms responsible for the degradation of lignin.

Table 43. Reaction mechanisms of lignin degradation.

No.	Name	Reactions	Phase	Range of temperature / Observations
L1	Dehydration of alkyl chains in H units	$C_9H_{10}O_2 (uH) \rightarrow C_9H_8O + H_2O$	S → S + G	180?-425°C?
L2	Dehydration of alkyl chains in G units	$C_{10}H_{12}O_3 (uG) \rightarrow C_{10}H_{10}O_2 + H_2O$	S → S + G	180?-425°C?
L3	Dehydration of alkyl chains in S units	$C_{11}H_{14}O_4 (uS) \rightarrow C_{11}H_{12}O_3 + H_2O$	S → S + G	180?-425°C?
L4	Fragmentation of C _β -C _γ bonds in H units	$C_9H_{10}O_2 (uH) \rightarrow CH_2O (Fo) + C_8H_8O (Ch)$	S → S + G	180?-900°C?
L5	Fragmentation of C _β -C _γ bonds in G units	$C_{10}H_{12}O_3 (uG) \rightarrow CH_2O (Fo) + C_9H_{10}O_2 (uH)$	S → S + G	180?-900°C?
L6	Fragmentation of C _β -C _γ bonds in S units	$C_{11}H_{14}O_4 (uS) \rightarrow CH_2O (Fo) + C_{10}H_{12}O_3 (uG)$	S → S + G	180?-900°C?
L7	Fragmentation and formation of eugenol from G units	$C_{10}H_{12}O_3 (uG) + CO \rightarrow C_{10}H_{12}O_2 (Eu) + CO_2$	S + G → G	250-300°C?
L8	Fragmentation and formation of eugenol from S units	$C_{11}H_{14}O_4 (uS) \rightarrow C_{10}H_{12}O_2 (Eu) + CH_2O_2 (FA)$	S → G	250-300°C?
L9	Fragmentation and formation of 2-methoxy-4-vinylphenol from G units	$C_{10}H_{12}O_3 (uG) \rightarrow C_9H_{10}O_2 (2M4V) + CH_2O (Fo)$	S → G	250-380°C?
L10	Fragmentation and formation of 2-methoxy-4-vinylphenol from S units	$C_{11}H_{14}O_4 (uS) \rightarrow C_9H_{10}O_2 (2M4V) + 2 CH_2O (Fo)$	S → G	250-380°C?
L11	Fragmentation and formation of vanillin from G units	$C_{10}H_{12}O_3 (uG) \rightarrow C_8H_8O_3 (V) + C_2H_4 (Et)$	S → G	200-500°C?
L12	Fragmentation and formation of vanillin from S units	$C_{11}H_{14}O_4 (uS) \rightarrow C_8H_8O_3 (V) + C_3H_6O (Pr \text{ or } Ac)$	S → G	200-500°C?

4.3.1. Dehydration of alkyl chains

Reactions L1, L2 and L3 describe the dehydration mechanisms of alkyl chains of H, G and S units in lignin, respectively, which form water.

However, in the present work, the water formation has not been measured. In literature, the reaction has been reported to take place from 180°C (Jakab et al., 1995; Monteil-Rivera et al., 2013; Shen et al., 2010).

4.3.2. Fragmentation of C_β-C_γ bonds

Reactions L4, L5 and L6 consist of the fragmentation of C_β-C_γ bonds in H, G and S units, respectively, which give rise to formaldehyde.

In the present work, formaldehyde has not been detected during torrefaction experiments for any biomass. In literature, these reactions have been reported to be activated when hydroxyl groups are located on a C_γ carbon. Then a fragmentation between C_β and C_γ carbons would take place, provoking the release of formaldehyde (Collard and Blin, 2014; Jakab et al., 1995; Liu et al., 2008).

Reactions L4, L5 and L6 would also form solid by-products. Fragmentation on H units in reaction L4 would form char – whose chemical formula is C₈H₈O –, fragmentation on G units in reaction L5 would form H units, and fragmentation on S units in reaction L6 would form G units.

4.3.3. Formation of eugenol

Reactions L7 and L8 involve G and S units, respectively, in the formation of eugenol.

Eugenol has been quantified in the present work. It has been shown that eugenol production increases with temperature, present from 250°C although significant from 270°C. Eugenol is produced by pine, ash-wood and wheat straw (no data available for miscanthus). In parallel, aromatic structures in lignin appear to be stable until 260°C. From this temperature, their proportion increases, from more to less abundance, as

follows: wheat straw, miscanthus, pine and ash-wood. This could lead to think that reactions L7 and L8 take place from 250°C but are more significant from 260°C. This contrasts with literature, where formation of eugenol has been reported to begin at lower temperature, around 200°C (Fenner and Lephardt, 1981; Shen et al., 2010).

Reaction L7 would take place in the presence of carbon monoxide and give rise to carbon dioxide, for which higher quantities have been measured during torrefaction by works in literature, such as Nocquet et al. (2014a). Reaction L8 would give rise to formic acid as by-product, whose formation has been semi-quantified and observed to significantly increase from 260-270°C.

According to literature, mechanisms of these reactions would be based on the reactivity of chemical bonds between lignin monomers, such as α -O-4 and β -O-4, which are quite unstable and reactive at low temperatures. Concretely, α -O-4 bond would begin to react at 200°C, whereas β -O-4 bond would react from 245°C. This could lead to a reorganization in lignin structure, releasing phenolic molecules with a structure similar to that of lignin units. This means that released species would contain a propyl or ethyl side chain (Candelier et al., 2011; Collard and Blin, 2014; Huang et al., 2012; Kibet et al., 2012; Mu et al., 2013; Shen et al., 2010). This is the case of eugenol, which keeps the phenolic structure with a propyl chain (see Table 39).

4.3.4. Formation of 2-methoxy-4-vinylphenol

Reactions L9 and L10 involve G and S units, respectively, in the production of 2-methoxy-4-vinylphenol, also called 4-vinylguaiacol, and formaldehyde.

2-Methoxy-4-vinylphenol has been semi-quantified in the present work. It has been shown that 2-methoxy-4-vinylphenol production increases with temperature, being released from 250°C although its formation starts to be significant from 260-270°C. 2-Methoxy-4-vinylphenol is produced by pine, ash-wood and wheat straw (no data available for miscanthus). In parallel, aromatics in lignin appear to be stable until 260°C, then their proportion rises, from more to less abundancy, as follows: wheat straw, miscanthus, pine and ash-wood. This could mean that reactions L9 and L10 take place from 250°C with relatively slow kinetics then from 260°C with faster kinetics. To our knowledge, no

temperature intervals have been reported in literature for the mechanisms of production of 2-methoxy-4-vinylphenol.

Both reactions involved in the production of 2-methoxy-4-vinylphenol would take place for the same reasons as reaction L7 and L8 involved in the formation of eugenol, since 2-methoxy-4-vinylphenol keeps the phenolic structure with an ethyl chain (see Table 39) (Candelier et al., 2011; Collard and Blin, 2014; Huang et al., 2012; Kibet et al., 2012; Mu et al., 2013; Shen et al., 2010).

4.3.5. Formation of vanillin

Reactions L11 and L12 involve G and S units, respectively, in the formation of vanillin.

Vanillin has been semi-quantified in the present work. Experimental results have shown that vanillin production increases with temperature, as this species is detected from 200°C although its formation starts to be significant from 250-270°C. Vanillin is present in torrefaction of pine, ash-wood and wheat straw (no data available for miscanthus). In parallel, as already mentioned, aromatics in lignin appear to be stable until 260°C, then their proportion rises, from more to less abundance, as follows: wheat straw, miscanthus, pine and ash-wood. This could mean that reaction L11 and L12 take place from 200°C with slower kinetics, then from 250°C with faster kinetics. This hypothesis differs from literature (Candelier et al., 2011), where reaction is reported to take place only from 300°C.

Regarding formation of by-products, reaction L11 would produce ethylene, while reaction 12 would produce propanal or acetone. Neither ethylene nor acetone has been detected in the present work.

Reactions which form vanillin might take place at approximately the same temperature as reactions which form 2-methoxy-4-vinylphenol and eugenol, since both condensable species keep the phenolic structure. Vanillin keeps a one-carbon side chain (see Table 39), while 2-methoxy-4-vinylphenol keeps a two-carbon side chain, and eugenol keeps a three-carbon chain.

5. CONCLUSION

The conceptual model proposed has been elaborated using in a complementary way both the original experimental results of the present work and literature. The main innovations of our model compared with the existing ones lie in:

- The detailed approach of hemicellulose and lignin compositions, which enables to predict the differences of behavior observed among the different types of biomass;
- The elemental balance of reactions with stoichiometric coefficients;
- The chemical meaning of the mechanisms proposed.

CHAPTER VI: CONCLUSIONS AND PERSPECTIVES

The general objective of this work was to contribute to better understand the chemical evolution of the solid and gaseous phases produced during biomass torrefaction. In order to attain this general objective, three specific objectives were considered:

- Identify and quantify chemical evolution of functional groups in the solid phase during biomass torrefaction, versus temperature and versus biomass species;
- Identify and quantify production of condensable species formed in the gaseous phase during biomass torrefaction, versus temperature and versus biomass species;
- Elucidate the reaction pathway which leads from reactants to products during biomass torrefaction.

Torrefaction experiments were carried out with a dynamic profile of temperatures (heating rate of 5°C/min), between 200 and 300°C and under inert atmosphere. Four different biomasses were torrefied: pine, ash-wood, miscanthus and wheat straw. The TGA-GC-MS coupled to the loops storage was employed to analyze the mass loss of the solid phase and the production of condensable species in the gaseous phase during biomass torrefaction; the ^{13}C CP/MAS solid-state NMR was employed to characterize the chemical evolution of functional groups in the solid phase. Torrefaction reaction mechanisms were elucidated on the basis of the original ^{13}C CP/MAS solid-state NMR and TGA-GC-MS data obtained, as well as on the existing literature.

The characterization of the solid phase carried out on raw and torrefied biomass at different temperatures through ^{13}C CP/MAS solid-state NMR enabled to get information about the chemical structure of the solid, i.e. functional groups such as aromatics and methoxyl groups in lignin, or acetyl groups in hemicellulose. It was mainly found:

- A significant difference between spectra profiles of woody and non-woody biomasses, related to their lignin content;

- A decrystallization of crystalline fraction of cellulose from 200-280°C – this temperature depends on the type of biomass – with no further recrystallization, in disagreement with some literature;
- Hemicellulose is the most degraded constituent during the whole torrefaction interval of temperatures, while cellulose turns out to be rapidly degraded at high temperatures, and lignin is degraded to a less extent during torrefaction;
- Charring is the predominant mechanism of solid conversion at high temperatures: char initially comes from lignin degradation, then also from polysaccharides;
- Methoxyl groups in lignin appear to remain unaffected by torrefaction, and there is no enrichment in this group, in disagreement with some literature;
- Acetyl groups in hemicellulose are, at 280°C, completely degraded for non-woody biomasses and almost completely degraded for ash-wood, whereas acetyl groups of pine are conserved throughout torrefaction;
- In view of the experimental results, the three parameters which would mainly affect solid chemical evolution are: the lignin content in biomass, the cellulose crystallinity index and the xylan content in hemicellulose.

The analysis of the condensable species in the gaseous phase produced at different temperatures through GC-MS coupled with TGA has shown that:

- The formation of the major condensable species observed has been reported in literature, only the formation of some minor species, e.g. 3-butanedione and 2(5H)-furanone-5-methyl-, has not been reported before;
- One can find formation of condensable species within the whole range of torrefaction temperatures explored;
- Around a half of condensable species are produced within the whole range of torrefaction temperatures, around a fourth are produced within the first half of this range, and around a fourth within the second half;
- Around a third of condensable species are produced from all types of biomass;

- A little amount of extractive species were measured only during torrefaction of pine (softwood);
- For the majority of condensable species, trends of formation versus temperature appear to be different among biomasses, in agreement with results found on solid characterization and thus probably also due to difference in compositions of hemicellulose and lignin among biomasses;
- In view of the experimental results, the three parameters which would mainly affect the formation of condensable species are: the proportion and composition of lignin in biomass, and the proportion of xylan in hemicellulose.

In literature, only three kinetic models predict the formation of specific gaseous species linked to solid decomposition during biomass torrefaction. The conceptual model proposed in the present work will be the fourth one, and includes several innovative aspects in comparison to existing models:

- Proposes reaction mechanisms based on a detailed approach of reactants, which are: cellulose (crystalline and amorphous), C5 and C6 sugars of hemicellulose, and H, G and S units of lignin. This approach would enable to predict the differences of behavior among different types of biomass;
- Considers the formation of twenty-six species: twenty-one are gaseous species – sixteen are condensable species and five are non-condensable species –, and five are forms of solid char;
- Reactions proposed have chemical meaning;
- Presents reactions which satisfy the elemental balances in C, H and O.

The main perspectives on experimentation that arise from this work for future studies are:

- Development of experimental procedures in order to increase the amount of condensable species detected and improve the quantification methods;

- Analysis of condensable species produced during torrefaction of cellulose, hemicellulose and lignin extracted from biomass, and torrefaction of mixtures of the three extracted constituents;
- Characterization of the chemical evolution of the solid during torrefaction of cellulose, hemicellulose and lignin extracted from biomass, and torrefaction of mixtures of the three extracted constituents;
- Comparison of the previous experiments on analysis of condensable species and characterization of the solid phase with results obtained during torrefaction of raw biomass to investigate the potential interactions among constituents.

The main perspectives on modelling that arise from this work for future studies are:

- Detail the approach of solid reactants to the level of composition in functional groups: the type and proportion of functional groups are a function of type of biomass, thus this even more detail approach would improve the prediction of the behavior of different biomass species;
- Elaborate a numeric model based on the conceptual model: our model already has chemical coherence, thus the next step would be to add mathematical coherence;
- Elucidate reaction mechanisms for other condensable species;
- Elucidate intermediate mechanisms between reactants and products of each reaction in order to better understand the pathway of reaction;
- Consider interactions among biomass constituents in the model, insofar as they are proved to exist with experimental results;
- Consider not only kinetic aspects, but also thermodynamic aspects, like the enthalpy and the Gibbs free energy of formation;
- Elucidate the kinetic laws, during both dynamic and isothermal torrefaction.

BIBLIOGRAPHY

- Alén, R., Kuoppala, E., Oesch, P., 1996. Formation of the main degradation compound groups from wood and its components during pyrolysis. *J. Anal. Appl. Pyrolysis* 36, 137–148.
- Almeida, G., Brito, J.O., Perré, P., 2010. Alterations in energy properties of eucalyptus wood and bark subjected to torrefaction: The potential of mass loss as a synthetic indicator. *Bioresour. Technol.* 101, 9778–9784.
- Anca-Couce, A., Mehrabian, R., Scharler, R., Obernberger, I., 2014. Kinetic scheme to predict product composition of biomass torrefaction, *Chemical Engineering Transactions*.
- Aziz, M.A., Sabil, K.M., Uemura, Y., Ismail, L., 2012. A study on torrefaction of oil palm biomass. *J. Appl. Sci.* 12, 1130–1135. doi:10.3923/jas.2012.1130.1135
- Bach, Q.-V., Khalil, R.A., Tran, K.-Q., Skreiberg, O., 2014. Torrefaction kinetics of norwegian biomass fuels, *Chemical Engineering Transactions*.
- Banoub, J., Delmas, G.-H., Jr., Joly, N., Mackenzie, G., Cachet, N., Benjelloun-Mlayah, B., Delmas, M., 2015. A critique on the structural analysis of lignins and application of novel tandem mass spectrometric strategies to determine lignin sequencing. *J. Mass Spectrom.* 50, 5–48. doi:10.1002/jms.3541
- Bates, R.B., Ghoniem, A.F., 2012. Biomass torrefaction: Modeling of volatile and solid product evolution kinetics. *Bioresour. Technol.* 124, 460–469.
- Ben, H., Ragauskas, A.J., 2012. Torrefaction of Loblolly pine. *Green Chem.* 14, 72–76.
- Bergman, P.C.A., Boersma, A.R., Zwart, R.W.H., Kiel, J.H.A., 2005. Torrefaction for biomass co-firing in existing coal-fired power stations.
- Boonstra, M.J., Van Acker, J., Tjeerdsma, B.F., Kegel, E.V., 2007. Strength properties of thermally modified softwoods and its relation to polymeric structural wood constituents. *Ann. For. Sci.* 64, 679–690. doi:10.1051/forest:2007048
- Branca, C., Di Blasi, C., Mango, C., Hrablay, I., 2013. Products and Kinetics of Glucomannan Pyrolysis. *Ind. Eng. Chem. Res.* 52, 5030–5039. doi:10.1021/ie400155x
- Bridgeman, T.G., Jones, J.M., Shield, I., Williams, P.T., 2008. Torrefaction of reed canary grass, wheat straw and willow to enhance solid fuel qualities and combustion properties. *Fuel* 87, 844–856.
- Candelier, K., Chaouch, M., Dumaray, S., Pétrissans, A., Pétrissans, M., Gérardin, P., 2011. Utilization of thermodesorption coupled to GC-MS to study stability of different wood species to thermodegradation. *J. Anal. Appl. Pyrolysis* 92, 376–383.
- Casajus, C., Marias, F., Perard, P., De Guillebon, B., 2012. Overview of torrefaction technology.
- Castellano, J.M., Gómez, M., Fernández, M., Esteban, L.S., Carrasco, J.E., 2015. Study on the effects of raw materials composition and pelletization conditions on the quality and properties of pellets obtained from different woody and non woody biomasses. *Fuel* 139, 629–636. doi:10.1016/j.fuel.2014.09.033
- Cavagnol, S., Sanz, E., Nastoll, W., Roesler, J.F., Zymła, V., Perré, P., 2013. Inverse analysis of wood pyrolysis with long residence times in the temperature range 210-290 C: Selection of multi-step kinetic models based on mass loss residues. *Thermochim. Acta* 574, 1–9.
- Chang, S., Zhao, Z., Zheng, A., He, F., Huang, Z., Li, H., 2012. Characterization of products from torrefaction of sprucewood and bagasse in an auger reactor. *Energy Fuels* 26, 7009–7017. doi:10.1021/ef301048a

- Chen, D., Zhou, J., Zhang, Q., Zhu, X., Lu, Q., 2014. Torrefaction of Rice Husk using TG-FTIR and its Effect on the Fuel Characteristics, Carbon, and Energy Yields. *Bioresour.* Vol 9 No 4 2014.
- Chen, W.-H., Hsu, H.-C., Lu, K.-M., Lee, W.-J., Lin, T.-C., 2011a. Thermal pretreatment of wood (Lauan) block by torrefaction and its influence on the properties of the biomass. *Energy* 36, 3012–3021.
- Chen, W.-H., Hsu, H.-C., Lu, K.-M., Lee, W.-J., Lin, T.-C., 2011b. Thermal pretreatment of wood (Lauan) block by torrefaction and its influence on the properties of the biomass. *Energy* 36, 3012–3021.
- Chen, W.-H., Kuo, P.-C., 2011. Torrefaction and co-torrefaction characterization of hemicellulose, cellulose and lignin as well as torrefaction of some basic constituents in biomass. *Energy* 36, 803–811. doi:10.1016/j.energy.2010.12.036
- Chen, W.-H., Peng, J., Bi, X.T., 2015. A state-of-the-art review of biomass torrefaction, densification and applications. *Renew. Sustain. Energy Rev.* 44, 847–866. doi:10.1016/j.rser.2014.12.039
- Chew, J.J., Doshi, V., 2011. Recent advances in biomass pretreatment - Torrefaction fundamentals and technology. *Renew. Sustain. Energy Rev.* 15, 4212–4222.
- Collard, F.-X., Blin, J., 2014. A review on pyrolysis of biomass constituents: Mechanisms and composition of the products obtained from the conversion of cellulose, hemicelluloses and lignin. *Renew. Sustain. Energy Rev.* 38, 594–608.
- Commandré, J.M., Leboeuf, A., 2015. Volatile yields and solid grindability after torrefaction of various biomass types.
- Da Silva Perez, D., Dupont, C., Guillemain, A., Jacob, S., Labalette, F., Briand, S., Marsac, S., 2015. Characterisation of the Most Representative Agricultural and Forestry Biomasses in France for Gasification. *Waste Biomass Valorization*.
- David, K., Pu, Y., Foston, M., Muzzy, J., Ragauskas, A., 2009. Cross-polarization/magic angle spinning (CP/MAS) ¹³C nuclear magnetic resonance (NMR) analysis of chars from alkaline-treated pyrolyzed softwood. *Energy Fuels* 23, 498–501.
- Di Blasi, C., Lanzetta, M., 1997. Intrinsic kinetics of isothermal xylan degradation in inert atmosphere. *J. Anal. Appl. Pyrolysis* 40-41, 287–303.
- Dorado, J., Claassen, F.W., Van Beek, T.A., Lenon, G., Wijnberg, J.B.P.A., Sierra-Alvarez, R., 2000. Elimination and detoxification of softwood extractives by white-rot fungi. *J. Biotechnol.* 80, 231–240. doi:10.1016/S0168-1656(00)00264-9
- Dupont, C., Commandré, J.M., Ould Marrakchy, E.K., Nocquet, T., Verne-Tournon, C., Da Silva Perez, D., Labalette, F., Rousset, P., 2011. Torrefaction behaviour of various biomass types: Kinetics of solid mass loss and release of volatiles. *TCBiomass*, Chicago.
- Englisch M., 2011. Fundamentals and basic principles of torrefaction. Central European Biomass Conference, Austria.
- Faulon, J., Carlson, G.A., al., 1994. A three-dimensional model for lignocellulose from gymnospermous wood. *Org. Geochem.* 1169–1179.
- Fenner, R.A., Lephardt, J.O., 1981. Examination of the thermal decomposition of kraft pine lignin by Fourier transform infrared evolved gas analysis. *J. Agric. Food Chem.* 29, 846–849. doi:10.1021/jf00106a042
- Fisher, E.M., Dupont, C., Darvell, L.I., Commandré, J.-M., Saddawi, A., Jones, J.M., Grateau, M., Nocquet, T., Salvador, S., 2012. Combustion and gasification

- characteristics of chars from raw and torrefied biomass. *Bioresour. Technol.* 119, 157–165.
- Fougeroux, M., 2014. Étalonnages des analyseurs GC-MS et GC-FID pour l'analyse de composés issus de la torréfaction de biomasse. Préparation de solutions et analyses de prélèvements.
- Frank M. White, n.d. *Fluid Mechanics*, Fourth Edition. ed. McGraw-Hill.
- González-Martínez, M., 2015. Calculations on reaction characteristic time during biomass TGA torrefaction.
- Grigiente, M., Antolini, D., 2015. Mass yield as guide parameter of the torrefaction process. An experimental study of the solid fuel properties referred to two types of biomass. *Fuel* 153, 499–509. doi:10.1016/j.fuel.2015.03.025
- Hakkou, M., Pétrissans, M., Gérardin, P., Zoulalian, A., 2006. Investigations of the reasons for fungal durability of heat-treated beech wood. *Polym. Degrad. Stab.* 91, 393–397. doi:10.1016/j.polymdegradstab.2005.04.042
- Hansen, N.M.L., Plackett, D., 2008. Sustainable films and coatings from hemicelluloses: A review. *Biomacromolecules* 9, 1493–1505. doi:10.1021/bm800053z
- Harmsen, P.F.H., Huijgen, W.J.J., Bermúdez López, L.M., Bakker, R.R.C., 2010. Literature Review of Physical and Chemical Pretreatment Processes for Lignocellulosic Biomass.
- Heux, L., Dinand, E., Vignon, M.R., 1999. Structural aspects in ultrathin cellulose microfibrils followed by ¹³C CP-MAS NMR. *Carbohydr. Polym.* 40, 115–124. doi:10.1016/S0144-8617(99)00051-X
- Ho, D.P., Ngo, H.H., Guo, W., 2014. A mini review on renewable sources for biofuel. *Bioresour. Technol.* 169, 742–749. doi:10.1016/j.biortech.2014.07.022
- Holtman, K.M., Chen, N., Chappell, M.A., Kadla, J.F., Xu, L., Mao, J., 2010. Chemical structure and heterogeneity differences of two lignins from loblolly pine as investigated by advanced solid-state NMR spectroscopy. *J. Agric. Food Chem.* 58, 9882–9892.
- Huang, Y., Wei, Z., Qiu, Z., Yin, X., Wu, C., 2012. Study on structure and pyrolysis behavior of lignin derived from corncob acid hydrolysis residue. *J. Anal. Appl. Pyrolysis* 93, 153–159. doi:10.1016/j.jaap.2011.10.011
- IEA, 2013. *World Energy Outlook 2013*.
- IEA, 2012. *World Energy Outlook 2012*.
- Jacob, S., Da Silva Perez, D., Dupont, C., Commandré, J.-M., Broust, F., Carriau, A., Sacco, D., 2013. Short rotation forestry feedstock: Influence of particle size segregation on biomass properties. *Fuel* 111, 820–828. doi:10.1016/j.fuel.2013.04.043
- Jakab, E., Faix, O., Till, F., Székely, T., 1995. Thermogravimetry/mass spectrometry study of six lignins within the scope of an international round robin test. *J. Anal. Appl. Pyrolysis* 35, 167–179. doi:10.1016/0165-2370(95)00907-7
- Kaplan, D.L., 1998. *Biopolymers from Renewable Sources*. Springer-Verlag.
- Khazraie Shoulaifar, T., Demartini, N., Willför, S., Pranovich, A., Smeds, A.I., Virtanen, T.A.P., Maunu, S.-L., Verhoeff, F., Kiel, J.H.A., Hupa, M., 2014. Impact of torrefaction on the chemical structure of birch wood. *Energy Fuels* 28, 3863–3872.
- Kibet, J., Khachatryan, L., Dellinger, B., 2012. Molecular Products and Radicals from Pyrolysis of Lignin. *Environ. Sci. Technol.* 46, 12994–13001. doi:10.1021/es302942c
- Kiel, J.H.A., 2012. Torrefaction to improve biomass logistics (and enduse).

- Kirk-Otmer, 2001. Kirk-Othmer Encyclopedia of Chemical Technology, 4th edition. ed.
- Klinger, J., Bar-Ziv, E., Shonnard, D., 2013. Kinetic study of aspen during torrefaction. *J. Anal. Appl. Pyrolysis* 104, 146–152. doi:10.1016/j.jaap.2013.08.010
- Lê Thành, K., Commandré, J.M., Valette, J., Volle, G., Meyer, M., 2015. Detailed identification and quantification of the condensable species released during torrefaction of lignocellulosic biomasses. *Fuel Process. Technol.*
- Liu, G., Qiu, X., Yang, D., 2008. Properties of wheat straw soda lignin of different molecular weights and its influence on properties of LPF adhesive. *Huagong Xuebao* *J. Chem. Ind. Eng. China* 59, 1590–1594.
- Lupoi, J.S., Singh, S., Parthasarathi, R., Simmons, B.A., Henry, R.J., 2015. Recent innovations in analytical methods for the qualitative and quantitative assessment of lignin. *Renew. Sustain. Energy Rev.* 49, 871–906. doi:10.1016/j.rser.2015.04.091
- McKendry, P., 2002. Energy production from biomass (part 2): conversion technologies. *Rev. Issue* 83, 47–54. doi:10.1016/S0960-8524(01)00119-5
- Melkior, T., Jacob, S., Gerbaud, G., Hediger, S., Le Pape, L., Bonnefois, L., Bardet, M., 2012. NMR analysis of the transformation of wood constituents by torrefaction. *Fuel* 92, 271–280.
- Monteil-Rivera, F., Phuong, M., Ye, M., Halasz, A., Hawari, J., 2013. Isolation and characterization of herbaceous lignins for applications in biomaterials. *Ind. Crops Prod.* 41, 356–364. doi:10.1016/j.indcrop.2012.04.049
- Mu, W., Ben, H., Ragauskas, A., Deng, Y., 2013. Lignin Pyrolysis Components and Upgrading—Technology Review. *BioEnergy Res.* 6, 1183–1204. doi:10.1007/s12155-013-9314-7
- Nocquet, T., 2012. *Torréfaction du bois et de ses constituants: expériences et modélisation des rendements en matières volatiles.* Université de Toulouse, Toulouse.
- Nocquet, T., Dupont, C., Commandre, J.-M., Gâteau, M., Thiery, S., Salvador, S., 2014a. Volatile species release during torrefaction of wood and its macromolecular constituents: Part 1 - Experimental study. *Energy* 72, 180–187.
- Nocquet, T., Dupont, C., Commandre, J.-M., Gâteau, M., Thiery, S., Salvador, S., 2014b. Volatile species release during torrefaction of biomass and its macromolecular constituents: Part 2 - Modeling study. *Energy* 72, 188–194. doi:10.1016/j.energy.2014.05.023
- Ochoa-Villarreal, M., Aispuro-Hernández, E., Vargas-Arispuro, I., Martínez-Téllez, M.A., 2012. Polymerization - Chapter 4: Plant Cell Wall Polymers: Function, Structure and Biological Activity of Their Derivatives. Ailton De Souza Gomes.
- Park, J., Li, X., Rojas, O., Park, S., 2011. Chemistry of lignocellulosic biomass transformation during torrefaction. Presented at the ACS National Meeting Book of Abstracts.
- Park, J., Meng, J., Lim, K.H., Rojas, O.J., Park, S., 2013a. Transformation of lignocellulosic biomass during torrefaction. *J. Anal. Appl. Pyrolysis* 100, 199–206.
- Park, J., Meng, J., Lim, K.H., Rojas, O.J., Park, S., 2013b. Transformation of lignocellulosic biomass during torrefaction. *J. Anal. Appl. Pyrolysis* 100, 199–206.
- Park, S., Baker, J.O., Himmel, M.E., Parilla, P.A., Johnson, D.K., 2010. Cellulose crystallinity index: measurement techniques and their impact on interpreting cellulase performance. *Biotechnol. Biofuels* 3, 10–10. doi:10.1186/1754-6834-3-10

- Pastorova, I., Botto, R.E., Arisz, P.W., Boon, J.J., 1994. Cellulose char structure: A combined analytical Py-GC-MS, FTIR, and NMR study. *Carbohydr. Res.* 262, 27–47.
- Patuzzi, F., Mimmo, T., Cesco, S., Gasparella, A., Baratieri, M., 2013a. Common reeds (*Phragmites australis*) as sustainable energy source: Experimental and modelling analysis of torrefaction and pyrolysis processes. *GCB Bioenergy* 5, 367–374. doi:10.1111/gcbb.12000
- Patuzzi, F., Mimmo, T., Cesco, S., Gasparella, A., Baratieri, M., 2013b. Common reeds (*Phragmites australis*) as sustainable energy source: Experimental and modelling analysis of torrefaction and pyrolysis processes. *GCB Bioenergy* 5, 367–374. doi:10.1111/gcbb.12000
- Pelaez-Samaniego, M.R., Yadama, V., Garcia-Perez, M., Lowell, E., McDonald, A.G., 2014. Effect of temperature during wood torrefaction on the formation of lignin liquid intermediates. *J. Anal. Appl. Pyrolysis* 109, 222–233. doi:10.1016/j.jaap.2014.06.008
- Peng, Y., Wu, S., 2010. The structural and thermal characteristics of wheat straw hemicellulose. *J. Anal. Appl. Pyrolysis* 88, 134–139.
- Prins, M.J., 2005. Thermodynamic analysis of biomass gasification and torrefaction. Technische Universiteit Eindhoven, The Netherlands.
- Prins, M.J., Ptasiński, K.J., Janssen, F.J.J.G., 2006a. Torrefaction of wood. Part 2. Analysis of products. *J. Anal. Appl. Pyrolysis* 77, 35–40.
- Prins, M.J., Ptasiński, K.J., Janssen, F.J.J.G., 2006b. Torrefaction of wood. Part 1. Weight loss kinetics. *J. Anal. Appl. Pyrolysis* 77, 28–34.
- Ragauskas, A.J., 2008. Typical H:G:S ratio for lignin from biomass. Institute for Paper Science and Technology (IPST).
- Ranzi, E., Cuoci, A., Faravelli, T., Frassoldati, A., Migliavacca, G., Pierucci, S., Sommariva, S., 2008. Chemical kinetics of biomass pyrolysis. *Energy Fuels* 22, 4292–4300.
- Raven, P.H., Evert, R.F., al., 1992. *Biology of plants*, 6th edition. ed. W.H. Freeman and company/Worth Publishers.
- Ren, S., Lei, H., Wang, L., Bu, Q., Chen, S., Wu, J., 2013. Thermal behaviour and kinetic study for woody biomass torrefaction and torrefied biomass pyrolysis by TGA. *Biosyst. Eng.* 116, 420–426.
- Rousset, P., Davrieux, F., Macedo, L., Perré, P., 2011. Characterisation of the torrefaction of beech wood using NIRS: Combined effects of temperature and duration. *Biomass Bioenergy* 35, 1219–1226. doi:10.1016/j.biombioe.2010.12.012
- Rutherford, D.W., Wershaw, R.L., Rostad, C.E., Kelly, C.N., 2012. Effect of formation conditions on biochars: Compositional and structural properties of cellulose, lignin, and pine biochars. *Biomass Bioenergy* 46, 693–701. doi:10.1016/j.biombioe.2012.06.026
- Sabil, K.M., Aziz, M.A., Lal, B., Uemura, Y., 2013. Synthetic indicator on the severity of torrefaction of oil palm biomass residues through mass loss measurement. *Appl. Energy* 111, 821–826.
- Sarvaramini, A., Assima, G.P., Larachi, F., 2013. Dry torrefaction of biomass - Torrefied products and torrefaction kinetics using the distributed activation energy model. *Chem. Eng. J.* 229, 498–507.
- Scheirs, J., Camino, G., Avidano, M., Tumiatti, W., 1998. Origin of furanic compounds in thermal degradation of cellulosic insulating paper. *J. Appl. Polym. Sci.* 69, 2541–2547.

- Scheirs, J., Camino, G., Tumiatti, W., 2001. Overview of water evolution during the thermal degradation of cellulose. *Eur. Polym. J.* 37, 933–942. doi:10.1016/S0014-3057(00)00211-1
- Sebio-Puñal, T., Naya, S., López-Beceiro, J., Tarrío-Saavedra, J., Artiaga, R., 2012. Thermogravimetric analysis of wood, holocellulose, and lignin from five wood species. *J. Therm. Anal. Calorim.* 109, 1163–1167.
- Shang, L., Ahrenfeldt, J., Holm, J.K., Barsberg, S., Zhang, R.-Z., Luo, Y.-H., Egsgaard, H., Henriksen, U.B., 2013. Intrinsic kinetics and devolatilization of wheat straw during torrefaction. *J. Anal. Appl. Pyrolysis* 100, 145–152. doi:10.1016/j.jaap.2012.12.010
- Shebani, A.N., van Reenen, A.J., Meincken, M., 2008. The effect of wood extractives on the thermal stability of different wood species. *Thermochim. Acta* 471, 43–50. doi:10.1016/j.tca.2008.02.020
- Shen, D.K., Gu, S., 2009. The mechanism for thermal decomposition of cellulose and its main products. *Bioresour. Technol.* 100, 6496–6504.
- Shen, D.K., Gu, S., Luo, K.H., Wang, S.R., Fang, M.X., 2010. The pyrolytic degradation of wood-derived lignin from pulping process. *Bioresour. Technol.* 101, 6136–6146. doi:10.1016/j.biortech.2010.02.078
- Sierra, R., Smith, A., Granda, C., Holtzapple, M.T., 2008. Producing fuels and chemicals from lignocellulosic biomass. *Chem. Eng. Prog.* 104, S10–S18.
- Sivonen, H., Maunu, S.L., Sundholm, F., Jämsä, S., Viitaniemi, P., 2002. Magnetic resonance studies of thermally modified wood. *Holzforschung* 56, 648–654.
- Sjostrom, E., 1993. *Wood chemistry. Fundamentals and applications*, 2nd edition. ed. Academic Press.
- Theng, E.Y., Doshi, V., 2014. Characterisation of By-Products from Torrefaction of Palm Mesocarp Fiber.
- Tsubaki, S., Azuma, J., 2011. *Advances in Induction and Microwave Heating of Mineral and Organic Materials - chapter 30: Application of Microwave Technology for Utilization of Recalcitrant Biomass*. InTech.
- Tumuluru, J.S., Sokhansanj, S., Hess, J.R., Wright, C.T., Boardman, R.D., 2011. A review on biomass torrefaction process and product properties for energy applications. *Ind. Biotechnol.* 7, 384–401.
- Van der Stelt, M.J.C., Gerhauser, H., Kiel, J.H.A., Ptasinski, K.J., 2011. Biomass upgrading by torrefaction for the production of biofuels: A review. *Biomass Bioenergy* 35, 3748–3762.
- Vassilev, S.V., Baxter, D., Andersen, L.K., Vassileva, C.G., 2010. An overview of the chemical composition of biomass. *Fuel* 89, 913–933. doi:10.1016/j.fuel.2009.10.022
- Vassilev, S.V., Baxter, D., Andersen, L.K., Vassileva, C.G., Morgan, T.J., 2012. An overview of the organic and inorganic phase composition of biomass. *Fuel* 94, 1–33. doi:10.1016/j.fuel.2011.09.030
- Vermerris, W., Abril, A., 2015. Enhancing cellulose utilization for fuels and chemicals by genetic modification of plant cell wall architecture. *Curr. Opin. Biotechnol.* 32, 104–112. doi:10.1016/j.copbio.2014.11.024
- Wang, S., Guo, X., Wang, K., Luo, Z., 2011. Influence of the interaction of components on the pyrolysis behavior of biomass. *J. Anal. Appl. Pyrolysis* 91, 183–189.
- Wang, Z., McDonald, A.G., Westerhof, R.J.M., Kersten, S.R.A., Cuba-Torres, C.M., Ha, S., Pecha, B., Garcia-Perez, M., 2013. Effect of cellulose crystallinity on the formation

- of a liquid intermediate and on product distribution during pyrolysis. *J. Anal. Appl. Pyrolysis* 100, 56–66.
- Wen, J.-L., Sun, S.-L., Yuan, T.-Q., Xu, F., Sun, R.-C., 2014. Understanding the chemical and structural transformations of lignin macromolecule during torrefaction. *Appl. Energy* 121, 1–9.
- Wikberg, H., Maunu, S.L., 2004. Characterisation of thermally modified hard- And softwoods by ¹³C CPMAS NMR. *Carbohydr. Polym.* 58, 461–466.
- Windeisen, E., Bachle, H., Zimmer, B., Wegener, G., 2009. Relations between chemical changes and mechanical properties of thermally treated wood. *Holzforschung* 63, 773–778.
- Wooten, J.B., Seeman, J.I., Hajaligol, M.R., 2004. Observation and Characterization of Cellulose Pyrolysis Intermediates by ¹³C CPMAS NMR. A New Mechanistic Model. *Energy Fuels* 18, 1–15. doi:10.1021/ef0300601
- Worasuwannarak, N., Sonobe, T., Tanthapanichakoon, W., 2007. Pyrolysis behaviors of rice straw, rice husk, and corncob by TG-MS technique. *J. Anal. Appl. Pyrolysis* 78, 265–271. doi:10.1016/j.jaap.2006.08.002
- Wu, Y.-M., Zhao, Z.-L., Li, H.-B., He, F., 2009. Low temperature pyrolysis characteristics of major components of biomass. *Ranliao Huaxue Xuebao* Journal Fuel Chem. Technol. 37, 427–432.
- Yang, H., Yan, R., Chen, H., Lee, D.H., Zheng, C., 2007. Characteristics of hemicellulose, cellulose and lignin pyrolysis. *Fuel* 86, 1781–1788.
- Yu, Y., Liu, D., Wu, H., 2012. Characterization of water-soluble intermediates from slow pyrolysis of cellulose at low temperatures. *Energy Fuels* 26, 7331–7339. doi:10.1021/ef3013097
- Zanzi, R., Ferro, D.T., Torres, A., Soler, P.B., Bjornbom, E., 2002. Biomass torrefaction.
- Zheng, A., Zhao, Z., Chang, S., Huang, Z., He, F., Li, H., 2012. Effect of torrefaction temperature on product distribution from two-staged pyrolysis of biomass. *Energy Fuels* 26, 2968–2974.
- Zheng, A., Zhao, Z., Chang, S., Huang, Z., Wang, X., He, F., Li, H., 2013. Effect of torrefaction on structure and fast pyrolysis behavior of corncobs. *Bioresour. Technol.* 128, 370–377.